ORNL-TM-3063

Contract No. W-7405-eng-26

METALS AND CERAMICS DIVISION

AN EVALUATION OF THE MOLTEN-SALT REACTOR EXPERIMENT HASTELLOY N SURVEILLANCE SPECIMENS — FOURTH GROUP

H. E. McCoy, Jr.

MARCH 1971

OAK RIDGE NATIONAL LABORATORY
Oak Ridge, Tennessee
operated by
UNION CARBIDE CORPORATION
for the
U.S. ATOMIC ENERGY COMMISSION

CONTENTS

AN EVALUATION OF THE MOLTEN-SALT REACTOR EXPERIMENT HASTELLOY N SURVEILLANCE SPECIMENS – FOURTH GROUP

H. E. McCoy, Jr.

ABSTRACT

Two heats of standard Hastelloy N were removed from the core of the MSRE after 22,533 hr at 650°C and exposed to a thermal fluence of 1.5×10^{21} neutrons/cm^2 and a fast fluence > 50 kev of 1.1×10^{21} neutrons/cm^2. The mechanical properties have systematically deteriorated with increasing fluence. However, the change in properties is due to the helium produced by the $^{10}B(n,\alpha)^{7}Li$ transmutation and can be reduced by changes in chemical composition. Some of these modified heats have been exposed to the core of the MSRE and show improved resistance to irradiation.

The corrosion of the Hastelloy N has been largely due to the selective removal of chromium. The rates of removal are much as predicted from the measured diffusion rate of chromium. Other superficial structure modifications have been observed, but they likely result from carbide precipitation along slip bands that were formed during machining.

INTRODUCTION

The Molten-Salt Reactor Experiment (MSRE) is a single region reactor that is fueled by a molten fluoride salt (65 LiF–29.1 BeF_2–5 ZrF_4–0.9 UF_4, mole %), moderated by unclad graphite, and contained by Hastelloy N (Ni–16 Mo–7 Cr–4 Fe–0.05 C, wt %). The details of the reactor design and construction can be found elsewhere.[1] We knew that the neutron environment would produce some changes in the two structural materials – graphite and Hastelloy N. Although we were very confident of the compatibility of these materials with the fluoride salt, we needed to keep abreast of the possible development of corrosion problems within

[1] R. C. Robinson, MSRE Design and Operations Report, Pt. 1, Description of Reactor Design, ORNL-TM-728 (1965).

the reactor itself. For these reasons, we developed a surveillance program that would allow us to follow the property changes of graphite and Hastelloy N specimens as the reactor operated.

The reactor went critical on June 1, 1965. After many small problems were solved, normal operation began in May 1966. We removed four groups of surveillance samples. The results of tests on the first three groups were reported.[2–4] This report deals primarily with the results of tests on samples removed with the fourth group. The fourth group included two heats of standard Hastelloy N used in fabricating the MSRE and three heats with modified chemistry that had better mechanical properties after irradiation and appear attractive for use in future molten-salt reactors. The respective history of each lot was (1) standard Hastelloy N, annealed 2 hr at 900°C and exposed to the MSRE core for 22,533 hr at 650°C to a thermal fluence of 1.5×10^{22} neutrons/cm^2, (2) two heats of modified Hastelloy N, annealed 1 hr at 1177°C and exposed to the MSRE core for 7244 hr at 650°C to a thermal fluence of 5.1×10^{22} neutrons/cm^2, and (3) a single heat of modified Hastelloy N, annealed for 1 hr at 1177°C and exposed to the MSRE cell environment of N_2 + 2 to 5% O_2 for 17,033 hr at 650°C to a thermal fluence of 2.5×10^{19} neutrons/cm^2. The results of tests on these materials will be presented in detail, and some comparisons will be made with the data from the groups removed previously.

EXPERIMENTAL DETAILS

Surveillance Assemblies

The core surveillance assembly[5] was designed by W. H. Cook and others, and the details have been reported previously. The specimens

---

[2]H. E. McCoy, An Evaluation of the Molten-Salt Reactor Experiment Hastelloy N Surveillance Specimen — First Group, ORNL-TM-1997 (1967).

[3]H. E. McCoy, An Evaluation of the Molten-Salt Reactor Experiment Hastelloy N Surveillance Specimen — Second Group, ORNL-TM-2359 (1969).

[4]H. E. McCoy, An Evaluation of the Molten-Salt Reactor Experiment Hastelloy N Surveillance Specimen — Third Group, ORNL-TM-2647 (1970).

[5]W. H. Cook, MSR Program Semiann. Progr. Rept. Aug. 31, 1965, ORNL-3872, p. 87.

are arranged in three stringers. Each stringer is about 62 in. long and consists of two Hastelloy N rods and a graphite section made up of various pieces that are joined by pinning and tongue-and-groove joints. The Hastelloy N rod has periodic-reduced sections 1 1/8 in. long by 1/8 in. in diameter and can be cut into small tensile specimens after it is removed from the reactor. Three stringers are joined together so that they can be separated in a hot cell and reassembled with one or more new stringers for reinsertion into the reactor. The assembled stringers fit into a perforated Hastelloy N basket that is inserted into an axial position about 3.6 in. from the core center line.

A control facility is associated with the surveillance program. It utilizes a "fuel salt" containing depleted uranium in a static pot that is heated electrically. The temperature is controlled by the MSRE computer so that the temperature matches that of the reactor. Thus, these specimens are exposed to conditions similar to those in the reactor except for the static salt and the absence of a neutron flux.

There is another surveillance facility for Hastelloy N located outside the core in a vertical position about 4.5 in. from the vessel. These specimens are exposed to the cell environment of N_2 + 2 to 5% O_2.

Materials

The compositions of the two heats of standard Hastelloy N are given in Table 1. These heats were air melted by the Stellite Division of Union Carbide Corporation. Heat 5085 was used for making the cylindrical portion of the reactor vessel and heat 5065 was used for forming the top and bottom heads. These materials were given a mill anneal of 1 hr at 1177°C and a final anneal of 2 hr at 900°C at ORNL after fabrication.

The chemical compositions of the three modified alloys are given in Table 1. The modifications in composition were made principally to improve the alloy's resistance to radiation damage and to bring about general improvements in the fabricability, weldability, and ductility.[6]

[6]H. E. McCoy and J. R. Weir, Materials Development for Molten-Salt Breeder Reactors, ORNL-TM-1854 (1967).

Table 1. Chemical Analysis of Surveillance Heats

Element	Content, wt %				
	Heat 5065	Heat 5085	Heat 7320	Heat 67-551	Heat 67-504
Cr	7.3	7.3	7.2	7.0	6.94
Fe	3.9	3.5	< 0.05	0.02	0.05
Mo	16.5	16.7	12.0	12.2	12.4
C	0.065	0.052	0.059	0.028	0.07
Si	0.60	0.58	0.03	0.02	0.010
Co	0.08	0.15	0.01	0.03	0.02
W	0.04	0.07	< 0.05	0.001	0.03
Mn	0.55	0.67	0.17	0.12	0.12
V	0.22	0.20	< 0.02	< 0.001	0.01
P	0.004	0.0043	0.002	0.0006	0.002
S	0.007	0.004	0.003	< 0.002	0.003
Al	0.01	0.02	0.15	< 0.05	0.03
Ti	0.01	< 0.01	0.65	1.1	< 0.02
Cu	0.01	0.01	0.02	0.01	0.03
O	0.0016	0.0093	0.001	0.0004	< 0.0001
N	0.011	0.013	0.0002	0.0003	0.0003
Zr	< 0.1	< 0.002	< 0.05	< 0.01	0.01
Hf	< 0.1				0.50
B	0.0024	0.0038	0.00002	0.0002	0.00003

Alloys 67-551 and 67-504 were small, 100-lb heats made by the Stellite Division of Union Carbide Corporation by vacuum melting. They were finished to 1/2 in. plate by working at 870°C. We cut strips 1/2 in. by 1/2 in. from the plates and swaged them to 1/4-in.-diam rod. Two sections of rod were welded together to make 62-in.-long rods for fabricating the samples. The rods were annealed for 1 hr at 1177°C in argon and then the reduced sections were machined. Heat 7320 was a 5000-lb melt made by the Materials Systems Division of Union Carbide Corporation. Part of the heat was fabricated by the vendor to 5/16-in.-diam rod and was sinterless ground to obtain the needed 1/4 in. stock. The material was annealed 1 hr at 1177°C and then the reduced sections were machined.

Test Specimens

The surveillance rods inside the core are 62 in. long and those outside the vessel are 84 in. long. They both are 1/4 in. in diameter with reduced sections 1/8 in. in diameter by 1 1/8 in. long. After removal from the reactor, the rods are sawed into small mechanical property specimens having a gage section 1/8 in. in diameter by 1 1/8 in. long.

The first rods were machined as segments and then welded together, but we described previously an improved technique in which we use a milling cutter to machine the reduced sections in the rod.[3] This technique is quicker, cheaper, and requires less handling of the relatively fragile rods than the previous method of making the rods into segments. The standard Hastelloy N rods were machined and welded together and the modified alloys were prepared by milling.

IRRADIATION CONDITIONS

The irradiation conditions for the various groups of surveillance specimens that have been removed are summarized in Table 2. The reactor operated from June 1965 until March 1968 with a single change of fuel salt in which there was a 33% enrichment of ^{235}U. After this period of operation the uranium in the fuel was stripped by fluorination and replaced with ^{233}U (ref. 7). This charge of salt was used until the present group of samples was removed. Referring again to Table 2, the standard Hastelloy N in the core was exposed to both salts and the modified Hastelloy N in the core was exposed only to the latter salt. The same salt has been used in the control facility throughout operation.

The specimens outside the core (designated "vessel" specimens) were exposed to the cell environment of N_2 + 2 to 5% O_2.

---

[7]P. N. Haubenreich and J. R. Engle, "Experience with the Molten-Salt Reactor Experiment," Nucl. Appl. Technol. 8(2), 118 (1970).

Table 2. Summary of Exposure Conditions of Surveillance Samples[a]

	Group 1 Core Standard Hastelloy N	Group 2, Hastelloy N		Group 3, Hastelloy N			Group 4, Hastelloy N		
		Core Modified	Vessel Standard	Core Standard	Core Modified	Vessel Standard	Core Standard	Core Modified	Vessel Modified
Date inserted	9/8/65	9/13/66	8/24/65	9/13/66	6/5/67	8/24/65	9/13/66	4/10/68	5/7/68
Date removed	7/28/66	5/9/67	6/5/67	4/3/68	4/3/68	5/7/68	6/69	6/69	6/69
Megawatt-hour on MSRE at time of insertion	0.0066	8682	0	8682	36,247	0	8682	72,441	36,247
Megawatt-hour on MSRE at time of removal	8682	36,247	36,247	72,441	72,441	72,441	92,805	92,805	92,805
Temperature, °C	650 ± 10	650 ± 10	650 ± 10	650 ± 10	650 ± 10	650 ± 10	650 ± 10	650 ± 10	650 ± 10
Time at temperature, hr	4800	5500	11,000	15,289	9789	20,789	22,533	7244	17,033
Peak fluence, neutrons/cm^2									
Thermal (< 0.876 ev)	1.3×10^{20}	4.1×10^{20}	1.3×10^{19}	9.4×10^{20}	5.3×10^{20}	2.6×10^{19}	1.5×10^{21}	5.1×10^{20}	2.5×10^{19}
Epithermal (> 0.876 ev)	3.8×10^{20}	1.2×10^{21}	2.5×10^{19}	2.8×10^{21}	1.6×10^{21}	5.0×10^{19}	3.7×10^{21}	9.1×10^{20}	3.9×10^{19}
(> 50 kev)	1.2×10^{20}	3.7×10^{20}	2.1×10^{19}	8.5×10^{20}	4.8×10^{20}	4.2×10^{19}	1.1×10^{21}	1.1×10^{20}	3.3×10^{19}
(> 1.22 Mev)	3.1×10^{19}	1.0×10^{20}	5.5×10^{18}	2.3×10^{20}	1.3×10^{20}	1.1×10^{19}	3.1×10^{20}	0.8×10^{20}	8.6×10^{18}
(> 2.02 Mev)	1.6×10^{19}	0.5×10^{20}	3.0×10^{18}	1.1×10^{20}	0.7×10^{20}	6.0×10^{18}	1.5×10^{20}	0.4×10^{20}	3.5×10^{18}
Heat	5081	21545	5065	5065	67-502	5065	5065	7320	67-504
Designations	5085	21554	5085	5085	67-504	5085	5085	67-551	

[a]Information compiled by R. C. Steffy, Reactor Division, ORNL, July 1969. Revised for full-power operation at 8 Mw.

Testing Techniques

The laboratory creep-rupture tests of unirradiated control specimens were run in conventional creep machines of the dead-load and lever-arm types. The strain was measured by a dial indicator that showed the total movement of the specimen and part of the load train. The zero strain measurement was taken immediately after the load was applied. The temperature accuracy was ±0.75%, the guaranteed accuracy of the Chromel-P–Alumel thermocouples used.

The postirradiation creep-rupture tests were run in lever-arm machines that were located in hot cells. The strain was measured by an extensometer with rods attached to the upper and lower specimen grips. The relative movement of these two rods was measured by a linear differential transformer, and the transformer signal was recorded. The accuracy of the strain measurement is difficult to determine. The extensometer (mechanical and electrical portions) produced measurements that could be read to about ±0.02% strain; however, other factors (temperature changes in the cell, mechanical vibrations, etc.) probably combine to give an overall accuracy of ±0.1% strain. This is considerably better than the specimen-to-specimen reproducibility that one would expect for relatively brittle materials. The temperature measuring and control system was the same as that used in the laboratory with only one exception. In the laboratory, the control system was stabilized at the desired temperature by use of a recorder with an expanded scale. In the tests in the hot cells, the control point was established by setting the controller without the aid of the expanded-scale recorder. This error and the thermocouple accuracy combine to give a temperature uncertainty of about ±1%.

The tensile tests were run on Instron Universal Testing Machines. The strain measurements were taken from the crosshead travel and generally are accurate to ±2% strain.

The test environment was air in all cases. Metallographic examination showed that the depth of oxidation was small, and we feel that the environment did not appreciably influence the test results.

EXPERIMENTAL RESULTS

Visual and Metallographic Examination

W. H. Cook was in charge of the disassembly of the core surveillance fixture. As shown in Fig. 1, the assembly was in excellent mechanical condition when removed. The Hastelloy N samples were more discolored than noted previously; however, surface marking such as numbers were readily visible. The detailed appearance of the stringer has been described previously by Cook.[8] The Hastelloy N surveillance rods located outside the core were oxidized, but the oxide was tenacious.

Metallographic examination of the Hastelloy N straps that held the graphite and metal together revealed intergranular cracks. A typical

[8]W. H. Cook, MSR Program Semiann. Progr. Rept. Aug. 31, 1965, ORNL-3872, pp. 87–92.

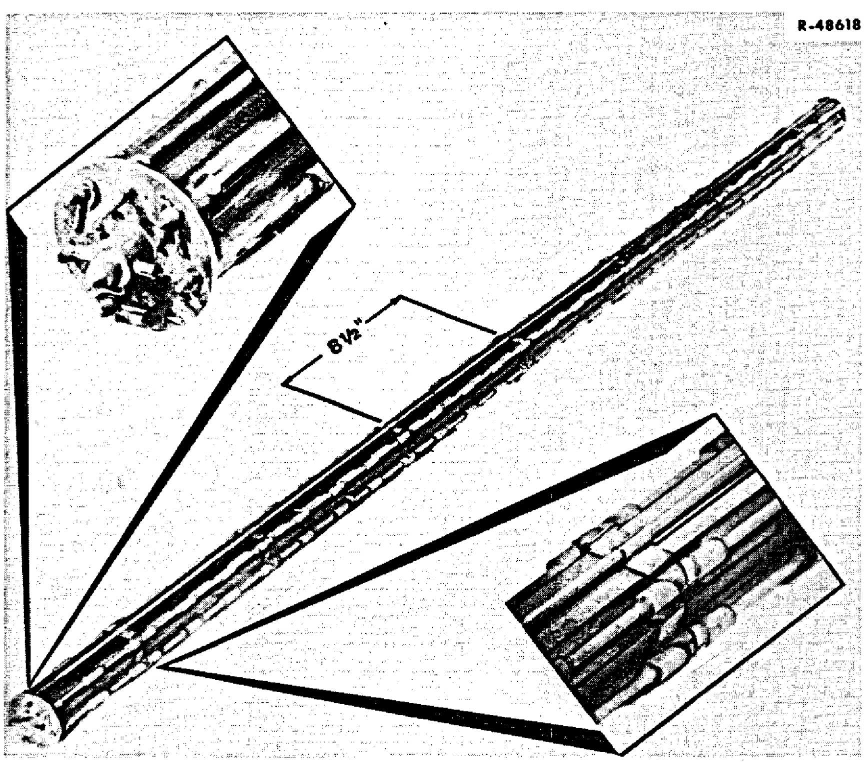

Fig. 1. Overall View of MSRE Surveillance Assembly Removed After Run 18. Parts of this assembly had been exposed to the salt for 22,533 hr at 650°C. The center portion is graphite and the long rods are Hastelloy N.

crack is shown in Fig. 2 and extends to a depth of about 3 mils. A similar strap on the modified samples which had been in the reactor for 7244 hr had cracks to a depth of about 1.5 mils. These straps are about 0.020 in. thick and they likely encountered some deformation while being removed. However, the cracks were quite uniformly spaced on both surfaces of the straps, and their general appearance attests to a general corrosion that rendered the grain boundaries extremely brittle. Examination of unirradiated control straps failed to reveal a similar type of cracking.

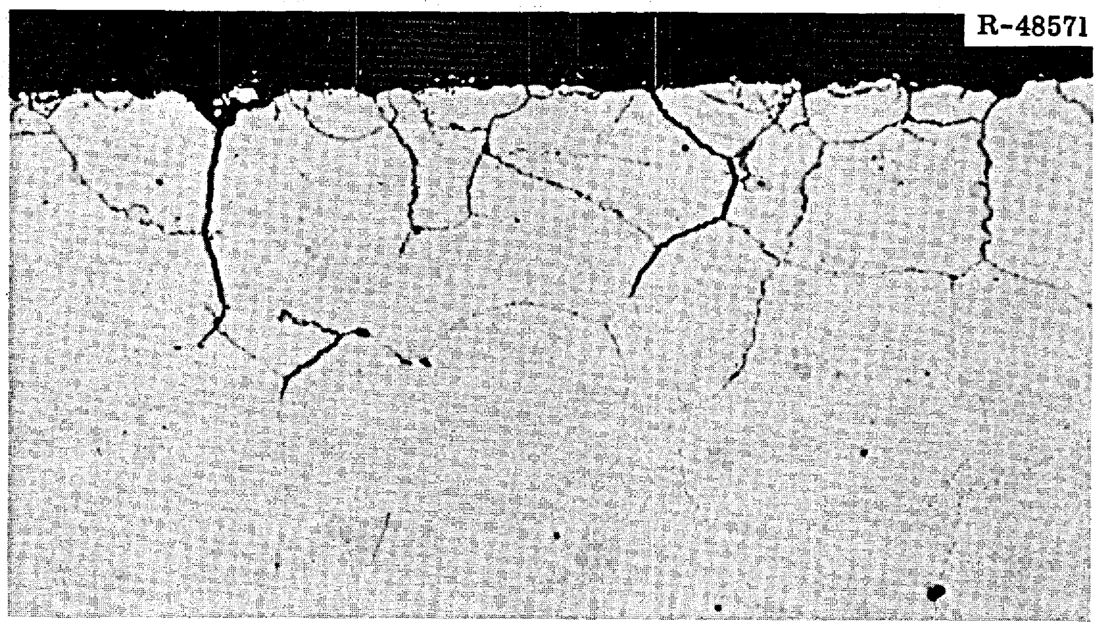

Fig. 2. Typical Microstructure of a Hastelloy N (Heat 5055) After Exposure to the MSRE Core for 22,533 hr at 650°C. This material was used for straps for the surveillance assembly. As polished. 500×.

These observations led to the examination of tabs from the surveillance stringers. Small sections were cut from the centers of the Hastelloy N surveillance rods. Typical photomicrographs of heat 5065 after exposure to the core for 22,533 hr are shown in Fig. 3. The unetched view in Fig. 3(a) shows the surface layer that led to the discolored appearance and a single grain boundary that is visible. Much of the surface layer looks metallic, but this is difficult to judge on

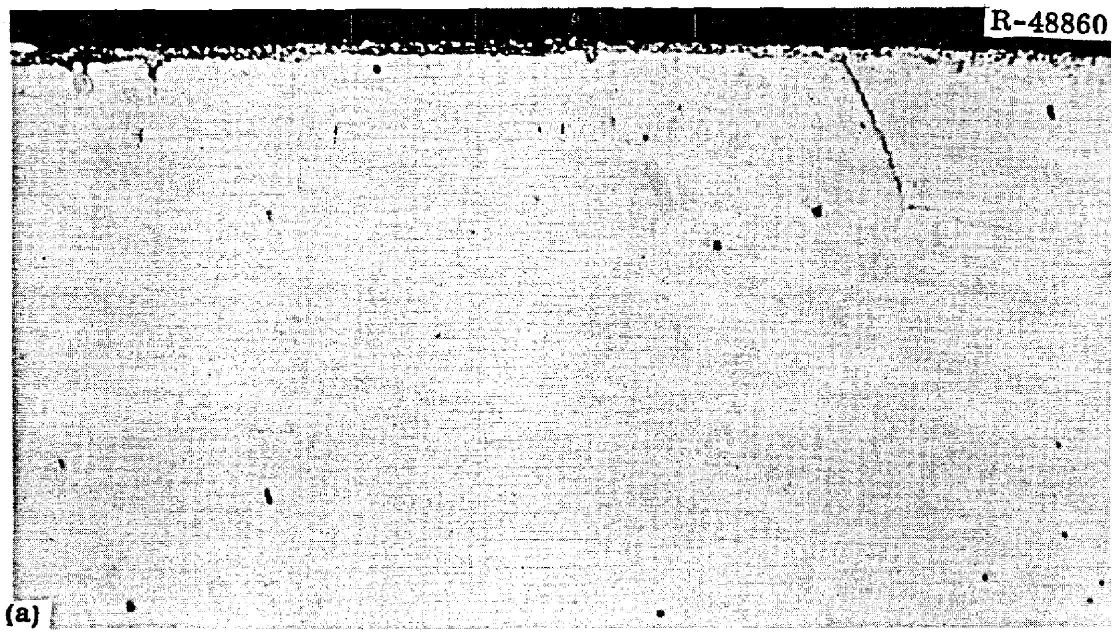

Fig. 3. Typical Photomicrographs of Hastelloy N (Heat 5065) Exposed to the MSRE Core for 22,533 hr at 650°C. (a) As polished. (b) Etchant: aqua regia. 500x.

such a thin film. The etched view in Fig. 3(b) reveals some carbide precipitation near the surface and grain boundaries that are generally lined with carbides. Heat 5085 was exposed an identical time and typical photomicrographs are shown in Fig. 4. The unetched view in Fig. 4(a) shows a modified grain boundary structure to a depth of about 2 mils. Etching [Fig. 4(b)] reveals a grain boundary network of carbides. The grain boundaries near the surface seem to etch differently from the rest of the sample, but little more can be said.

We interpreted these observations as being indicative of some corrosion and performed one further crude experiment to reveal the depth of this attack. One tensile sample had been cut too short for testing, and we bent the remaining portion in a vise. The sample was then sectioned and examined metallographically; the resulting photomicrographs are shown in Fig. 5. The tension side cracked to a depth of about 4 mils whereas the compression side did not crack. Both sides etched abnormally to a depth of about 4 mils.

Samples of heats 5065 and 5085 that were exposed to the static barren salt in the control facility were examined. Figure 6 shows typical photomicrographs of heat 5065 after exposure for 22,533 hr. There is some surface roughening, but no structure modification near the surface such as that shown in Fig. 3 for the sample from the reactor. Likewise, heat 5085 (Fig. 7) showed some surface effects that were minor compared with its irradiated counterpart in Fig. 4.

Thus, there is little doubt that the samples in the core experienced some modifications, apparently to a depth of 3 to 4 mils. This alters up to about 12% of the sample cross section and can be expected to influence the mechanical properties. We shall dwell further on this very important subject later in this report.

A sample of heat 5085 from the core was examined by transmission electron microscopy. This sample had received sufficient thermal fluence to transmute about 97% of the ^{10}B to helium. The helium bubbles are obvious in Fig. 8. Another point of concern was the formation of voids in the material due to fast neutrons. No defects other than helium bubbles and dislocations were present.

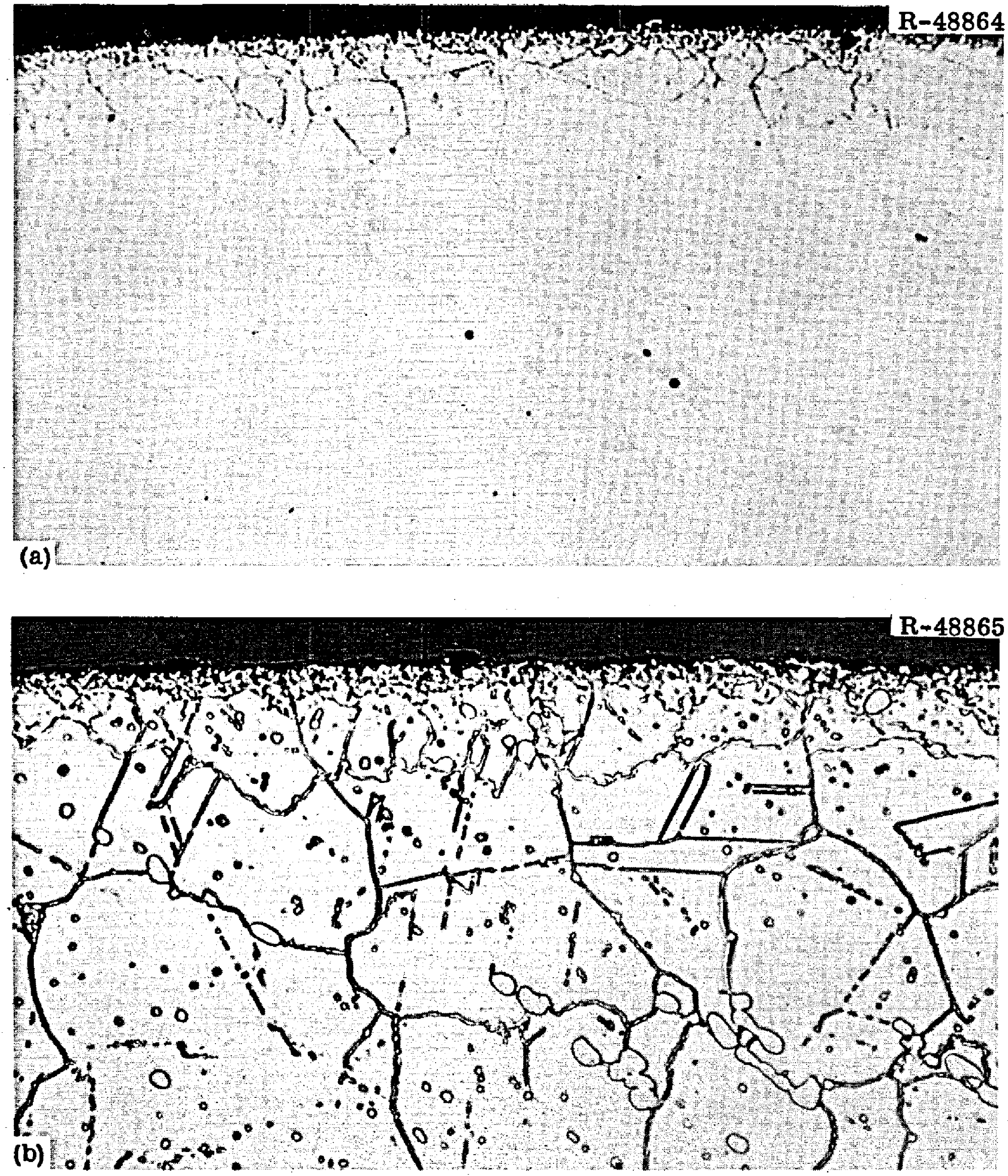

Fig. 4. Typical Photomicrographs of Hastelloy N (Heat 5085) Exposed to the MSRE Core for 22,533 hr at 650°C. (a) As polished. (b) Etchant: glyceria regia. 500×.

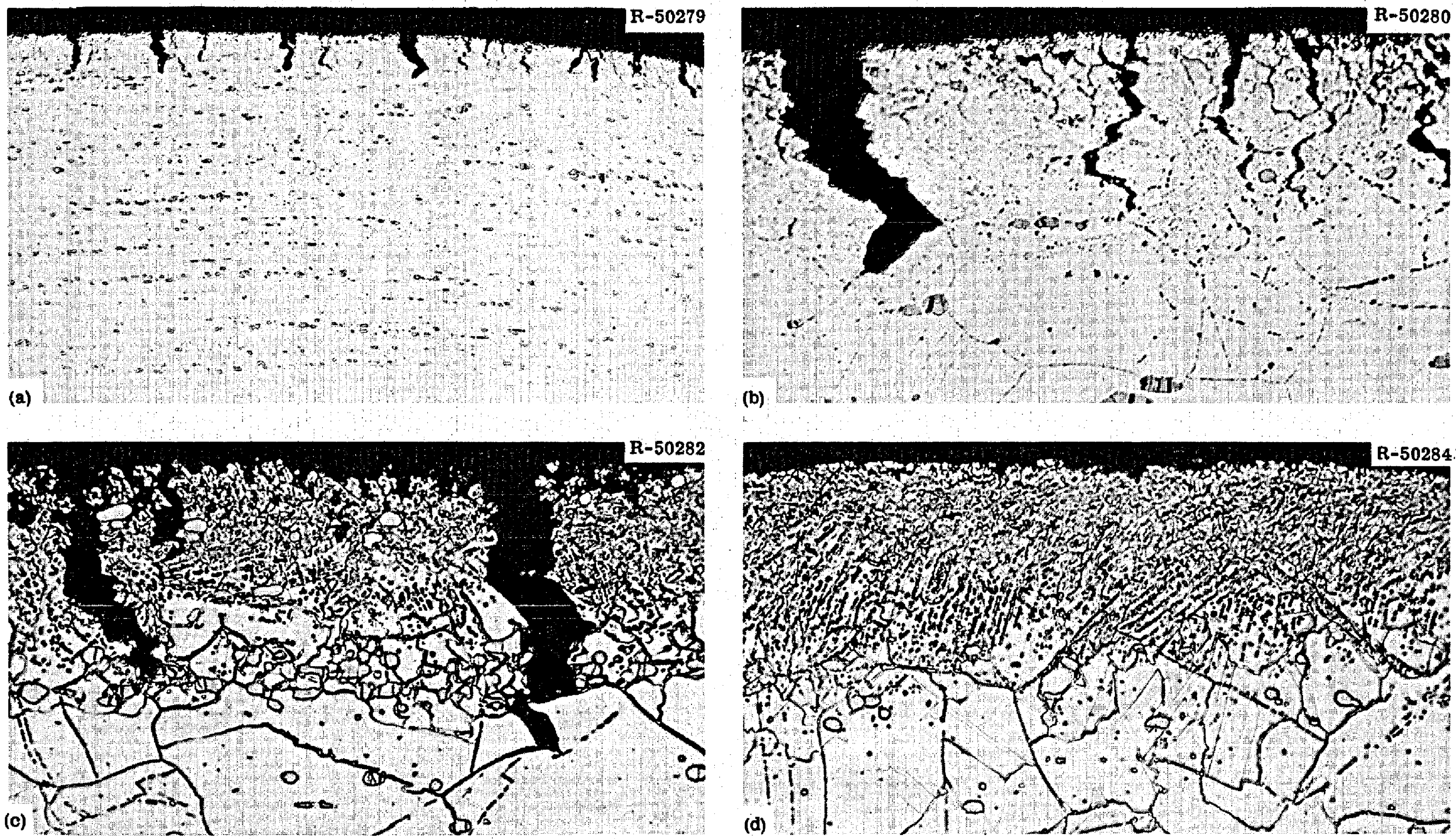

Fig. 5. Typical Photomicrographs of a Hastelloy N (Heat 5085) Sample Exposed to the MSRE Core for 22,533 hr at 650°C. The sample was bent in a vise. (a) As polished, tension side. (b) As polished, tension side. (c) Etched, tension side. (d) Etched, compression side. Etchant: aqua regia. 500X. Reduced 27%.

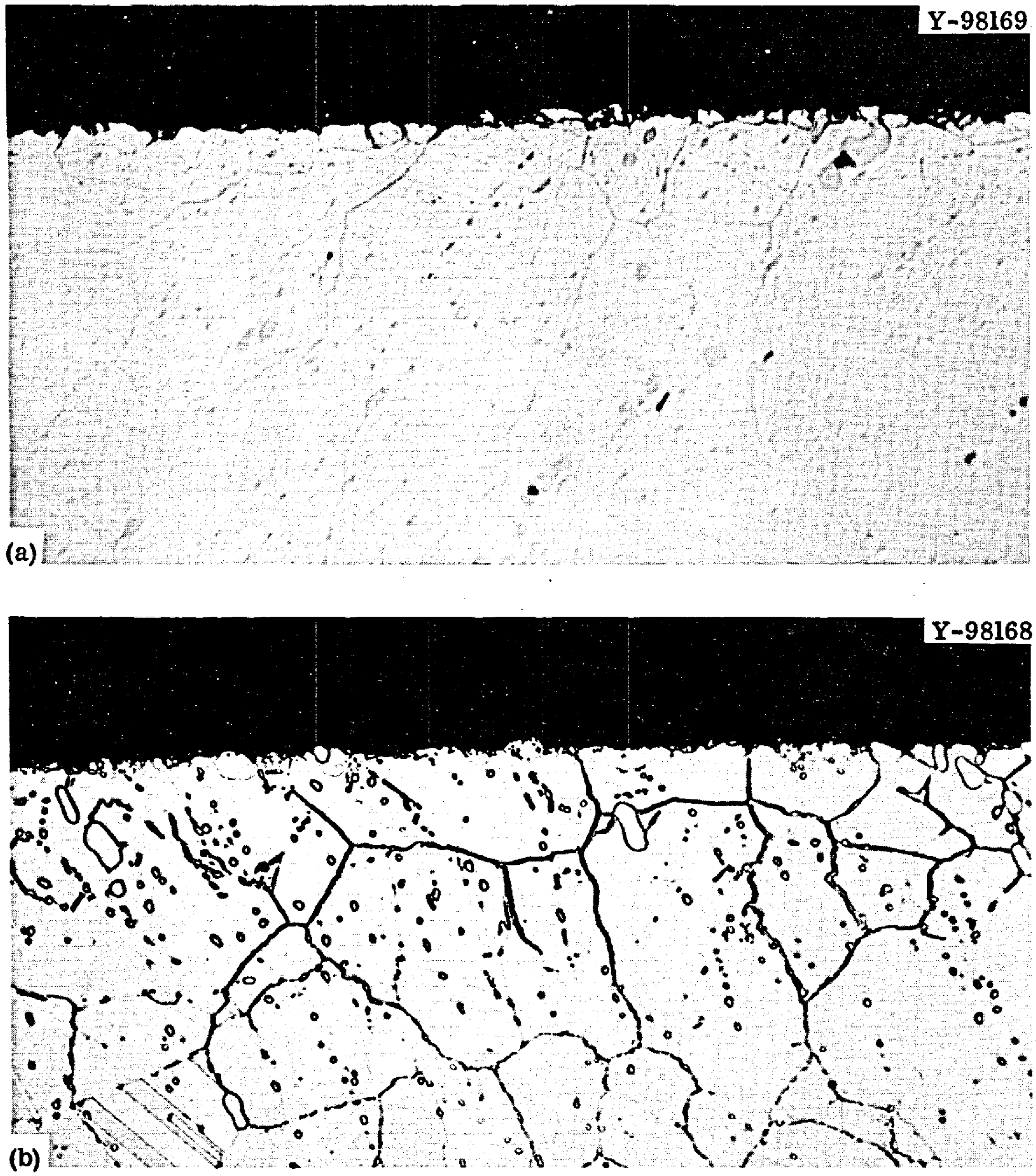

Fig. 6. Typical Photomicrographs of Heat 5065 After Exposure to Static Barren Fuel Salt for 22,533 hr at 650°C. (a) As polished. (b) Etched. Etchant: glyceria regia. 500X.

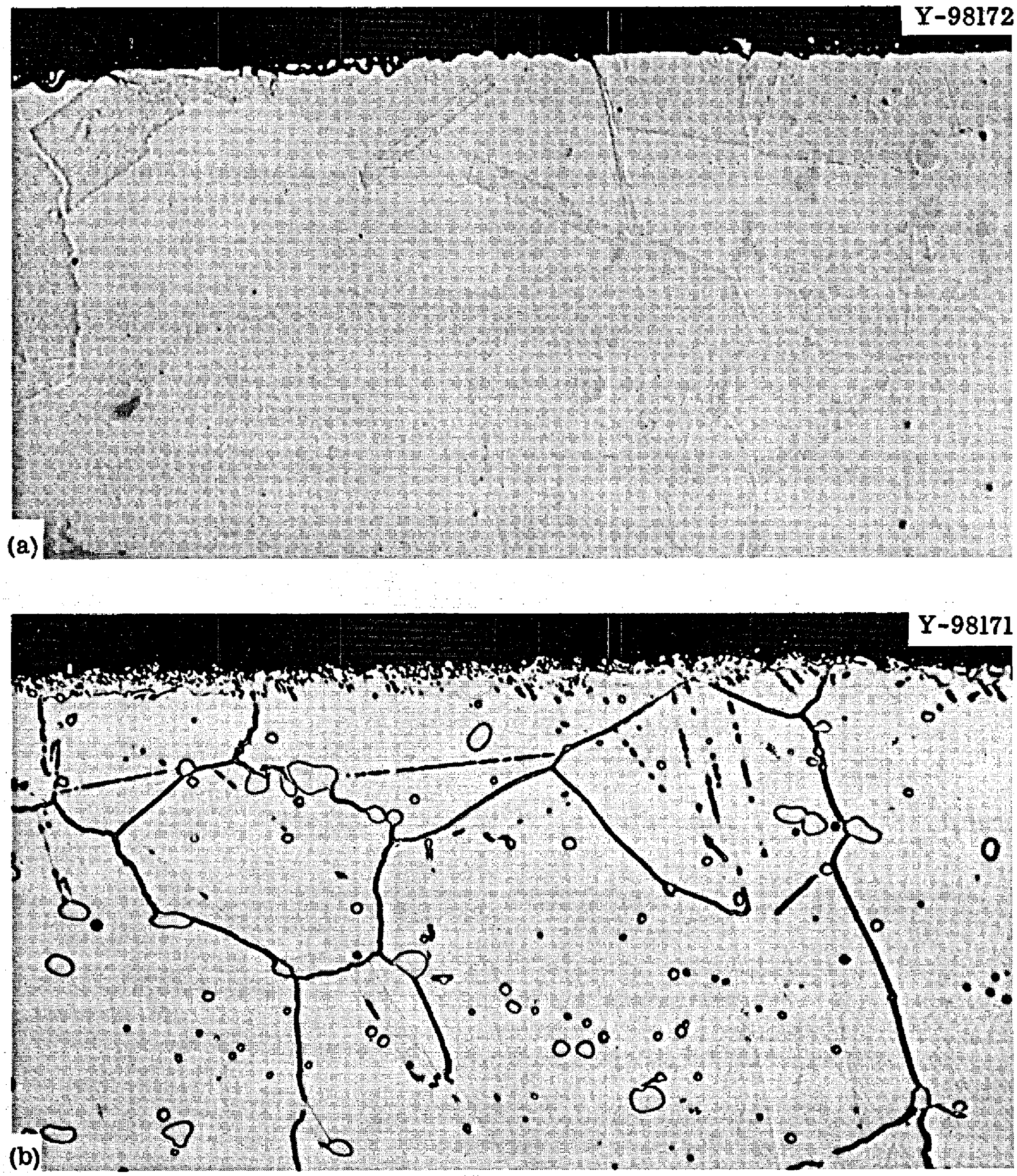

Fig. 7. Typical Photomicrographs of Heat 5085 After Exposure to Static Barren Fuel Salt for 22,533 hr at 650°C. (a) As polished. (b) Etched. Etchant: glyceria regia. 500X.

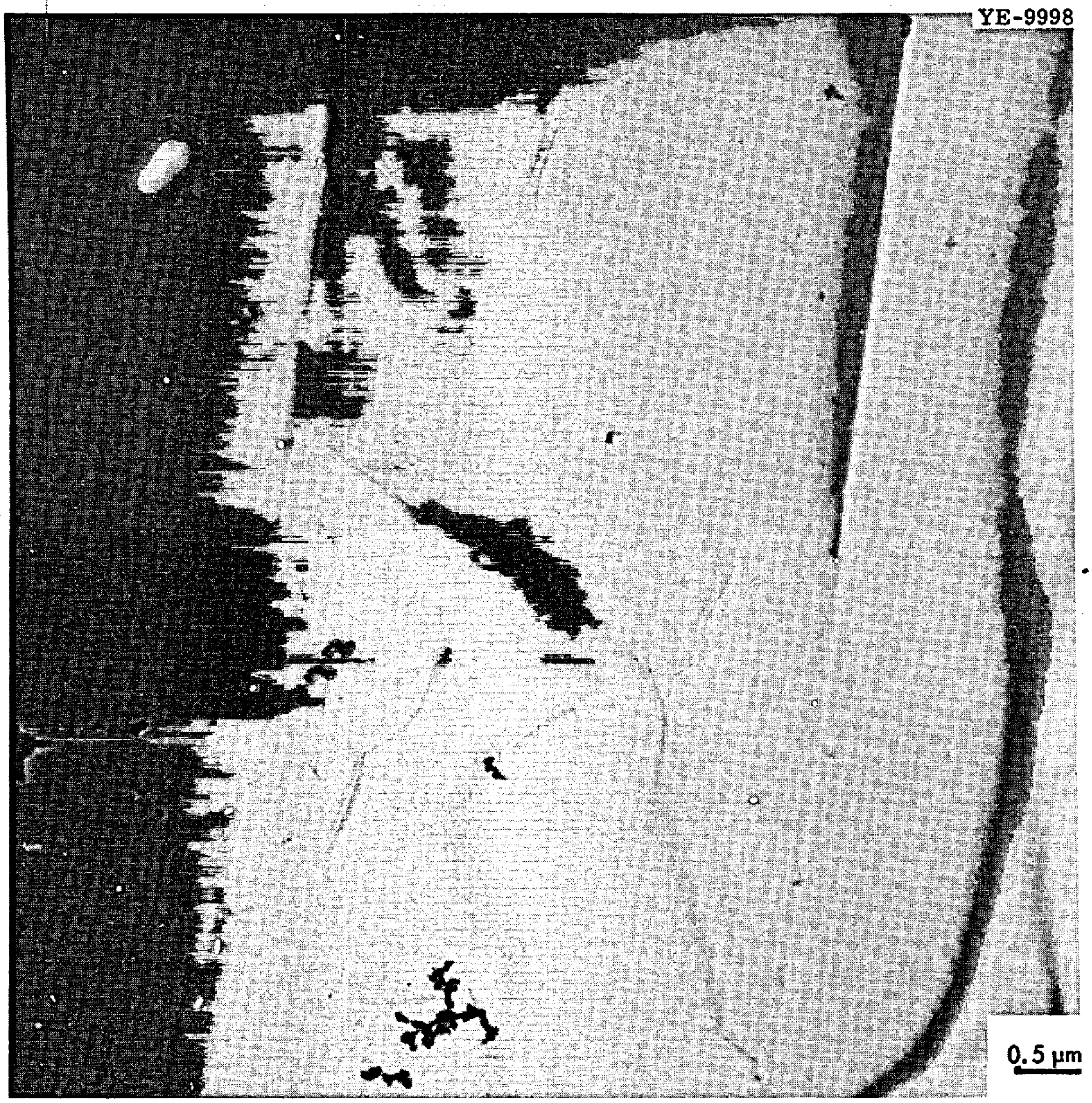

Fig. 8. Transmission Electron Micrograph of Hastelloy N (Heat 5085) Exposed to the MSRE Core for 22,533 hr at 650°C. Irradiated to a thermal neutron fluence of 1.5×10^{21} neutrons/cm^2 and a fast neutron fluence of 3.1×10^{20} neutrons/cm^2 (> 1.22 Mev). The white spots are helium bubbles that are located on a twin boundary. 25,000×. Reduced 16%.

Mechanical Property Data — Standard Hastelloy N

Two heats of standard Hastelloy N were exposed to the MSRE core environment for 22,533 hr at 650°C and received a thermal neutron fluence of 1.5×10^{21} neutrons/cm^2. Similar control samples were exposed to static barren fuel salt for a corresponding length of time. The results of tensile tests on heat 5085 are summarized in Tables 3 and 4 for unirradiated and irradiated samples, respectively. The fracture strains are shown as a function of test temperature in Fig. 9. With increasing temperature the unirradiated samples exhibit first an increase in fracture strain, then a sharp decrease, and then an increase. The irradiated samples follow the same general pattern except for the absence

Table 3. Results of Tensile Tests on Control Samples of Heat 5085[a]

Specimen Number	Test Temperature (°C)	Strain Rate (min^{-1})	Stress, psi		Elongation, %		Reduction in Area (%)	True Fracture Strain (%)
			Yield	Ultimate Tensile	Uniform	Total		
10410	25	0.05	48,100	108,500	40.5	40.6	32.8	40
10409	200	0.05	39,300	101,400	44.7	45.1	33.4	41
10408	400	0.05	35,400	94,900	48.2	48.9	39.3	50
10407	400	0.002	35,200	98,500	48.6	49.0	36.3	45
10406	500	0.05	34,000	92,800	48.0	48.8	40.0	51
10405	500	0.002	35,800	90,100	37.5	38.2	28.8	34
10416	550	0.05	32,700	88,900	51.6	52.2	37.1	46
10417	550	0.002	36,500	79,500	29.4	30.1	24.1	28
10418	600	0.05	33,400	82,200	37.3	37.9	28.6	34
10420	600	0.002	35,200	69,000	25.7	26.9	19.1	21
10421	650	0.05	32,600	75,200	31.0	32.0	28.9	34
10422	650	0.002	34,300	65,600	23.3	23.9	23.9	27
10404	650	0.0002	35,700	64,500	24.9	25.5	19.7	22
10412	650	0.000027	30,000	59,700	15.2	22.2	21.2	24
10423	760	0.05	33,900	64,900	25.6	27.5	19.7	22
10424	760	0.002	31,600	52,000	12.2	27.0	31.6	38
10426	850	0.05	33,600	50,600	10.0	33.0	37.1	46
10425	850	0.002	24,100	26,300	4.2	36.7	25.3	29

[a]Annealed 2 hr at 900°C; exposed to a static vessel of barren fuel salt for 22,533 hr at 650°C.

Table 4. Postirradiation Tensile Properties of Hastelloy N (Heat 5085)[a]

Specimen Number	Test Temperature (°C)	Strain Rate (min^{-1})	Stress, psi: Yield	Stress, psi: Ultimate Tensile	Elongation, %: Uniform	Elongation, %: Total	Reduction in Area (%)	True Fracture Strain (%)
8806	25	0.05	53,900	89,000	22.0	22.1	19.6	22
8805	200	0.05	44,800	85,600	26.4	27.0	26.4	31
8804	400	0.05	41,600	80,900	30.2	30.5	24.3	28
8803	400	0.002	41,300	80,100	28.4	29.2	26.8	31
8802	500	0.05	40,800	73,200	24.8	25.0	23.2	26
8801	500	0.002	39,400	61,100	11.7	12.4	13.9	15
8812	550	0.05	37,900	62,600	14.4	14.9	14.3	15
8813	550	0.002	36,200	49,100	5.8	6.2	9.1	10
8814	600	0.05	36,700	56,200	9.8	10.5	13.3	14
8816	600	0.002	39,000	48,500	4.5	4.9	6.7	7
8817	650	0.05	36,400	50,800	8.8	9.3	9.1	10
8818	650	0.002	37,200	42,800	4.7	5.0	5.8	6
8800	650	0.002	35,200	37,700	2.1	2.4	2.8	3
8799	650	0.000027	32,900	34,500	1.2	1.4	6.1	6
8819	760	0.05	30,700	36,300	6.1	6.4	6.4	7
8820	760	0.002	35,100	35,100	1.7	2.0	2.5	3
8821	850	0.05	32,100	32,700	2.3	2.3	2.1	2
8822	850	0.002	22,200	22,200	1.6	1.7	2.6	3

[a]Annealed 2 hr at 900°C prior to insertion in reactor. Irradiated to a thermal fluence of 1.5×10^{21} neutrons/cm^2 over a period of 22,533 hr at 650°C.

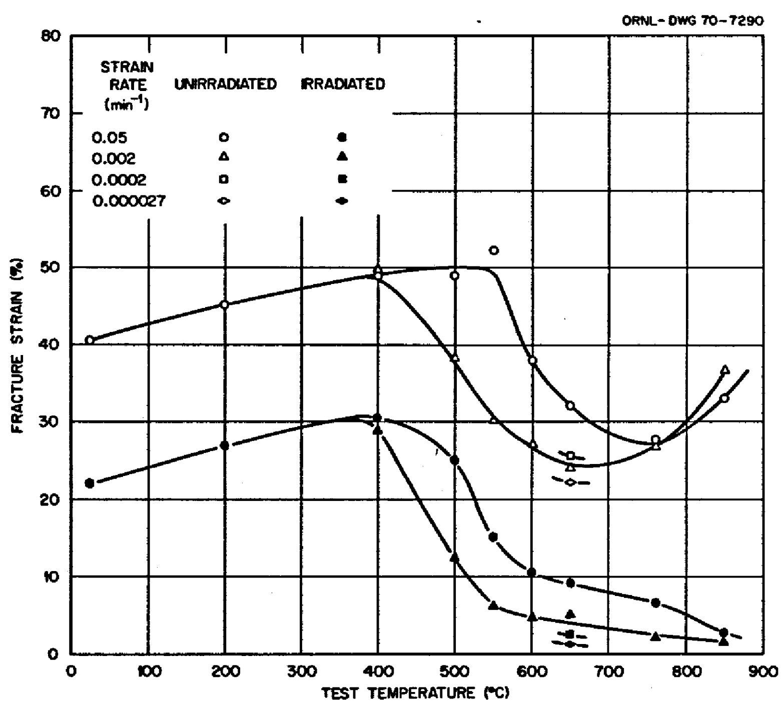

Fig. 9. Fracture Strains of Hastelloy N (Heat 5085) After Removal from the MSRE and from the Control Facility. All samples annealed 1 hr at 900°C before irradiation for 22,533 hr at 650°C to a thermal fluence of 1.5×10^{21} neutrons/cm^2.

of a ductility increase at high temperatures. However, the levels of the fracture strains are lower for the irradiated material over the entire temperature range. For both materials the fracture strain decreases with decreasing strain rate. Another difference in behavior between the irradiated and unirradiated samples is that at the highest strain rate (0.05 min^{-1}) the fracture strain begins its precipitious drop at a lower temperature for the irradiated material.

Further characteristics of the effects of irradiation on the tensile properties of heat 5085 are apparent when the ratios of the irradiated and unirradiated properties are compared (Fig. 10). The yield stress is from 10 to 20% higher for the irradiated material at test temperatures up to 760°C. The ultimate tensile stress is about 20% lower for the irradiated material and drops even further as the test temperature is increased above 500°C. The fracture strains of the irradiated samples are about 50% of those of the unirradiated samples up to about 500°C, above which the reduction is even greater.

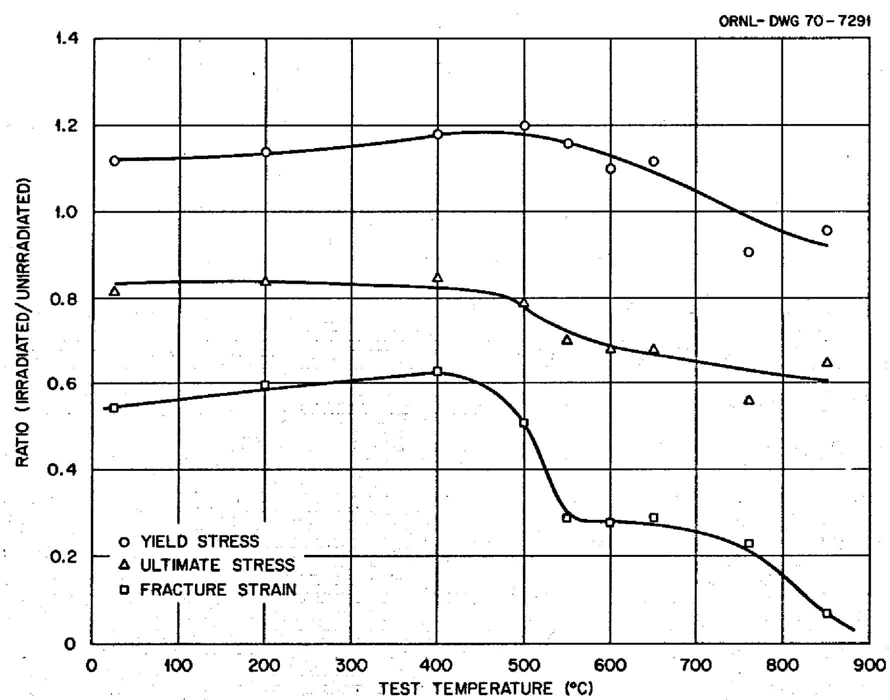

Fig. 10. Comparison of the Tensile Properties of Control and Irradiated Hastelloy N (Heat 5085). Samples irradiated to a fluence of 1.5×10^{21} neutrons/cm^2 over a period of 22,533 hr at 650°C. Tested at a strain rate of 0.05 min^{-1}.

The results of tensile tests on the samples of heat 5065 are summarized in Tables 5 and 6. The fracture strains of these samples are shown in Fig. 11 as a function of test temperature. The results are quite similar to those shown in Fig. 9 for heat 5085. A notable exception is the much higher fracture strains at low temperatures of heat 5065 after irradiation. The ratios of the irradiated and unirradiated tensile properties are shown in Fig. 12. The yield stress was not altered appreciably by irradiation. The ultimate tensile stress was decreased about 10% by irradiation at low test temperatures and up to 35% at high temperatures. Similarly, the fracture strain was reduced about 10% at low temperatures, and this reduction progressed to about 85% at high test temperatures.

The progressive change in the fracture strain with increasing fluence is illustrated in Fig. 13 for heat 5085. The fracture strain has been reduced over the entire range of test temperatures investigated. A similar trend was noted at a slower strain rate of 0.002 min^{-1} (Fig. 14), although the absolute values of the fracture strains were lower than noted in Fig. 13 at the higher strain rate of 0.05 min^{-1}. These samples have experienced various holding times at 650°C and some of the property changes can be attributed to thermal aging. The fracture strains for several sets of control samples of heat 5085 are compared in Fig. 15. At low test temperatures and at 760°C and above the fracture strain seems to show a progressive decrease with increasing holding time at 650°C. At intermediate temperatures the behavior is more complex. At a test temperature of 650°C, the results indicate a progressive decrease in fracture strain up to an exposure time of 15,289 hr and then an increase with further aging time.

Heat 5065 was not included in one set of surveillance samples, but there are sufficient data to follow the property changes with fluence and aging time at 650°C. The fracture strain is shown in Fig. 16 as a function of temperature for various fluences. At low test temperatures, excluding the one apparently anomalous point, the fracture strain was actually higher for irradiation to fluences of 1.3 and 2.6 × 10^{19} neutrons/cm^2. Higher fluences reduced the fracture strain at low test temperatures, but not to values as low as noted in Fig. 13 for heat 5085.

Table 5. Results of Tensile Tests on Control Samples of Heat 5065[a]

Specimen Number	Test Temperature (°C)	Strain Rate (min^{-1})	Stress, psi Yield	Stress, psi Ultimate Tensile	Elongation, % Uniform	Elongation, % Total	Reduction in Area (%)	True Fracture Strain (%)
10384	25	0.05	61,200	126,500	48.5	49.8	36.77	46
10388	200	0.05	44,000	107,900	47.5	49.4	40.16	51
10392	400	0.05	42,600	102,000	48.9	50.8	45.31	60
10383	400	0.002	43,900	106,000	47.5	47.7	39.30	50
10391	500	0.05	42,200	99,400	48.1	49.6	37.54	47
10378	500	0.002	45,800	98,700	45.5	46.2	34.08	42
10395	550	0.05	42,500	98,800	48.2	49.9	38.14	48
10375	550	0.002	43,800	84,600	25.5	26.1	27.51	32
10377	600	0.05	41,800	93,800	42.0	43.0	34.08	42
10393	600	0.002	39,400	76,700	25.6	26.1	34.29	42
10382	650	0.05	41,500	81,900	26.4	26.8	23.84	27
10394	650	0.002	39,200	71,700	23.1	23.6	20.89	23
10397	650	0.0002	41,800	71,200	18.8	19.6	17.88	20
10400	650	0.000027	42,900	60,800	7.5	19.7	24.57	28
10385	760	0.05	32,900	70,500	24.3	27.3	22.85	26
10398	760	0.002	41,100	42,100	5.7	39.6	45.48	61
10390	850	0.05	35,500	49,500	8.7	38.1	45.31	60
10379	850	0.002	24,800	25,100	2.9	56.5	47.15	64

[a]Annealed 2 hr at 900°C prior to insertion in the reactor. Exposed to a static vessel of barren fuel salt for 22,533 hr at 650°C.

Table 6. Postirradiation Tensile Properties of Hastelloy N (Heat 5065)[a]

Specimen Number	Test Temperature (°C)	Strain Rate (min^{-1})	Stress, psi Yield	Stress, psi Ultimate Tensile	Elongation, % Uniform	Elongation, % Total	Reduction in Area (%)	True Fracture Strain (%)
8833	25	0.05	56,700	109,500	42.5	42.8	3.32	3
8832	200	0.05	46,000	99,900	42.8	44.6	4.44	5
8831	400	0.05	43,700	94,300	39.0	39.3	31.22	37
8830	400	0.002	43,200	91,300	35.7	37.2	27.31	32
8829	500	0.05	43,600	82,100	29.1	29.5	22.98	26
8828	500	0.002	39,800	63,200	10.9	11.3	10.70	11
8839	550	0.05	41,200	68,700	15.5	15.7	16.83	18
8840	550	0.002	37,800	57,700	7.1	7.2	8.93	9
8841	600	0.05	40,500	60,100	8.6	9.0	9.30	10
8842	600	0.002	41,000	50,400	4.3	4.5	7.40	8
8843	650	0.05	39,700	52,100	6.0	6.2	7.37	8
8844	650	0.002	40,000	42,800	3.0	3.1	4.89	5
8827	650	0.0002	34,300	36,100	2.1	2.2	3.30	3
8826	650	0.000027	28,400	36,900	1.1	1.2	1.1	1
8845	760	0.05	37,800	41,400	2.5	2.7	3.33	3
8846	760	0.002	35,200	35,200	1.3	1.3	2.86	3
8847	850	0.05	35,400	35,400	1.5	1.6	2.22	2
8848	850	0.002	20,300	20,300	1.0	1.0	0.16	0

[a]Annealed 2 hr at 900°C prior to insertion in the reactor. Irradiated to a thermal fluence of 1.5×10^{20} neutrons/cm^2 over a period of 22,533 hr at 650°C.

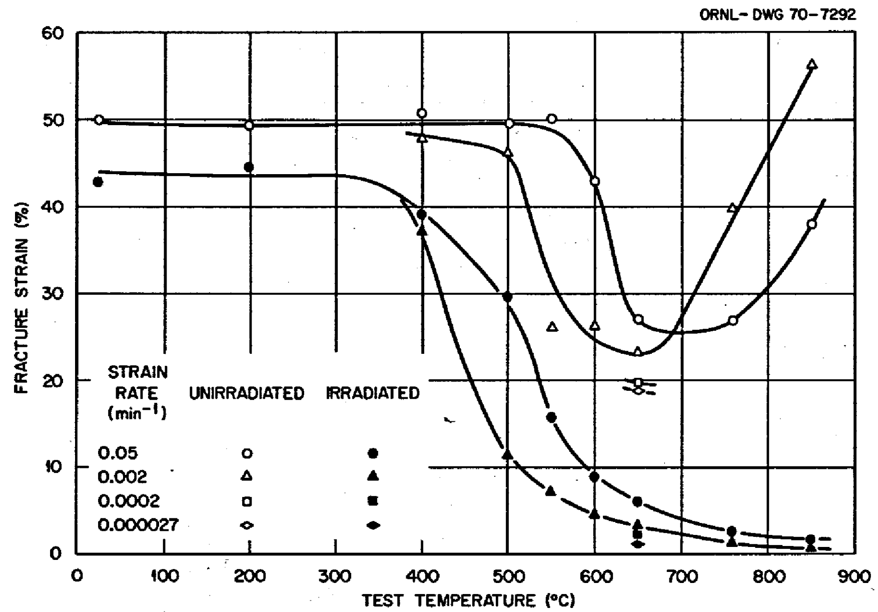

Fig. 11. Fracture Strains of Hastelloy N (Heat 5065) After Removal from the MSRE and from the Control Facility. All samples annealed 2 hr at 900°C before irradiation for 22,533 hr at 650°C to a fluence of 1.5×10^{21} neutrons/cm^2.

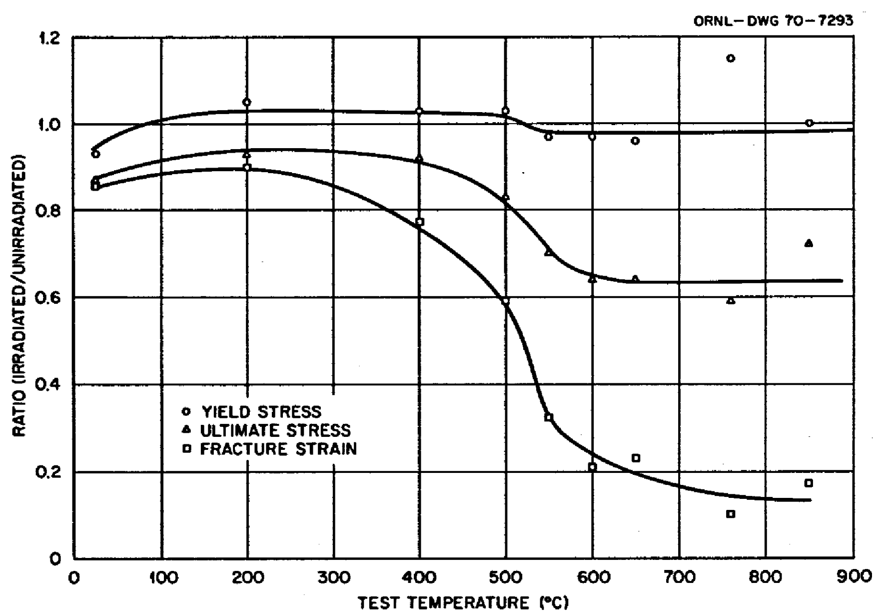

Fig. 12. Comparison of the Tensile Properties of Control and Irradiated Hastelloy N (Heat 5065). Samples irradiated to a fluence of 1.5×10^{21} neutrons/cm^2 over a period of 22,533 hr at 650°C. Tested at a strain rate of 0.05 min^{-1}.

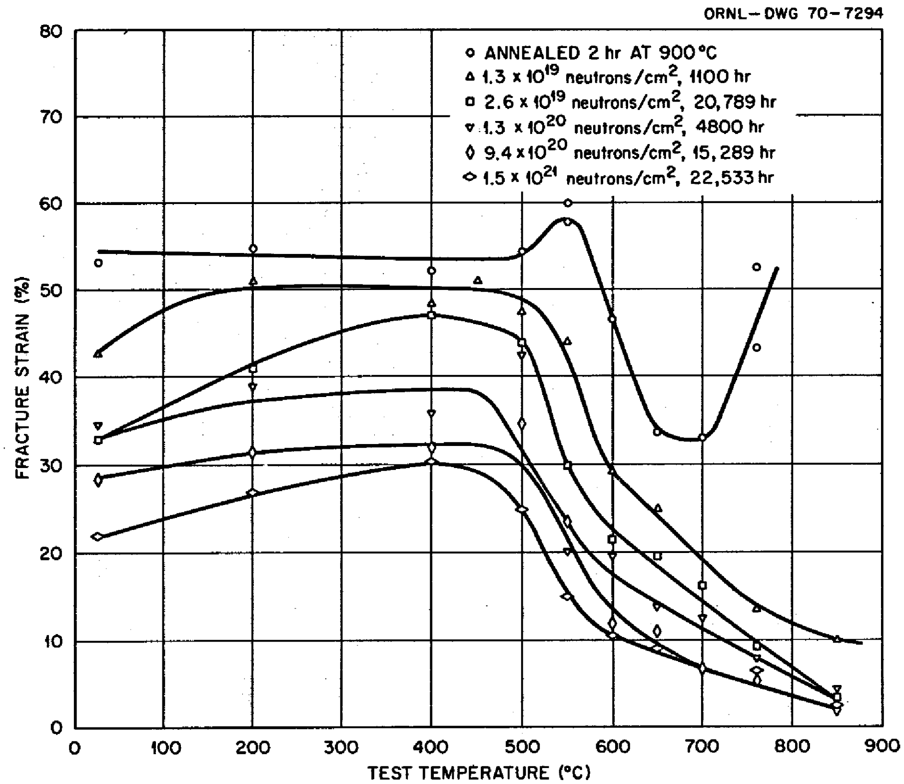

Fig. 13. Fracture Strains of Hastelloy N (Heat 5085) After Irradiation to Various Thermal Fluences in the MSRE. Tested at a strain rate of 0.05 min^{-1}.

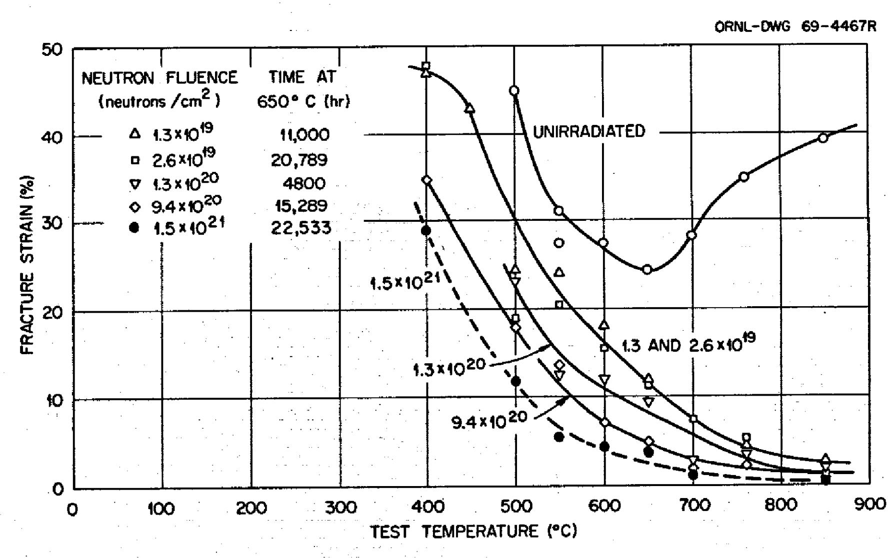

Fig. 14. Postirradiation Tensile Properties of Hastelloy N (Heat 5085) After Exposure to Various Neutron Fluences. Tested at a strain rate of 0.002 min^{-1}.

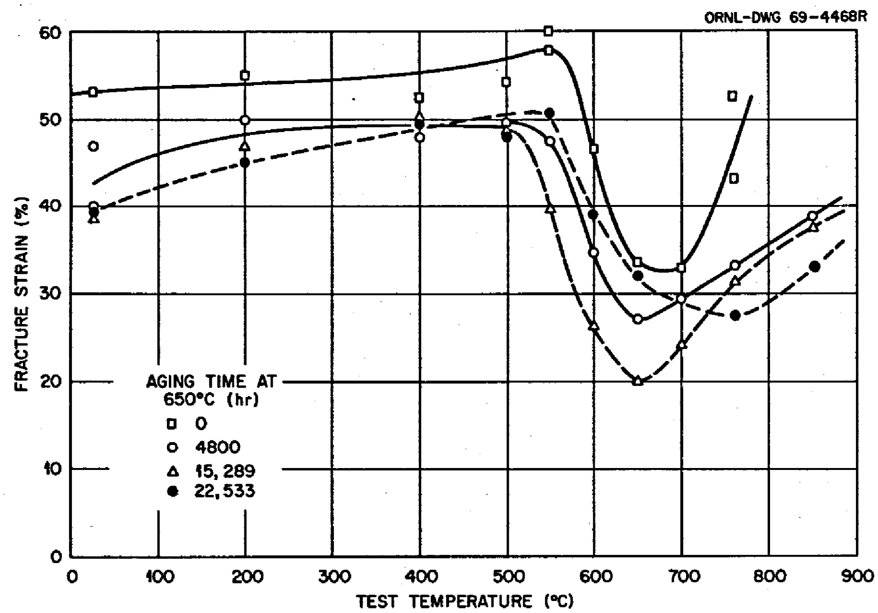

Fig. 15. Variation of the Tensile Properties of Hastelloy N (Heat 5085) with Aging Time in Barren Fuel Salt at 650°C. Tested at a strain rate of 0.05 min^{-1}.

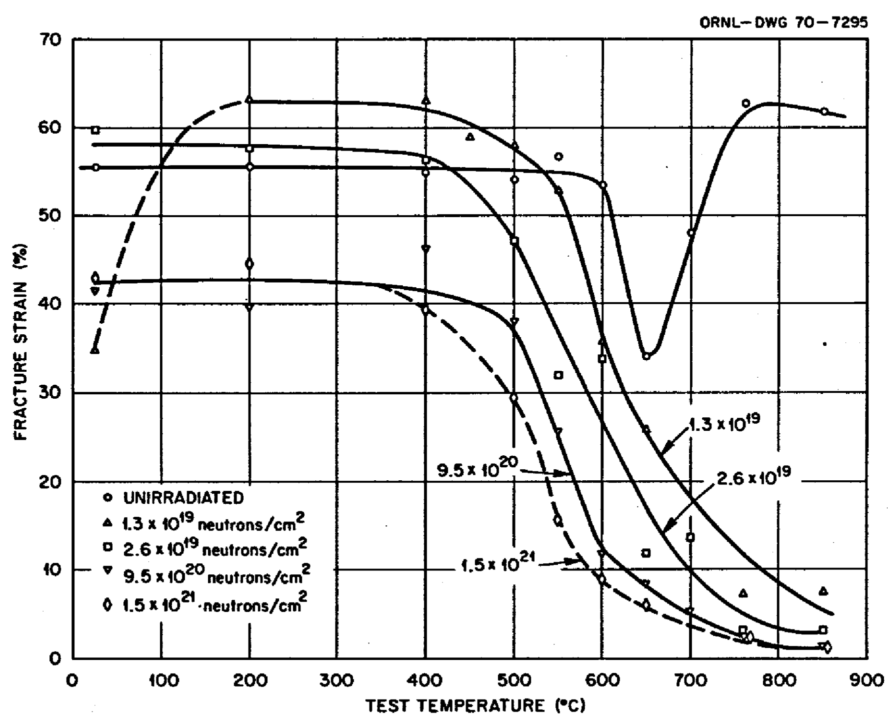

Fig. 16. Variation of the Postirradiation Tensile Properties of Hastelloy N (Heat 5065) with Thermal Neutron Fluence.

At test temperatures above 550°C the fracture strain decreases progressively with increasing fluence. As shown in Fig. 17 some of these changes in fracture strain can be attributed to thermal aging at 650°C. Except at test temperatures above 750°C, the fracture strain is lowest for the material aged 15,289 hr and is improved after aging 22,533 hr. The changes in properties at low test temperatures are less than those for heat 5085 (Fig. 15).

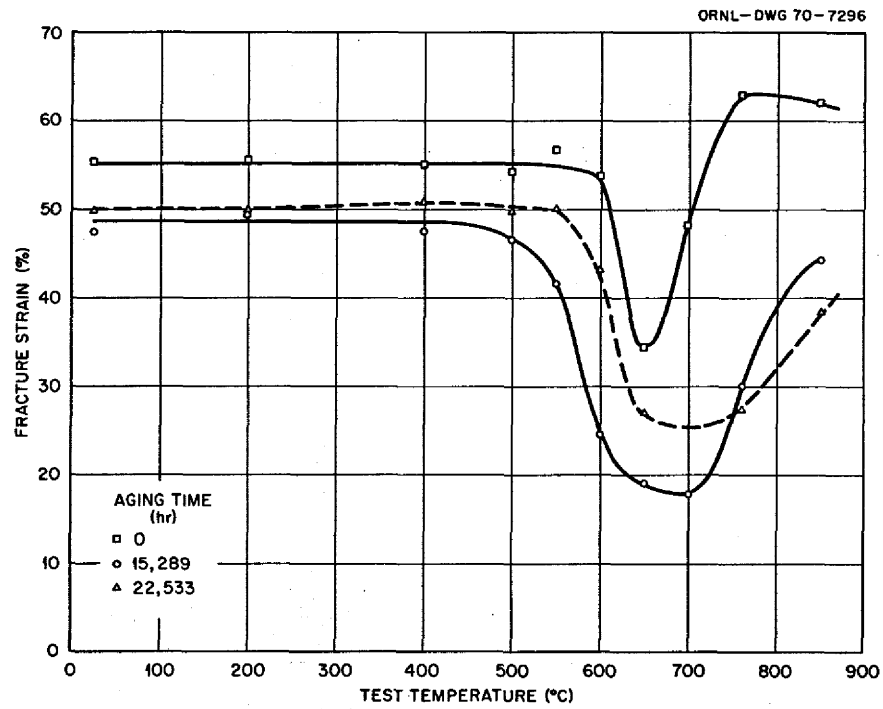

Fig. 17. Effects of Thermal Aging at 650°C on the Tensile Properties of Hastelloy N (Heat 5065) at a Strain Rate of 0.05 min^{-1}.

As discussed previously in this series of reports, the changes in fracture strain at low temperatures were not expected. Although the fracture strains have not reached values below 20%, we are still interested in its progression. Our experience to date is summarized in Fig. 18. If the noted effects were due simply to thermal aging, then the results should correlate with the time at 650°C. Obviously such a correlation does not exist. Where data are available for pairs of irradiated and unirradiated samples, the irradiated sample has the lower

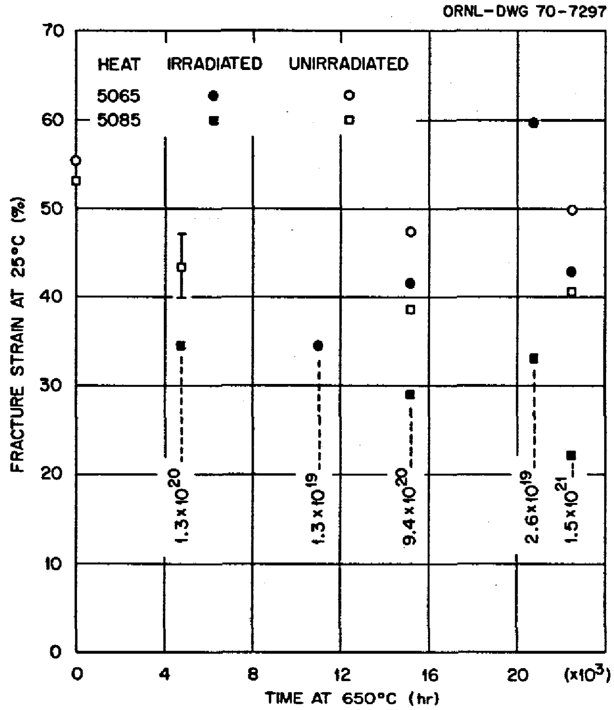

Fig. 18. Variation of the Fracture Strain at 25°C with Annealing Time and Thermal Fluence.

fracture strain. This indicates that irradiation has a role in the embrittlement. We previously showed that the ductility could be recovered by an anneal of 8 hr at 871°C and concluded that the changes must be associated with carbide precipitation.[9] The higher susceptibility of heat 5085 to this type of embrittlement is not understood, since heat 5065 actually has a higher carbon concentration (Table 1, p. 4). The data in Fig. 18 defy extrapolation, so one cannot conclude whether the room temperature embrittlement is likely to become worse.

In these discussions of tensile properties we have emphasized the changes in fracture strain and made little mention of strength changes. Some pertinent data are summarized in Table 7 for heat 5085. The samples were tested at 25 and 650°C and include three histories: (1) as annealed, (2) thermally aged, and (3) irradiated. The changes in yield strength are likely significant, but the main point is that they are

[9]H. E. McCoy, An Evaluation of the Molten-Salt Reactor Experiment Hastelloy N Surveillance Specimen — Third Group, ORNL-TM-2647 (1970), p. 17.

Table 7. Comparison of the Tensile Properties of Heat 5085 Before and After Irradiation[a]

Heat Treatment	Yield Stress, psi		Ultimate Tensile Stress, psi		Fracture Strain, %	
	at 25°C	at 650°C	at 25°C	at 650°C	at 25°C	at 650°C
Annealed 2 hr at 900°C	51,500	29,600	120,900	75,800	53.1	33.7
Annealed 2 hr at 900°C and aged 22,533 hr at 650°C	48,100	32,600	108,500	75,200	40.6	32.0
Annealed 2 hr at 900°C, irradiated for 22,533 hr at 650°C to a thermal fluence of 1.5×10^{21} neutrons/cm^2	53,900	36,400	89,000	50,800	22.1	9.3

[a]Strain rate of 0.05 min^{-1}.

small considering the long thermal history of 22,533 hr. The ultimate tensile strength is reduced due to the lower fracture strain and the resulting fact that the test is interrupted before it reaches the high ultimate strength noted for the as-annealed material. Similar results are shown in Table 8 for heat 5065. The yield strength is increased by aging, but the main effects are on the fracture strains and the ultimate tensile strengths.

Table 8. Comparison of the Tensile Properties of Heat 5065 Before and After Irradiation[a]

Heat Treatment	Yield Stress, psi		Ultimate Tensile Stress, psi		Fracture Strain, %	
	at 25°C	at 650°C	at 25°C	at 650°C	at 25°C	at 650°C
Annealed 2 hr at 900°C	56,700	32,100	126,400	81,200	55.3	34.3
Annealed 2 hr at 900°C and aged 22,533 hr at 650°C	61,200	41,500	126,500	81,900	49.8	26.8
Annealed 2 hr at 900°C, irradiated for 22,533 hr at 650°C to a thermal fluence of 1.5×10^{21} neutrons/cm^2	56,700	39,700	109,500	52,100	42.8	6.2

[a]Strain rate of 0.05 min^{-1}.

The results of creep-rupture tests on heats 5085 and 5065 from the fourth group of surveillance samples are summarized in Tables 9 and 10. The results are most interesting when they are compared with those obtained on previous groups of surveillance samples so that the progressive changes in properties can be noted. The stress-rupture properties of heat 5085 are shown in Fig. 19. The rupture lives of the last group of samples (1.5×10^{21} thermal neutrons/cm^2) are not detectably different from those irradiated previously to a thermal fluence of 9.4×10^{20} neutrons/cm^2. In the unirradiated condition, the rupture lives for the samples aged 22,533 hr are slightly less than in the as-annealed condition, but greater than those observed for samples aged for lesser times.

Table 9. Creep-Rupture Tests on Heat 5085 at 650°C

Test Number	Specimen Number	Stress (psi)	Rupture Life (hr)	Rupture Strain (%)	Reduction in Area (%)	Minimum Creep Rate (%/hr)
			Unirradiated[a]			
7978	10406	55,000	22.1	21.0	23.4	0.288
7897	10415	40,000	500.1	24.5	28.5	0.0299
7896[b]	10414	32,400	2500.7	12.7	9.4	0.0045
7895[b]	10413	27,000	2187.1	5.40	5.40	0.0026
7894[b]	10412	21,500	2064.9	2.10	2.44	0.0011
7893[b]	10411	17,000	2000.0	1.1	0	0.0007
			Irradiated[c]			
R-969	8811	40,000	0.6	1.1		0.78
R-958	8810	32,400	31.6	0.54		0.0067
R-956	8809	27,000	60.2	0.57		0.0055
R-957	8808	21,500	362.0	0.63		0.0010
R-964	8807	17,000	426.4	0.69		0.0004

[a]Annealed 2 hr at 900°C, exposed to static barren fuel salt for 22,533 hr at 650°C.

[b]Discontinued prior to failure.

[c]Annealed 2 hr at 900°C, exposed to MSRE core for 22,533 hr at 650°C, received thermal fluence of 1.5×10^{21} neutrons/cm^2.

Table 10. Creep-Rupture Tests on Heat 5065 at 650°C

Test Number	Specimen Number	Stress (psi)	Rupture Life (hr)	Rupture Strain (%)	Reduction in Area (%)	Minimum Creep Rate (%/hr)
			Unirradiated[a]			
7978	10406	55,000	22.1	21.0	23.4	0.34
7892	10388	40,000	651.2	36.3	29.9	0.0331
7891	10387	32,400	2144.3	44.7	37.7	0.0096
7890[b]	10386	27,000	2187.1	8.8	7.4	0.0040
7889[b]	10385	21,500	2373.3	3.6	2.2	0.0013
7888[b]	10384	17,000	2000.0	2.8	0	
			Irradiated[c]			
R-966	8838	40,000	0			
R-962	8836	32,400	22.7	0.25		0.0075
R-954	8836	27,000	40.5	0.44		0.0061
R-960	8835	21,500	46.2	0.47		0.0051
R-963	8834	17,000	1567.3	0.86		0.0004

[a]Annealed 2 hr at 900°C, exposed to static barren fuel salt for 22,533 hr at 650°C.

[b]Discontinued prior to failure.

[c]Annealed 2 hr at 900°C, exposed to MSRE core for 22,533 hr at 650°C, received thermal fluence of 1.5×10^{21} neutrons/cm^2.

The minimum creep rates are shown as a function of stress in Fig. 20 for heat 5085. As noted previously, neither irradiation nor aging has a detectable effect on the creep rate. The data deviate from the line shown in Fig. 20 at both extremes. At high stresses, the irradiated samples fail at such low strains that a minimum creep rate is not established over long enough period for measurement. At low stress levels the data deviate due to the semilog plot.

The fracture strain is the parameter most affected by irradiation, and a variation of this parameter with minimum creep rate is shown in Fig. 21 for heat 5085 at 650°C. There has been a continual deterioration of the fracture strain with increasing thermal fluence.

Tensile and creep tests were run at 650°C at several different strain rates and stresses. The fracture strains from these tests are plotted together in Fig. 22 although different parameters are controlled

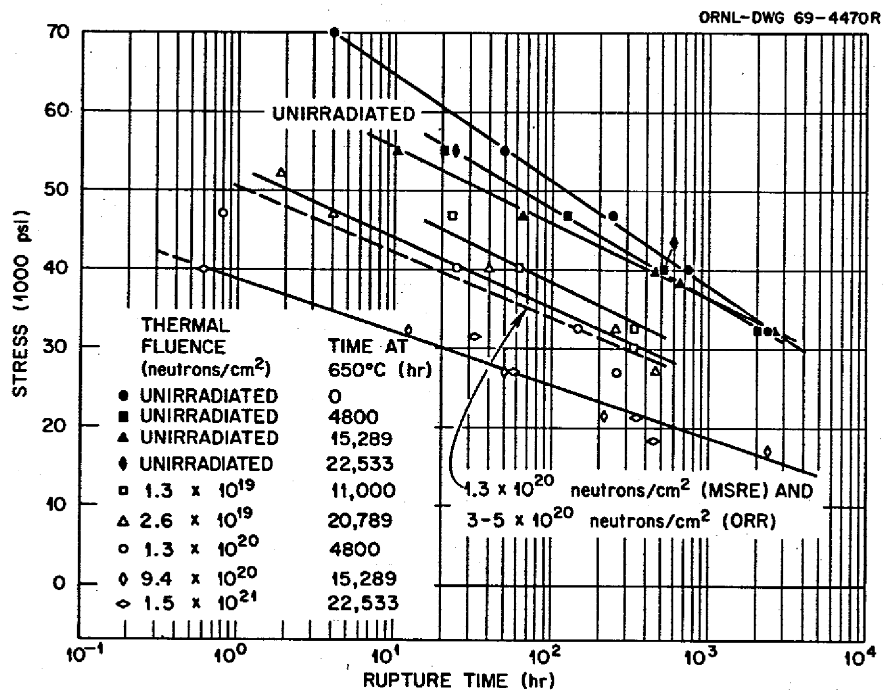

Fig. 19. Postirradiation Stress-Rupture Properties of MSRE Surveillance Specimens (Heat 5085) at 650°C.

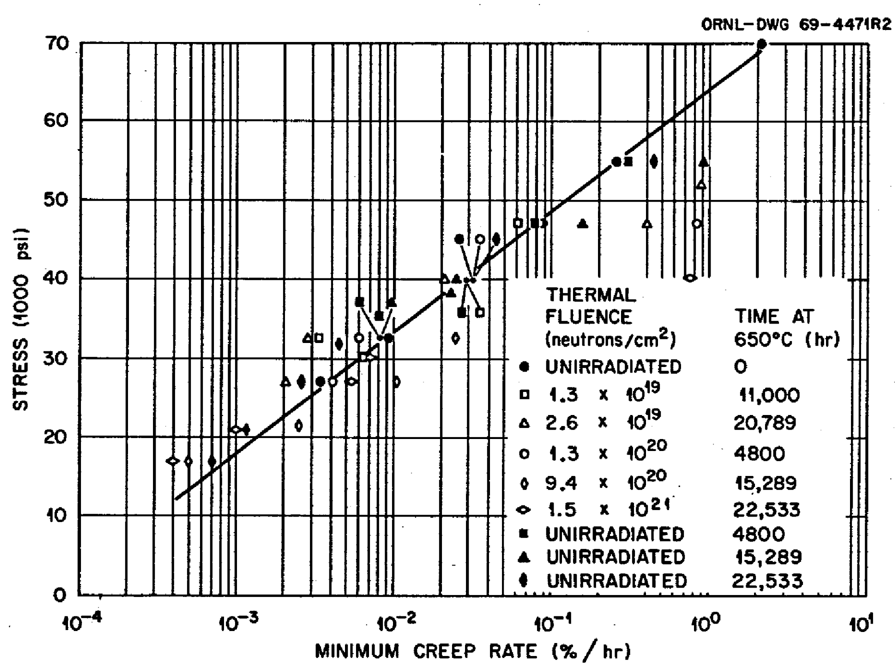

Fig. 20. Minimum Creep Rate of Hastelloy N (Heat 5085) Surveillance Specimens from the MSRE at 650°C.

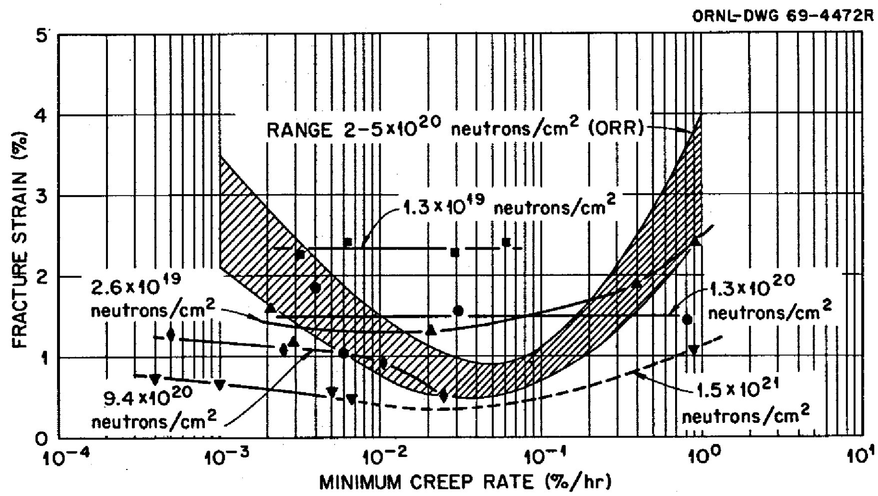

Fig. 21. Variation of Fracture Strain with Strain Rate for Hastelloy N (Heat 5085) Surveillance Specimens at 650°C.

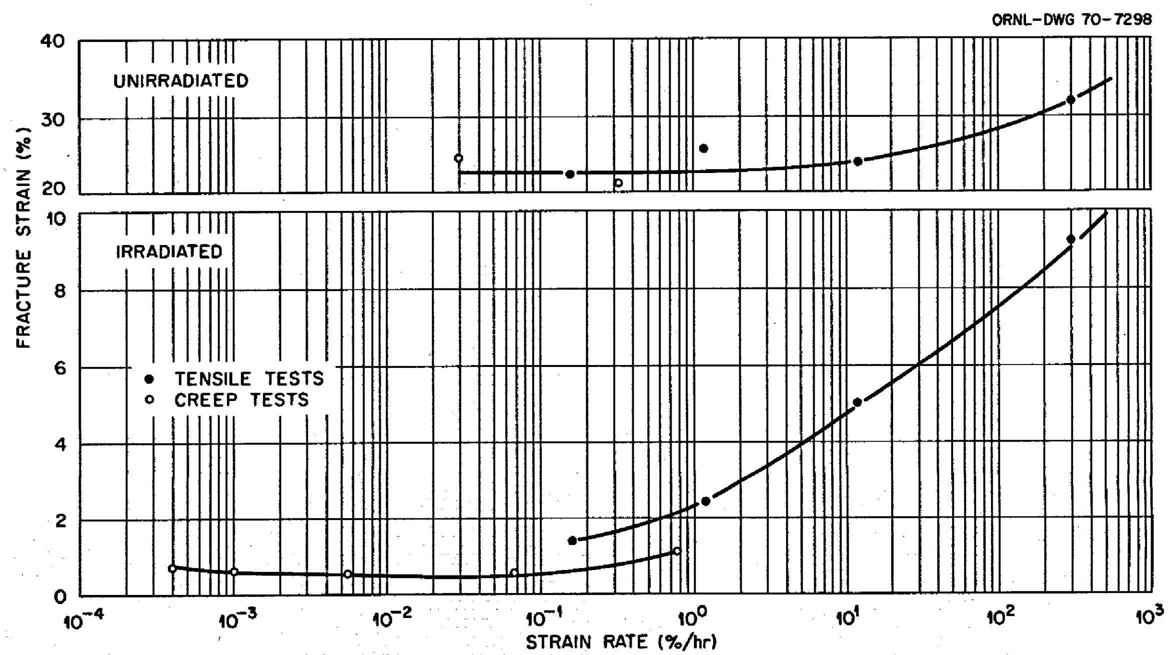

Fig. 22. Fracture Strain at 650°C of Heat 5085 in the Unirradiated and Irradiated Conditions. Irradiated to a thermal fluence of 1.5×10^{21} neutrons/cm^2 over a period of 22,533 hr at 650°C.

in the two types of tests. The most striking feature is the marked dependence of the fracture strain of the irradiated samples on the strain rate and the rather weak dependence of the fracture strains of the unirradiated samples on the strain rate. The irradiated samples at this high fluence level show a general decrease in fracture strain with decreasing strain rate, with a possible slight increase in fracture strain at very low strain rates.

The sensitivity of the fracture strain of heat 5085 at 650°C to the helium content is illustrated in Fig. 23 for three strain rates. This material contains 38 ppm B (Table 1, p. 4) that can yield an equivalent amount of helium when transmuted. (Several factors contribute to the relationship that 1 ppm of natural boron by weight leads to 1.1 ppm He on an atomic basis.) The points shown in Fig. 23 all come from surveillance samples from the MSRE. The two higher strain rates are obtained by tensile testing, and the fracture strain decreases with increasing helium content. The 0.1% strain rate is the creep rate that corresponds to the lowest fracture strain (Fig. 21). The fracture strain drops abruptly with the presence of 1 ppm He and then decreases gradually with increasing helium content.

The creep properties of heat 5065 are illustrated in a series of graphs similar to that just presented for heat 5085. The stress-rupture properties at 650°C are shown in Fig. 24 for heat 5065. The rupture

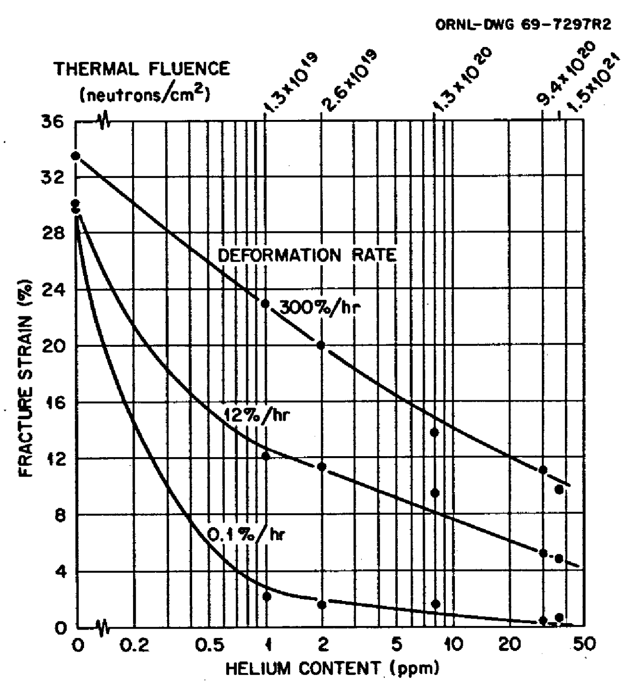

Fig. 23. Variation of the Fracture Strain with Calculated Helium Content and Strain Rate for Hastelloy N (Heat 5085) at 650°C.

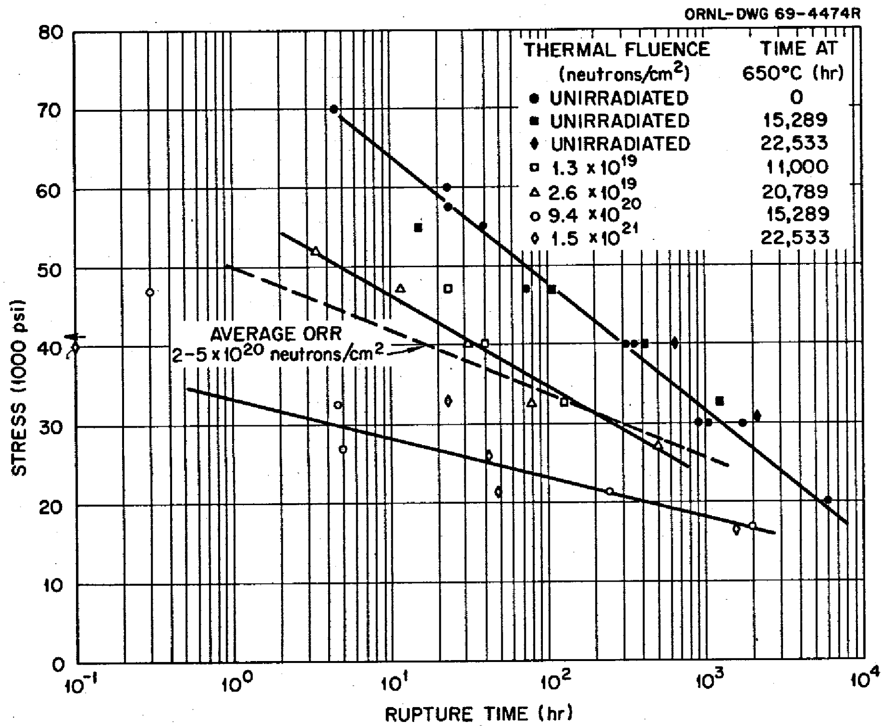

Fig. 24. Stress-Rupture Properties of MSRE Surveillance Specimens (Heat 5065) at 650°C.

times are equivalent for the samples irradiated to the two highest fluences. The rupture times are also quite comparable with those shown in Fig. 19 for heat 5085. The unirradiated samples that were aged for 22,533 hr at 650°C in static barren fuel salt have longer rupture lives than the as-received material. The minimum creep rates are shown in Fig. 25 and show a lack of sensitivity to any of the variables being studied. The fracture strain is shown as a function of strain rate in Fig. 26. The fracture strain decreases with increasing fluence up to the two highest fluence levels, where the strains are about equivalent. This heat of material shows a ductility minimum with the fracture strain increasing slightly with decreasing creep rate except for the samples showing the lowest fluence.

The tensile and creep test results for heat 5065 have been combined in Fig. 27. These results again show the marked dependence of the fracture strain on the strain rate for the irradiated material. A comparison with the similar plot for heat 5085 (Fig. 22) reveals some slight differences in the fracture strains of the two heats, but shows generally

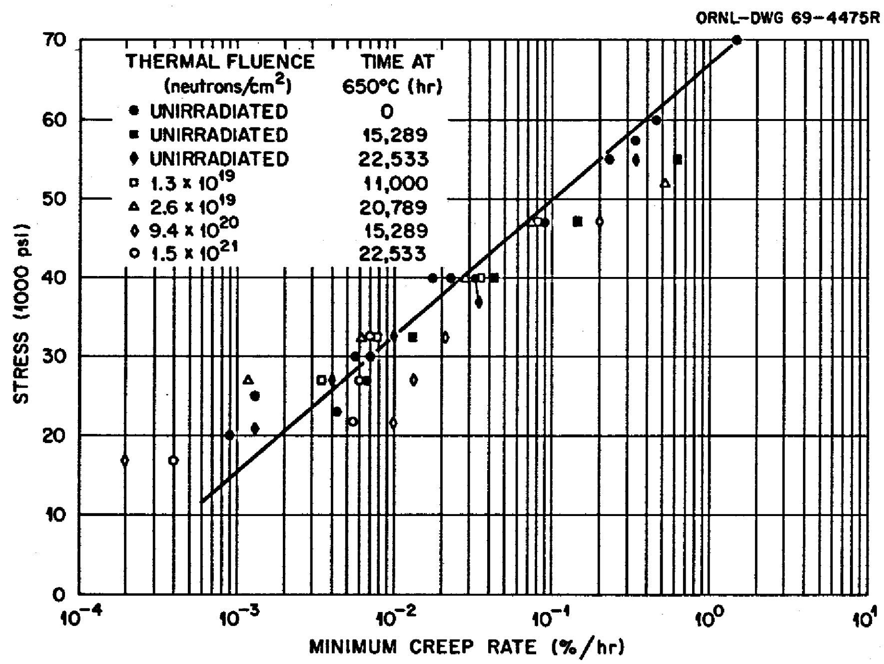

Fig. 25. Minimum Creep Rate of Hastelloy N (Heat 5065) Surveillance Samples from the MSRE at 650°C.

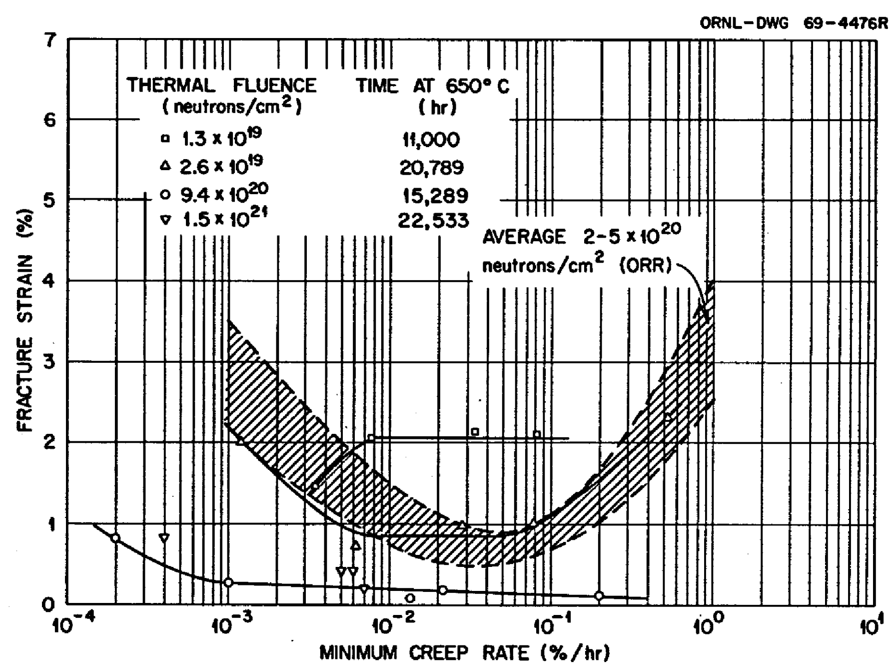

Fig. 26. Variation of Fracture Strain with Strain Rate for Hastelloy N (Heat 5065) Surveillance Specimens at 650°C.

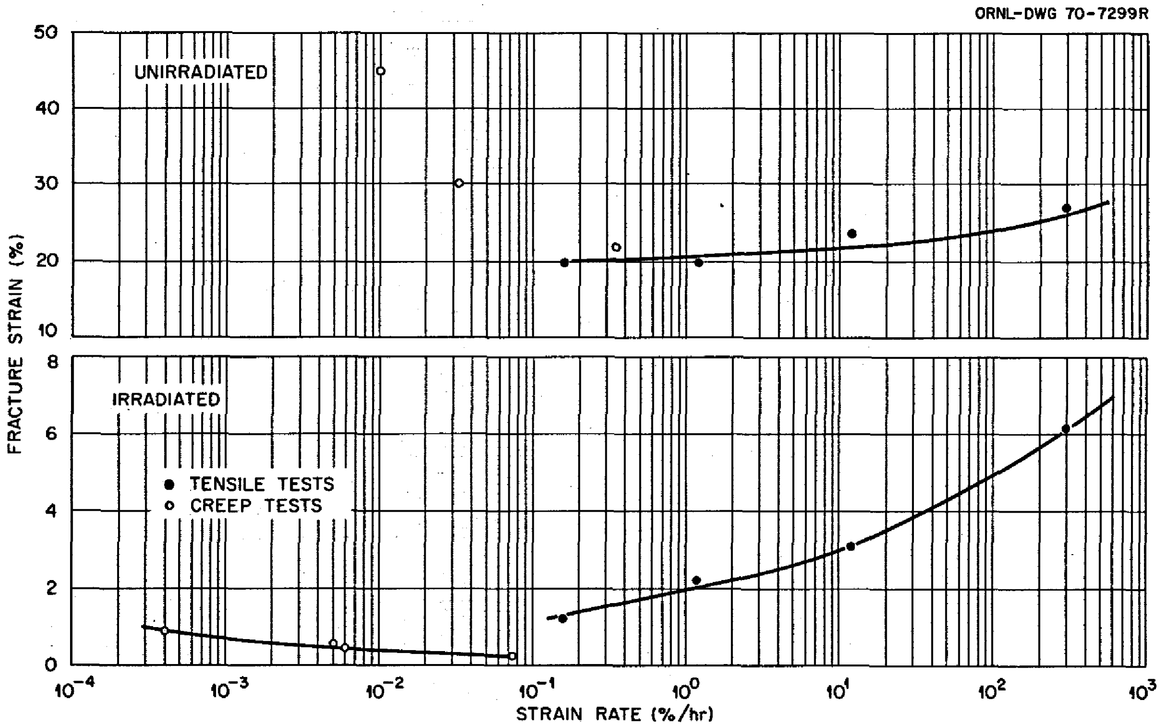

Fig. 27. Fracture Strains at 650°C of Heat 5065 in the Unirradiated and the Irradiated Conditions. Irradiated to a thermal fluence of 1.5×10^{21} neutrons/cm^2 over a period of 22,533 hr at 650°C.

that the two heats respond to irradiation quite similarly. Heat 5065 contains about 23 ppm B (average of the four values in Table 1, p. 4), and the variation of the fracture strain with helium content is shown in Fig. 28. The behavior is quite similar to that noted in Fig. 23 for heat 5085. Thus, the lower boron (and hence helium) concentration in heat 5065 results in about the same properties as the higher boron level in heat 5085.

Mechanical Property Data — Modified Hastelloy N

Two heats of modified Hastelloy N were exposed to the MSRE core for 6244 hr at 650°C and received a thermal neutron fluence of 5.1×10^{20} neutrons/cm^2 (Table 2, p. 6). Both of these alloys were modified with titanium — heat 7320 contained 0.65% and heat 67-551 contained 1.1%.

The tensile properties of heat 7320 are summarized in Tables 11 and 12 for the control and irradiated samples, respectively. The fracture

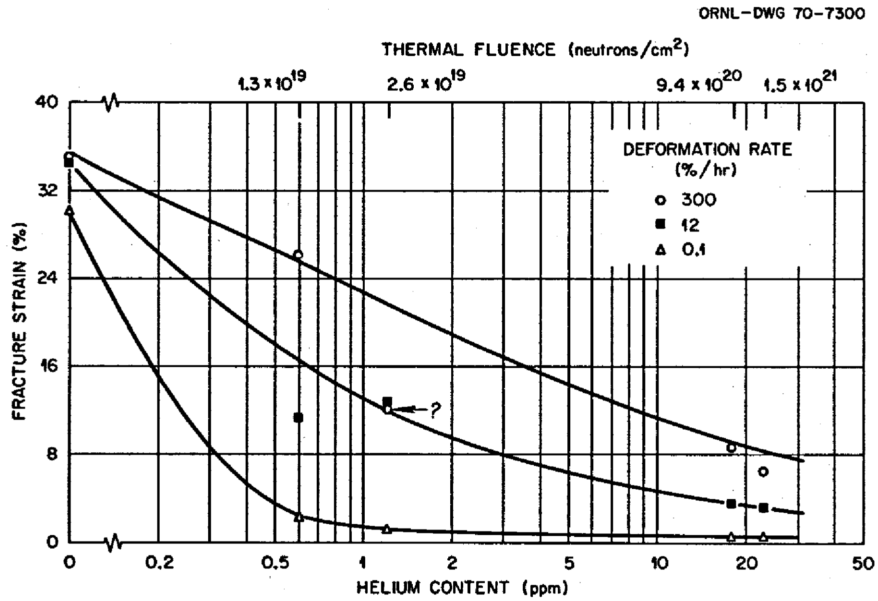

Fig. 28. Variation of Fracture Strain at 650°C with Calculated Helium Content and Strain Rate for Heat 5065.

Table 11. Results of Tensile Tests on Control Samples of Heat 7320[a]

Specimen Number	Test Temperature (°C)	Strain Rate (min^{-1})	Stress, psi Yield	Stress, psi Ultimate Tensile	Elongation, % Uniform	Elongation, % Total	Reduction in Area (%)	True Fracture Strain (%)
9464	25	0.05	68,800	122,600	48.2	49.7	40.83	52
9482	200	0.05	60,000	107,600	40.6	41.9	43.75	58
9470	400	0.05	56,600	103,300	46.9	49.1	43.09	56
9481	400	0.002	54,100	96,000	45.2	46.2	40.64	52
9472	500	0.05	54,500	99,200	47.9	51.1	44.38	59
9456	500	0.002	53,600	96,700	45.1	46.2	41.21	53
9467	550	0.05	51,700	95,500	49.2	52.0	45.39	61
9466	550	0.002	49,400	85,300	36.7	37.7	32.99	40
9458	600	0.05	52,500	91,900	41.4	45.5	41.11	53
9476	600	0.002	54,800	80,500	18.2	19.7	23.35	27
9478	650	0.05	49,300	78,600	28.4	30.6	36.67	46
9461	650	0.002	47,700	72,800	14.5	15.5	19.46	22
9475	650	0.0002	50,800	67,900	12.3	13.7	14.40	16
9474	650	0.000027	47,800	59,100	5.6	9.6	13.88	15
9477	760	0.05	50,100	71,500	12.0	13.1	11.69	12
9480	760	0.002	44,200	45,100	4.2	17.2	19.07	21
9471	850	0.05	45,000	48,200	5.6	10.2	12.39	13
9457	850	0.002	27,500	27,800	1.6	10.1	11.97	13

[a]Annealed 1 hr at 1177°C and exposed to a vessel of static barren fuel salt for 7244 hr at 650°C.

Table 12. Postirradiation Tensile Properties of Hastelloy N (Heat 7320)[a]

Specimen Number	Test Temperature (°C)	Strain Rate (min^{-1})	Stress, psi		Elongation, %		Reduction in Area (%)	True Fracture Strain (%)
			Yield	Ultimate Tensile	Uniform	Total		
9221	25	0.05	69,800	116,600	43.8	45.2	35.48	44
9222	200	0.05	59,000	102,900	40.7	41.7	35.69	44
9223	400	0.05	54,100	93,500	40.5	41.6	33.09	40
9224	400	0.002	58,200	94,100	38.0	38.7	31.67	38
9225	500	0.05	54,900	89,100	39.1	41.1	36.97	46
9226	500	0.002	55,400	83,300	31.1	32.5	26.61	31
9215	550	0.05	61,100	88,200	26.8	27.6	26.26	30
9214	550	0.002	61,000	74,700	9.2	11.1	21.27	24
9213	600	0.05	60,800	81,700	18.4	19.6	27.74	32
9212	600	0.002	61,700	69,800	4.3	5.5	11.83	13
9211	650	0.05	67,400	74,900	8.0	9.5	7.10	7
9210	650	0.002	57,100	68,500	4.3	5.1	9.08	10
9227	650	0.0002	49,500	58,200	4.3	4.7	7.54	8
9228	650	0.000027	37,500	49,400	2.0	2.9	3.00	3
9209	760	0.05	56,700	63,700	3.8	4.0	6.15	6
9208	760	0.002	48,700	48,900	1.6	3.0	6.15	6
9207	850	0.05	37,900	38,200	1.6	2.2	7.25	8
9206	850	0.002	24,800	24,800	1.0	1.6	2.23	2

[a]Annealed 1 hr at 1177°C. Irradiated to a thermal fluence of 5.1×10^{20} neutrons/cm^2 over a period of 7244 hr at 650°C.

strains are shown as a function of test temperature in Fig. 29. Irradiation reduces the fracture strain over the entire range of test temperatures, but the magnitude of the decrease is much greater at elevated temperatures. The sharp drop in fracture strain with increasing temperature occurs at a lower temperature for the irradiated material. The ratios of the irradiated and unirradiated properties are shown in Fig. 30. The yield stress is higher for the irradiated material over the test temperature range of 550 to 760°C. The ultimate tensile strength is about the same for the irradiated and unirradiated material but shows a gradual decline with increasing test temperature. The fracture strain decreased due to irradiation, with the reduction being about 80% at 850°C.

Some idea of the tensile properties of heat 7320 due to aging and irradiation can be obtained from Table 13. The yield strengths at 25 and 650°C are increased by aging; at a test temperature of 650°C a further increase occurs due to irradiation. The changes in ultimate tensile

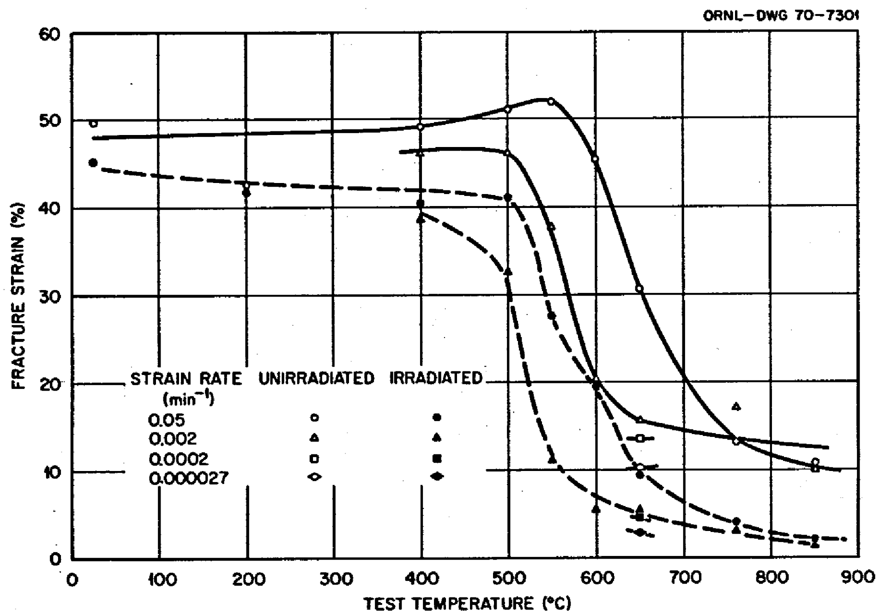

Fig. 29. Fracture Strains of Heat 7320 After Removal from the MSRE and from the Control Facility. All samples annealed 1 hr at 1177°C before irradiation to a thermal fluence of 5.1×10^{20} neutrons/cm^2 over a period of 7244 hr at 650°C.

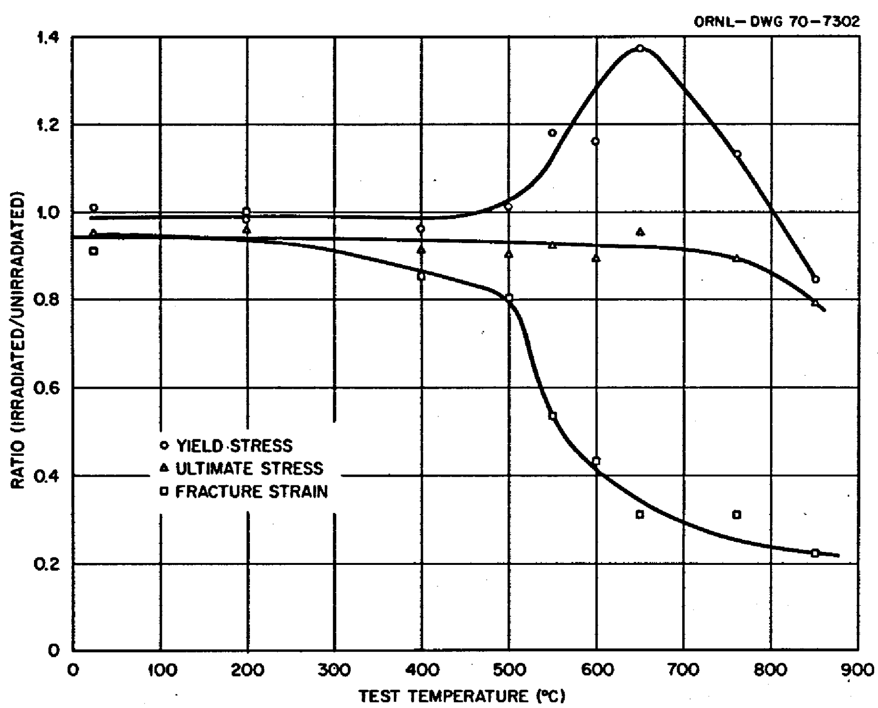

Fig. 30. Comparison of Unirradiated and Irradiated Tensile Properties of Heat 7320 After Irradiation to a Thermal Fluence of 5.1×10^{20} neutrons/cm^2 Over a Period of 7244 hr at 650°C. Tested at a strain rate of 0.05 min^{-1}.

Table 13. Comparison of the Tensile Properties of Heat 7320 Before and After Irradiation[a]

Heat Treatment	Yield Stress, psi at 25°C	Yield Stress, psi at 650°C	Ultimate Tensile Stress, psi at 25°C	Ultimate Tensile Stress, psi at 650°C	Fracture Strain, % at 25°C	Fracture Strain, % at 650°C
Annealed 1 hr at 1177°C	38,500	25,600	107,300	72,700	75.4	53.5
Annealed 1 hr at 1177°C, aged 7244 hr at 650°C	68,800	49,300	122,600	78,600	48.1	30.6
Annealed 1 hr at 1177°C, irradiated for 7244 hr at 650°C to a thermal fluence of 5.1×10^{20} neutrons/cm^2	69,800	67,400	116,600	74,900	45.2	9.5

[a]Tested at a strain rate of 0.05 min^{-1}.

strength are rather small and likely within experimental error. The fracture strain is decreased by aging and by irradiation; the magnitude of the decrease is much larger at the test temperature of 650°C.

The results of tensile tests on the control and irradiated samples of heat 67-551 are given in Tables 14 and 15, respectively. The fracture strain is shown as a function of test temperature in Fig. 31. The fracture strain at low temperatures is not influenced by irradiation, but above 400°C the fracture strain is decreased by irradiation. However, the fracture strains at high temperatures are higher than those for either heat 7320 (Fig. 29) or the standard alloy (Figs. 9 and 11, pp. 18 and 22, respectively). The ratios of the irradiated and unirradiated tensile properties are shown in Fig. 32. The yield stress is generally about 25% lower for the irradiated material. The ultimate tensile strength is reduced only about 10% by irradiation when tested below 550°C, but is reduced up to 30% as the test temperature is increased. The fracture strain is unaffected by irradiation up to test temperatures of 500°C; above this temperature the fracture strain decreases progressively with increasing test temperature. Some values of the tensile properties at 25 and 650°C are given in Table 16. Aging at 650°C seems to increase the yield strength at both 25 and 650°C; however, the strength of the irradiated material is quite close to that of the as-annealed material. The ultimate tensile strength is increased only slightly by aging and

Table 14. Results of Tensile Tests on Control Samples of Heat 67-551[a]

Specimen Number	Test Temperature (°C)	Strain Rate (min^{-1})	Stress, psi		Elongation, %		Reduction in Area (%)	True Fracture Strain (%)
			Yield	Ultimate Tensile	Uniform	Total		
9403	25	0.05	62,400	120,200	50.3	52.3	41.59	54
9419	200	0.05	54,100	108,700	47.5	50.1	45.22	60
9422	400	0.05	52,300	104,300	48.7	50.4	46.66	63
9417	400	0.002	51,400	101,700	50.4	51.5	43.84	58
9506	500	0.05	48,100	89,900	50.4	53.6	46.58	63
9423	500	0.002	50,400	92,100	42.0	43.6	36.67	46
9402	550	0.05	45,200	94,100	52.0	53.7	41.78	54
9418	550	0.002	47,600	80,400	26.3	27.9	31.67	38
9416	600	0.05	42,800	87,800	46.8	49.8	43.09	56
9428	600	0.002	46,200	79,600	23.1	25.3	26.37	31
9410	650	0.05	41,900	84,600	40.4	42.6	37.07	46
9407	650	0.002	42,700	76,300	27.3	31.5	25.42	29
9426	650	0.0002	46,000	74,800	22.3	30.2	28.87	34
9415	650	0.000027	39,900	60,900	11.9	21.7	23.23	26
9424	760	0.05	45,600	78,000	21.6	28.8	28.87	34
9421	760	0.002	43,000	45,200	5.5	36.2	33.98	42
9425	850	0.05	41,300	51,000	6.2	23.6	26.14	30
9420	850	0.002	25,500	26,200	2.3	22.4	18.81	21

[a]Annealed 1 hr at 1177°C prior to exposure to a vessel of static barren fuel salt for 7244 hr at 650°C.

Table 15. Postirradiation Tensile Properties of Hastelloy N (Heat 67-551)[a]

Specimen Number	Test Temperature (°C)	Strain Rate (min^{-1})	Stress, psi		Elongation, %		Reduction in Area (%)	True Fracture Strain (%)
			Yield	Ultimate Tensile	Uniform	Total		
9167	25	0.05	49,600	107,800	50.6	51.0	36.87	46
9168	200	0.05	39,800	94,700	50.0	53.2	42.15	55
9169	400	0.05	39,200	91,800	48.7	50.7	38.44	49
9175	400	0.002	40,400	88,100	51.3	52.6	39.69	51
9176	500	0.05	37,000	83,400	52.1	52.9	38.34	48
9172	500	0.002	37,000	67,900	25.8	27.4	29.21	35
9161	550	0.05	34,500	80,400	42.8	44.5	34.92	43
9160	550	0.002	39,500	57,100	14.7	17.0	23.35	27
9159	600	0.05	37,000	71,300	31.9	33.9	39.59	50
9158	600	0.002	41,900	61,800	18.0	19.2	22.68	26
9157	650	0.05	31,300	56,600	20.7	22.6	28.76	34
9156	650	0.002	31,200	53,300	16.0	16.9	19.20	21
9173	650	0.0002	35,100	57,100	12.3	14.5	13.74	15
9174	650	0.000027	34,800	51,300	7.5	12.9	12.5	13
9155	760	0.05	29,700	51,500	13.8	14.8	8.79	9
9154	760	0.002	29,200	38,400	5.7	9.2	10.74	11
9153	850	0.05	26,700	34,700	4.8	6.5	7.54	8
9152	850	0.002	22,300	22,700	2.2	6.2	5.24	5

[a]Annealed 1 hr at 1177°C. Irradiated to a thermal fluence of 5.1×10^{20} neutrons/cm^2 over a period of 7244 hr at 650°C.

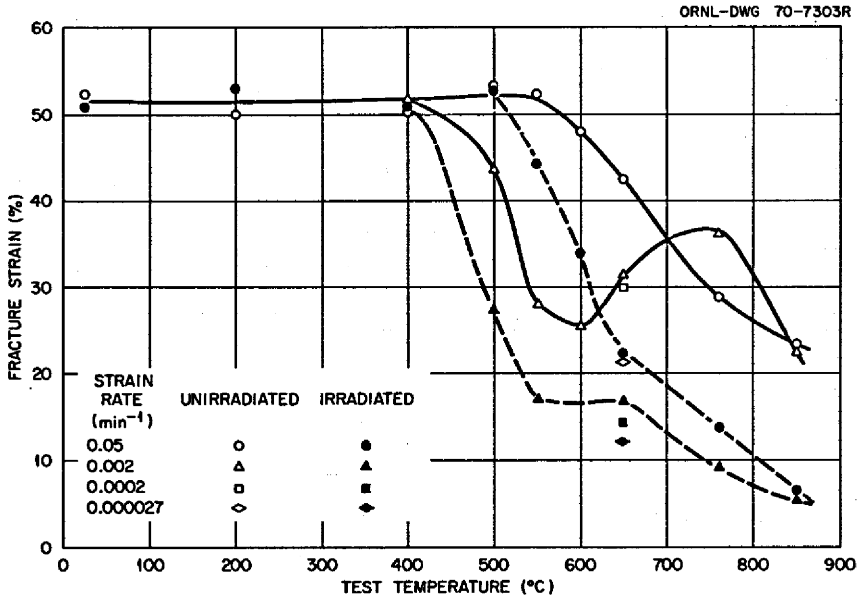

Fig. 31. Fracture Strains of Heat 67-551 After Removal from the MSRE and from the Control Facility. All samples annealed 1 hr at 1177°C before irradiation to a thermal fluence of 5.1 × 10^{20} neutrons/cm^2 over 7244 hr at 650°C.

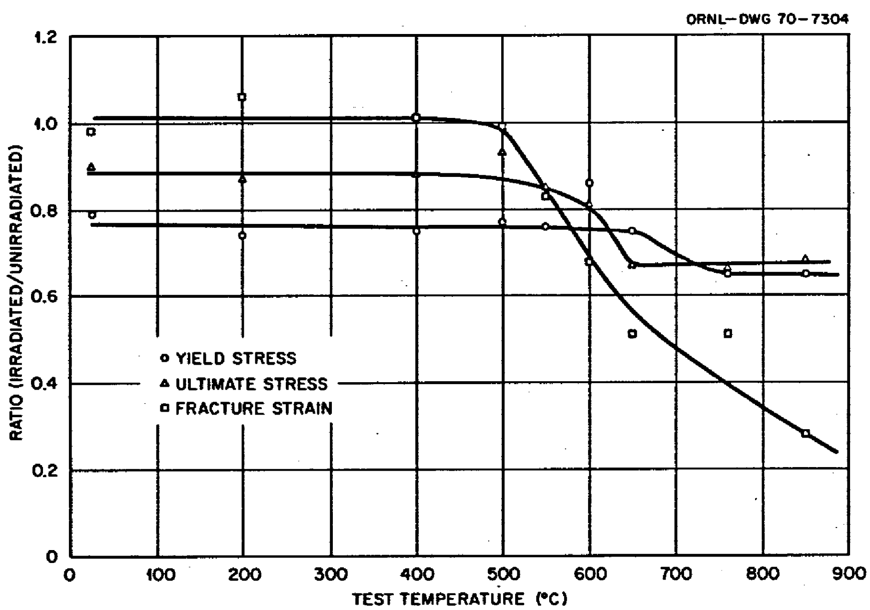

Fig. 32. Comparison of Unirradiated and Irradiated Tensile Properties of Heat 67-551 After Irradiation to a Thermal Fluence of 5.1 × 10^{20} neutrons/cm^2 over a period of 7244 hr at 650°C. Tested at a strain rate of 0.05 min^{-1}.

Table 16. Comparison of the Tensile Properties of Heat 67-551 Before and After Irradiation[a]

Heat Treatment	Yield Stress, psi		Ultimate Tensile Stress, psi		Fracture Strain, %	
	at 25°C	at 650°C	at 25°C	at 650°C	at 25°C	at 650°C
Annealed 1 hr at 1177°C	44,600	26,900	113,600	78,900	79.6	57.3
Annealed 1 hr at 1177°C, aged 7244 hr at 650°C	62,400	41,900	120,200	84,600	52.3	42.6
Annealed 1 hr at 1177°C, aged 7244 hr at 650°C, irradiated to a thermal fluence of 5.1×10^{20} neutrons/cm^2	49,600	31,300	107,800	56,600	51.0	22.6

[a]Tested at a strain rate of 0.05 min^{-1}.

decreased by irradiation. At 25°C the fracture strain is reduced from 79.6% to 52.3% by aging, and irradiation does not cause any further change. At 650°C the fracture strain is decreased by aging and decreased further by irradiation.

The creep-rupture properties of heat 7320 are summarized in Table 17. These results are compared in Figs. 33, 34, and 35 with those for unirradiated samples that were given a pretest anneal of 1 hr at 1177°C. The stress-rupture properties in Fig. 33 show that the aging treatment given the controls, 7244 hr at 750°C, increased the rupture life. The irradiated samples failed after longer times than did the unirradiated samples that were simply annealed 1 hr at 1177°C, but ruptured in shorter times than the control samples. However, the minimum creep rates shown in Fig. 34 seem to fall within a common scatter band for all conditions. Thus, neither irradiation nor aging seems to have a detectable effect on the minimum creep rate. The fracture strain is shown as a function of strain rate in Fig. 35. The fracture strains of the unirradiated samples vary from about 30% in a tensile test to about 10% in a long-term creep test. The irradiated samples have lower fracture strains that vary from 9.5% for the fastest tensile test to 2 to 3% for creep tests.

Table 17. Creep-Rupture Tests on Heat 7320 at 650°C

Test Number	Specimen Number	Stress (psi)	Rupture Life (hr)	Rupture Strain (%)	Reduction in Area (%)	Minimum Creep Rate (%/hr)
		Unirradiated — Annealed 1 hr at 1177°C prior to test				
7013	7276	55,000	4.7	28.7	29.6	0.190
7425	10329	50,000	11.5	21.2	28.3	0.125
7014	7277	47,000	49.9	21.8	31.3	0.0194
7016	7279	43,000	103.4	18.1	20.5	0.0069
7015	7278	40,000	384.6	16.3	17.6	0.0059
7424	10252	35,000	1602.1	27.3	30.6	0.0056
7017	7280	30,000	1949.5	10.9	19.9	0.0017
		Unirradiated Controls[a]				
7885	9462	55,000	32.5	14.2	32.9	0.25
7991	9468	47,000	224.1	15.3	26.3	0.045
7886	9463	40,000	653.7	17.9	29.3	0.019
7887	9465	40,000	501.9	7.9	21.4	0.015
7884[b]	9460	32,400	2420.2	6.9	4.8	0.0006
		Irradiated[c]				
R-1151	9204	63,000	1.7	12.2[d]		1.2
R-1016	9216	63,000	4.0	2.0		0.44
R-951	9217	55,000	12.3	2.7		0.20
R-955	9219	47,000	95.1	2.3		0.018
R-967	9218	40,000	329.9	3.2		0.0074
R-950	9220	32,400	2083.3	3.1		0.0058

[a]Annealed 1 hr at 1177°C and exposed to a vessel of static barren fuel salt for 7244 hr at 650°C.

[b]Discontinued prior to failure.

[c]Annealed 1 hr at 1177°C. Irradiated to a thermal fluence of 5.1×10^{20} neutrons/cm^2 over a period of 7244 hr at 650°C.

[d]Test loaded so that strain on loading was included. All other tests did not include this strain.

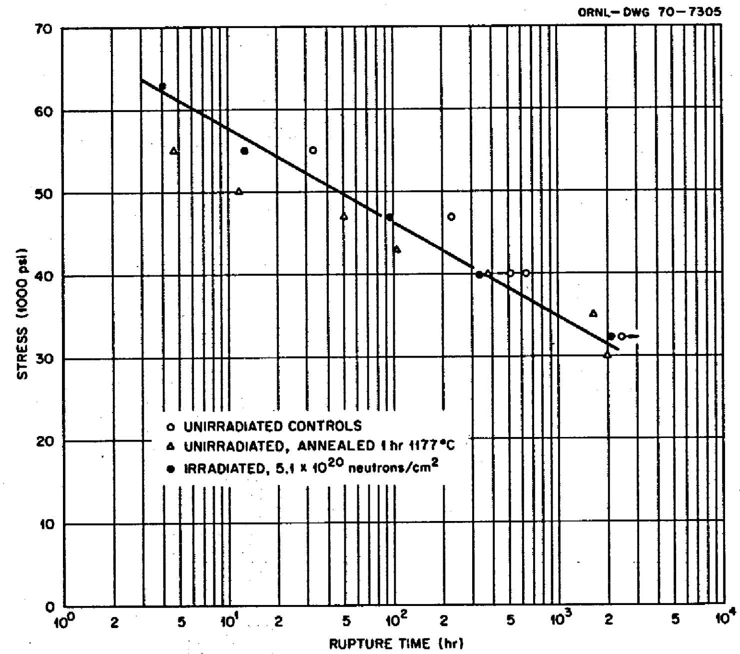

Fig. 33. Stress-Rupture Properties of Heat 7320 at 650°C.

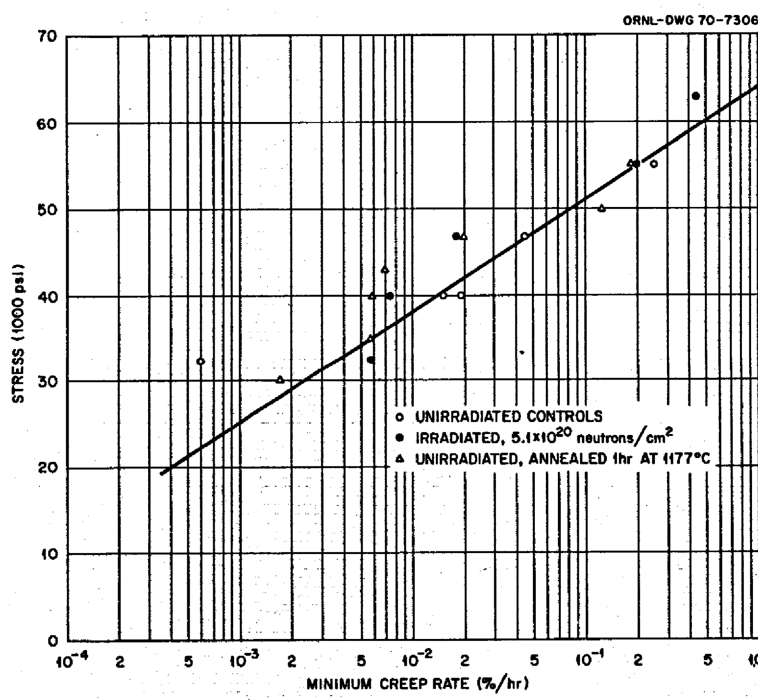

Fig. 34. Creep Properties at 650°C of Heat 7320.

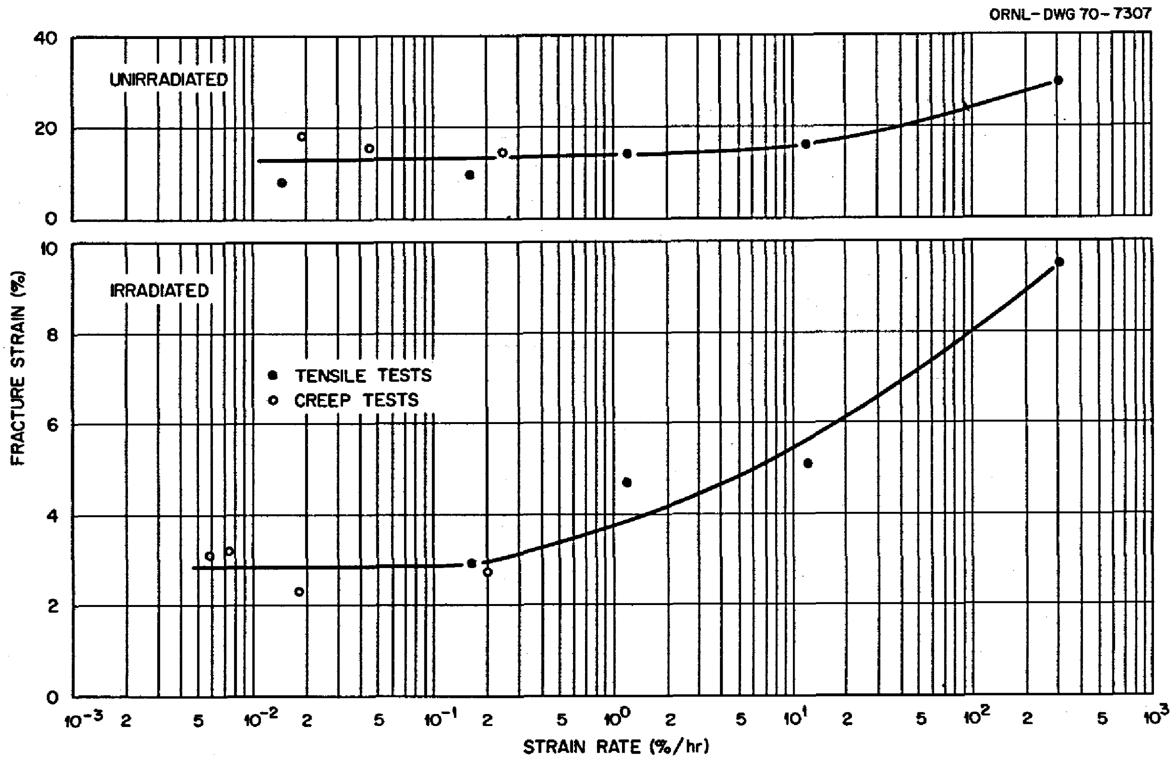

Fig. 35. Fracture Strains at 650°C of Heat 7320 in the Unirradiated and Irradiated Conditions. Irradiated to a thermal fluence of 5.1×10^{20} neutrons/cm^2 over a period of 7244 hr at 650°C.

The results of creep-rupture tests on heat 67-551 with 1.1% Ti are given in Table 18. The stress-rupture properties of the control and irradiated samples are compared in Fig. 36 for 650°C. The irradiated samples generally fail in slightly shorter times than the unirradiated samples. The minimum creep rate seems to be unaffected by irradiation, although there are two data points that seem to be anomalous (Fig. 37). The fracture strains of this alloy (Fig. 38) are higher in both the unirradiated and irradiated conditions than those for heat 7320. The fracture strains of the unirradiated samples varied over the range of 43 to 25% and those of the irradiated samples varied from 22.6 to 5.8% over the range of strain rates studied.

One heat of modified Hastelloy N containing 0.49% Hf (heat 67-504) was exposed to the cell environment for 17,033 hr at 650°C. The thermal fluence was 2.5×10^{19} neutrons/cm^2. This same heat of material was included previously in our surveillance program and was exposed to a

Table 18. Results of Creep-Rupture Tests on Heat 67-551 at 650°C

Test Number	Specimen Number	Stress (psi)	Rupture Life (hr)	Rupture Strain (%)	Reduction in Area (%)	Minimum Creep Rate (%/hr)
			Unirradiated, Annealed 1 hr at 1177°C before testing			
7872	6889	55,000	14.2	29.5	33.2	0.32
7871	6884	47,000	143.8	33.6	26.0	0.071
			Unirradiated Controls[a]			
7882	9409	55,000	44.7	25.5	28.5	0.190
7880	9404	47,000	271.2	29.1	29.6	0.067
7883	9411	40,000	956.2	30.4	25.5	0.018
7881	9408	32,400	2034.9	25.2	29.9	0.0053
			Irradiated[b]			
R-1150	9150	63,000	0.9	20.8[c]		2.2
R-1036	9151	63,000	0.6	2.2		2.6
R-949	9162	55,000	50.5	5.8		0.079
R-961	9165	47,000	117.1	8.3		0.058
R-948	9164	40,000	746.9	9.1		0.0079
R-947	9163	32,400	1485.6	12.5		0.0053

[a]Annealed 1 hr at 1177°C prior to exposure to a vessel of static barren fuel salt for 7244 hr at 650°C.

[b]Annealed 1 hr at 1177°C. Irradiated to a thermal fluence of 5.1×10^{20} neutrons/cm^2 over a period of 7244 hr at 650°C.

[c]Test loaded to include strain on loading. All other tests did not include this strain.

thermal fluence of 5.3×10^{20} neutrons/cm^2 while being at temperature in the core for 9789 hr (ref. 10). In the group of samples presently being discussed, there were two rods of heat 67-504. Two heats of material should have been involved, but postirradiation chemical analysis revealed that both rods were made of the same material. This was not discovered until after many of the samples were tested, so we have several tests under duplicate conditions.

[10]H. E. McCoy, An Evaluation of the Molten-Salt Reactor Experiment Hastelloy N Surveillance Specimen — Third Group, ORNL-TM-2647 (1970).

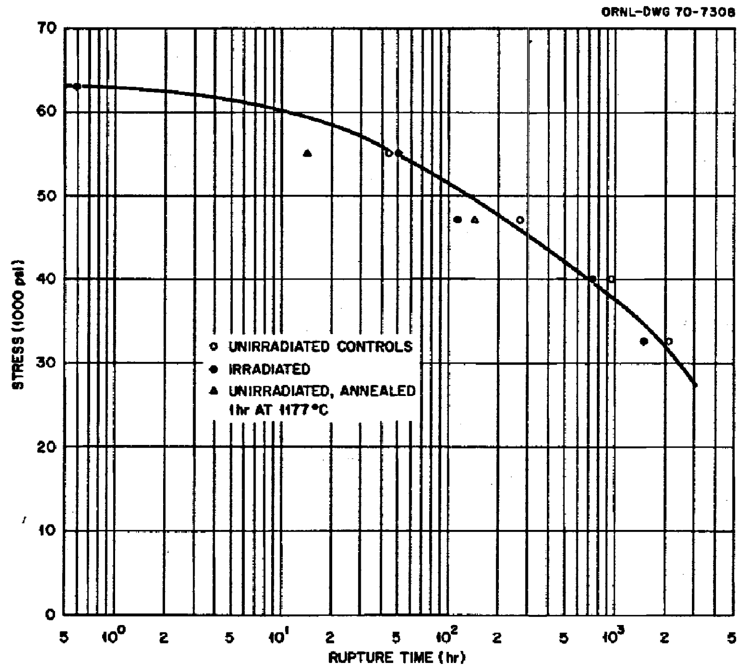

Fig. 36. Stress-Rupture Properties at 650°C of Heat 67-551. Irradiated to a thermal fluence of 5.1×10^{20} neutrons/cm^2 over a period of 7244 hr.

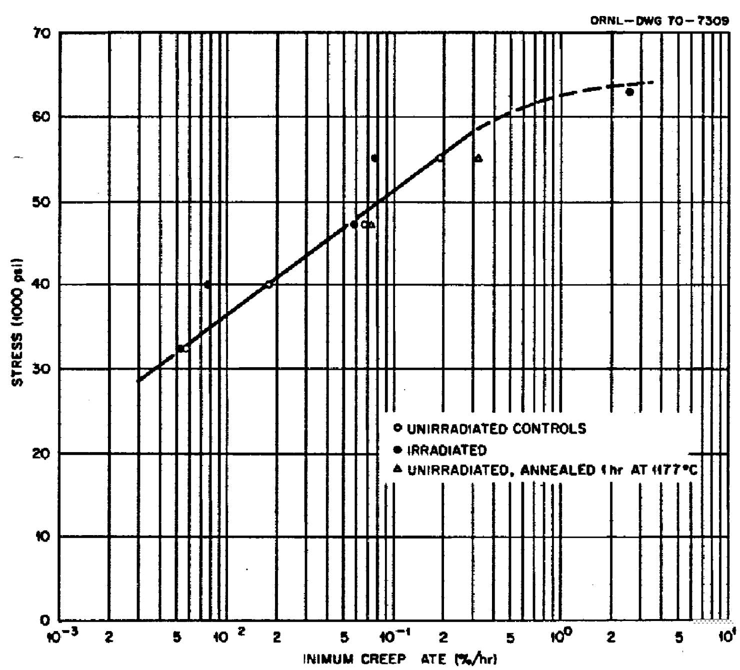

Fig. 37. Creep-Rupture Properties at 650°C of Heat 67-551. Irradiated to a thermal fluence of 5.1×10^{20} neutrons/cm^2 over a period of 7244 hr at 650°C.

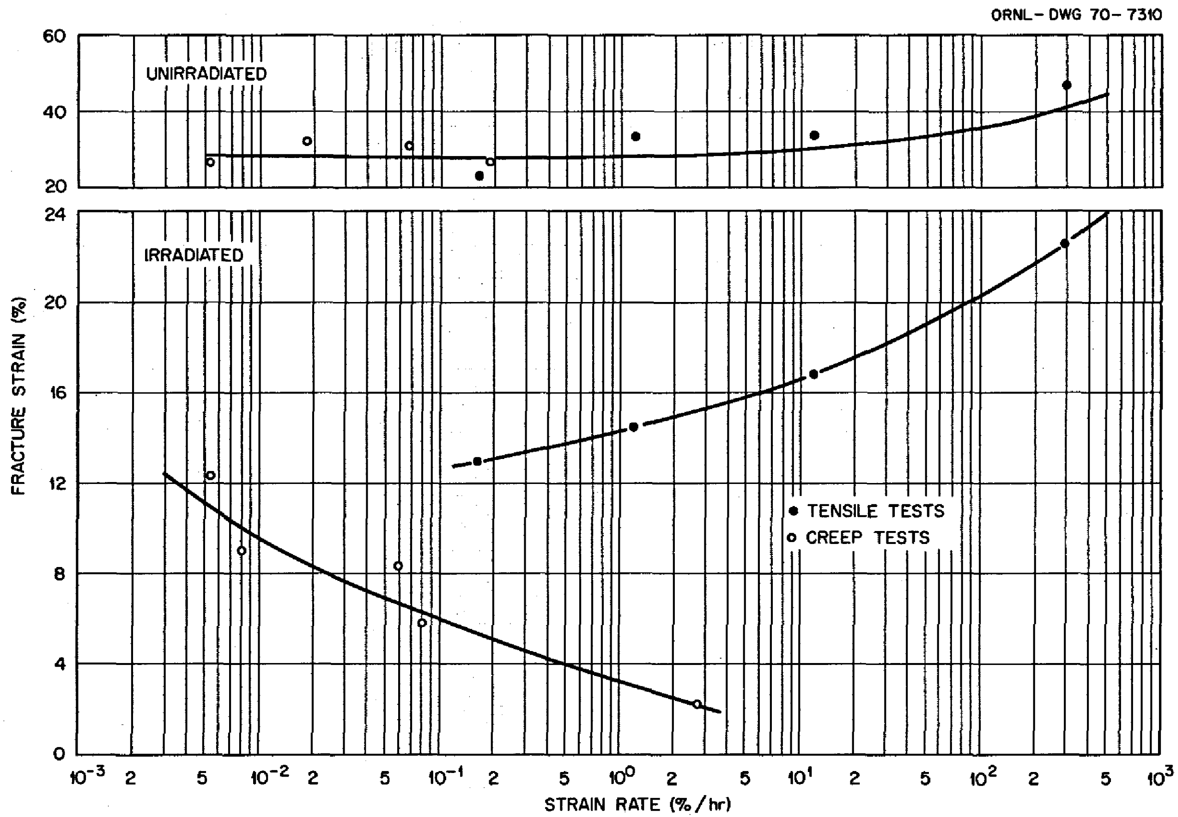

Fig. 38. Comparison of the Fracture Strains of Unirradiated and Irradiated Heat 67-551 at 650°C. Irradiated to a thermal fluence of 5.1×10^{20} neutrons/cm^2 over a period of 7244 hr at 650°C.

The results of the postirradiation tensile tests on heat 67-504 are given in Table 19. The postirradiation fracture strains are shown in Fig. 39 as a function of temperature and strain rate. The fracture strain generally decreases with increasing temperature above about 400°C and with decreasing strain rate. The results from the present tests and those reported previously[10] show some very striking changes in fracture strain with varying histories (Fig. 40). The samples were all initially annealed 1 hr at 1177°C before being given the treatment indicated in Fig. 40. In the as-annealed condition, the alloy has a fracture strain of 70 to 80% up to about 600°C, where the fracture strain drops precipitiously. Aging for 9789 hr at 650°C reduced the fracture strain at lower temperatures and increased it above about 700°C. However, the fracture strains are in the range of 40 to 50% over the entire range of temperatures studied. Irradiation to a thermal fluence of 2.5×10^{19} neutrons/cm^2 over a period of 17,033 hr in N_2 + 2 to 5% O_2 resulted in

Table 19. Postirradiation Tensile Properties of Hastelloy N (Heat 67-504)[a]

Specimen Number	Test Temperature (°C)	Strain Rate (min^{-1})	Stress, psi Yield	Stress, psi Ultimate Tensile	Elongation, % Uniform	Elongation, % Total	Reduction in Area (%)	True Fracture Strain (%)
5111	25	0.05	50,300	112,200	45.9	48.1	34.63	43
5147	25	0.05	50,700	112,800	54.6	56.6	36.54	45
5110	200	0.05	41,000	96,400	43.0	44.8	38.34	48
5162	200	0.05	40,900	95,300	45.7	47.3	46.66	63
5109	400	0.05	36,700	90,800	49.8	52.0	36.15	45
5145	400	0.05	37,500	90,800	52.8	54.8	34.84	43
5108	400	0.002	36,700	91,800	52.2	54.7	45.71	61
5144	400	0.002	41,100	97,900	52.7	53.7	33.31	41
5107	500	0.05	40,600	92,700	45.7	47.2	32.23	39
5143	500	0.05	40,900	94,000	49.6	50.6	39.97	51
5106	500	0.002	41,600	90,500	44.5	46.2	39.40	50
5142	500	0.002	33,800	78,600	41.1	42.6	36.00	45
5117	550	0.05	39,700	74,900	34.5	36.5	31.45	38
5153	550	0.05	34,700	77,800	39.7	43.5	37.94	48
5118	550	0.002	44,600	62,000	11.9	15.1	16.02	17
5154	550	0.002	33,200	59,900	20.5	21.5	20.38	23
5096	600	0.05	31,900	74,500	34.7	36.9	26.02	30
5164	600	0.05	32,900	70,800	32.9	34.0	35.69	44
5120	600	0.002	36,400	49,600	8.9	10.9	20.38	23
5156	600	0.002	30,900	49,500	12.6	15.7	23.35	27
5128	650	0.05	39,900	55,500	24.0	25.8	22.06	25
5121	650	0.05	38,800	59,600	14.6	16.5	19.15	21
5155	650	0.05	30,200	46,200	12.8	15.8	10.17	11
5122	650	0.002	52,200	54,500	2.2	6.2	3.51	4
5158	650	0.002	31,700	44,800	13.2	14.3	11.54	12
5105	650	0.0002	32,200	40,800	7.4	9.8	13.52	15
5141	650	0.0002	30,700	38,800	7.8	8.8	6.65	7
5140	650	~0.000027	30,200	37,100	4.4	6.5	5.1	5
5104	650	~0.000027	30,700	37,200	4.8	6.5	5.4	6
5098	760	0.05	27,000	38,600	9.0	23.7	18.94	21
5123	760	0.05	33,300	40,100	6.7	8.7	10.17	11
5159	760	0.05	28,800	38,000	9.6	13.5	13.19	14
5124	760	0.002	33,300	33,300	1.2	2.7	4.63	5
5160	760	0.002	28,200	34,600	4.2	5.6	6.00	6
5102	850	0.05	27,300	29,700	2.9	4.3	2.40	2
5138	850	0.05	27,500	30,900	3.2	4.5	7.10	7
5103	850	0.002	21,100	21,100	1.0	1.9	0.64	1
5139	850	0.002	23,700	23,700	1.0	2.5	0.48	0

[a]Annealed 1 hr at 1177°C. Irradiated to a thermal fluence of 0.25×10^{20} neutrons/cm^2 over a period of 17,033 hr at 650°C.

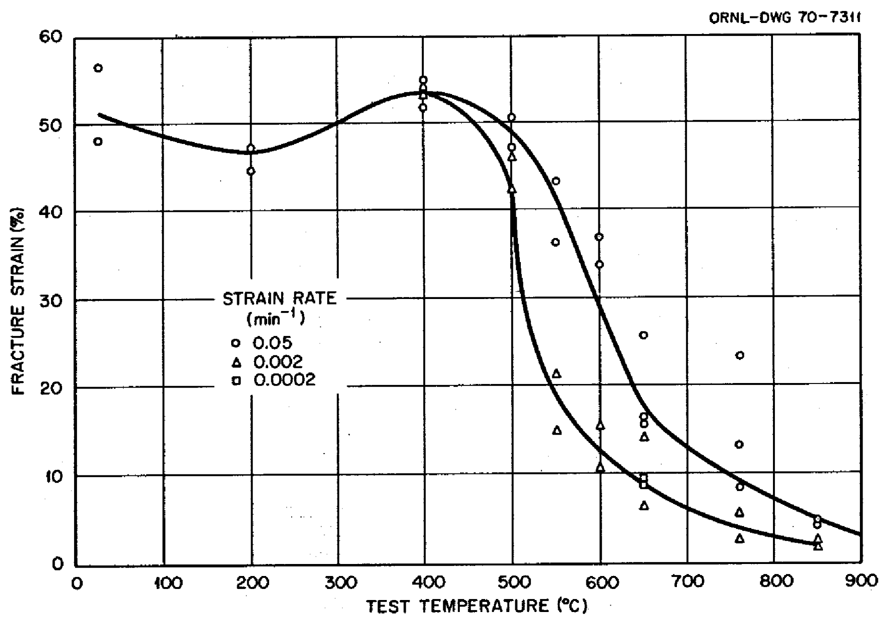

Fig. 39. Fracture Strains of Heat 67-504 After Irradiation to a Thermal Fluence of 2.5×10^{19} neutrons/cm^2 for 17,033 hr at 650°C.

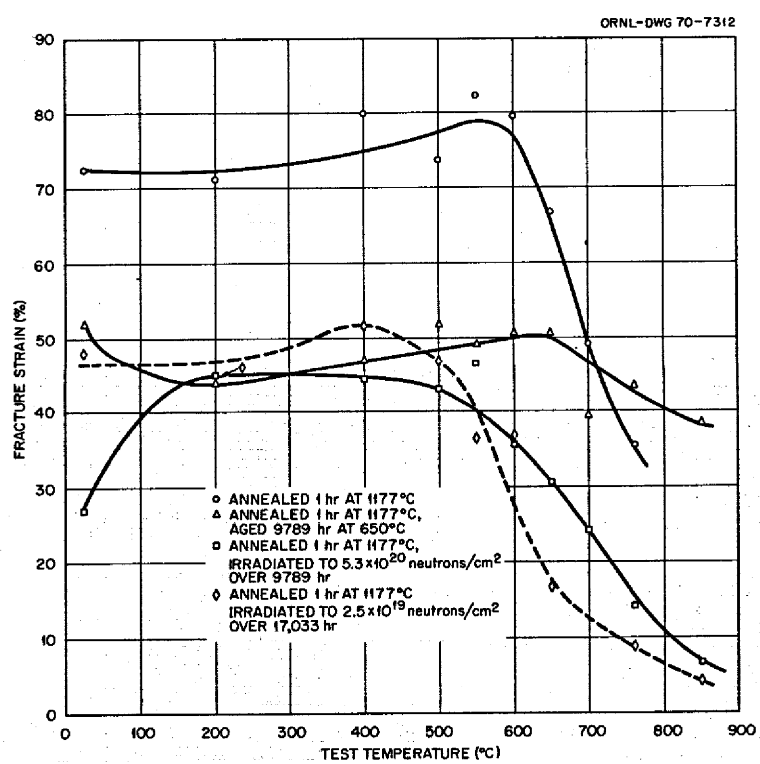

Fig. 40. Comparison of the Fracture Strains of Heat 67-504 in Various Conditions When Tested at a Strain Rate of 0.05 min^{-1}.

fracture strains of about 50% up to 500°C, above which the fracture strain dropped progressively with increasing temperature. Irradiation to a thermal fluence of 5.3×10^{20} neutrons/cm^2 at 650°C in fuel salt over a period of 9789 hr resulted in a low fracture strain at 25°C (which may be anomalous), fracture strains of about 45% up to 500°C, and decreasing fracture strains with increasing test temperature. The most striking feature is that above 550°C the fracture strains are lower for material irradiated in N_2 + 2 to 5% O_2 for 17,033 hr to a fluence of 2.5×10^{19} neutrons/cm^2 than for those irradiated in fuel salt for 9789 hr to a fluence of 5.3×10^{20} neutrons/cm^2.

Some values of the tensile properties at 25 and 650°C are given in Table 20. The yield stress at both test temperatures was increased by aging and by irradiation. The ultimate tensile stress at 25°C was increased by aging and by irradiation; at 650°C it was increased by aging, but decreased by irradiation. We have already discussed the changes in the fracture strain.

Table 20. Comparison of the Tensile Properties of Heat 67-504 After Various Treatments[a]

Heat Treatment	Yield Stress, psi		Ultimate Tensile Stress, psi		Fracture Strain, %	
	at 25°C	at 650°C	at 25°C	at 650°C	at 25°C	at 650°C
Annealed 1 hr at 1177°C	37,400	25,600	105,000	83,000	73.2	65.9
Annealed at 1177°C and aged 9789[b] hr at 650°C	67,500	43,300	133,000	94,300	52.3	50.9
Annealed at 1177°C, irradiated to[b] a thermal fluence of 5.3×10^{20} neutrons/cm^2 over 9789 hr (salt environment)	102,000	32,900	119,300	70,000	27.0	30.7
Annealed at 1177°C, irradiated to a thermal fluence of 2.5×10^{19} neutrons/cm^2 over 17,033 hr (N_2 + 2 to 5% O_2 environment)	50,300	38,800	112,000	59,600	48.1	16.5

[a]Tested at a strain rate of 0.05 min^{-1}.

[b]Data from: H. E. McCoy, Jr., An Evaluation of the Molten-Salt Reactor Experiment Hastelloy N Surveillance Specimens — Third Group, ORNL-TM-2647 (1970).

The results of creep-rupture tests on heat 67-504 are summarized in Table 21. These results and those obtained previously[11] were used to prepare Figs. 41, 42, and 43. The stress-rupture properties in Fig. 41 show that the rupture life was not changed appreciably by aging, at least for 9789 hr at 650°C. The stress-rupture life was reduced at least two orders of magnitude by the lower fluence and only a factor of 2 by the higher fluence. The minimum creep rates in Fig. 42 show that this property was not changed as much as the rupture life. Aging for 9789 hr increased the minimum creep, but samples irradiated over the same period had a lower creep rate than the aged samples. The samples irradiated to the lower fluence had a creep rate an order of magnitude higher than that of the as-annealed material. The fracture strains are

[11]H. E. McCoy, An Evaluation of the Molten-Salt Reactor Experiment Hastelloy N Surveillance Specimen — Third Group, ORNL-TM-2647 (1970).

Table 21. Creep-Rupture Tests on Heat 67-504 at 650°C

Test Number	Specimen Number	Stress (psi)	Rupture Life (hr)	Rupture Strain (%)	Minimum Creep Rate (%/hr)
Irradiated at 650°C to a thermal fluence of 2.5×10^{19} neutrons/cm^2					
R-952	5112	55,000	0.6	8.6	9.88
R-953	5148	55,000	1.0	10.6	6.6
R-959	5113	47,000	7.6	12.1	0.83
R-965	5149	47,000	3.3	6.2	0.52
R-971	5114	40,000	14.5	10.9	0.42
R-1017	5150	40,000	33.8	4.1	0.050
R-968	5115	32,400	235.5	3.8	0.0071
R-1033	5137	32,400	268.7	4.2	0.0066
R-1019	5116	27,000	1175.4	2.7	0.0016
Annealed 1 hr at 1177°C					
7432	6247	70,000	1.3	32.9	3.7
7431	6245	63,000	17.7	31.2	0.16
6255	4991	55,000	127.9	27.2	0.029
6254	4936	47,000	425.5	28.7	0.0068
6253	4933	40,000	876.9	16.3	0.0030

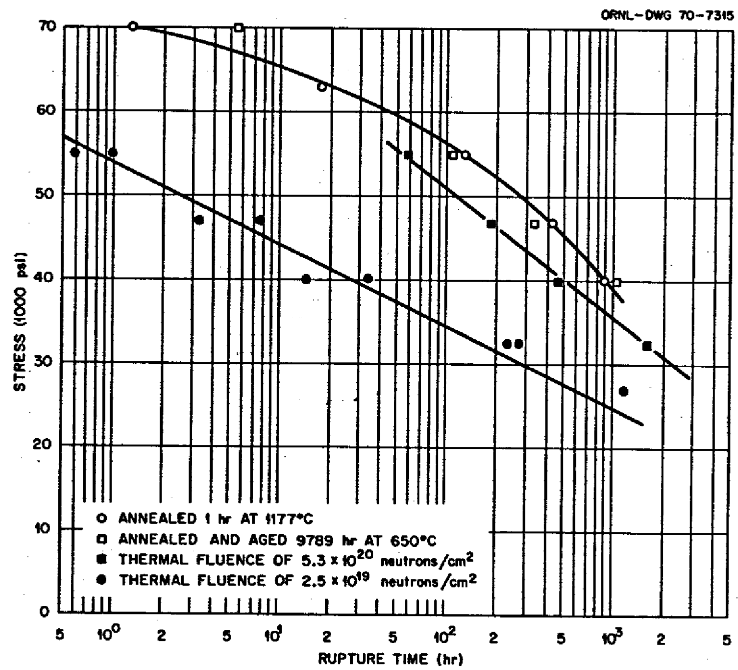

Fig. 41. Stress-Rupture Properties at 650°C of Heat 67-504.

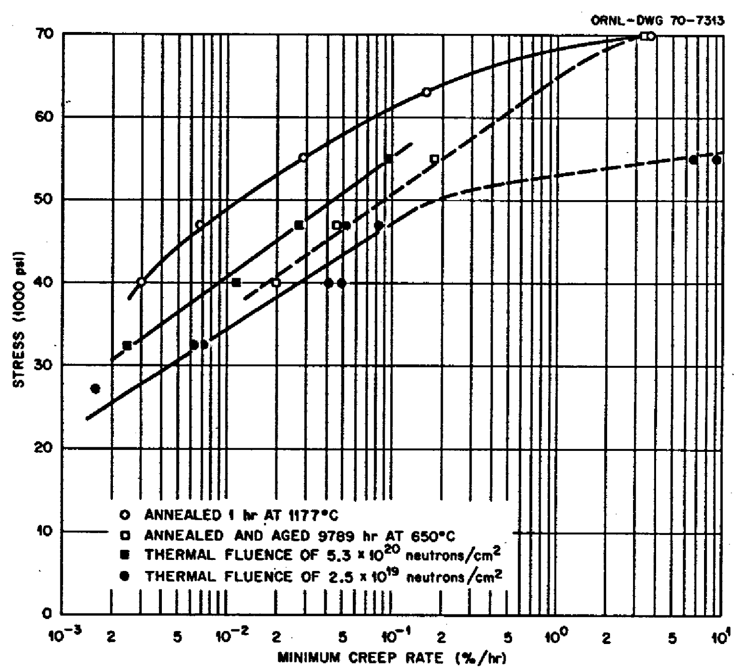

Fig. 42. Creep-Rupture Properties at 650°C of Heat 67-504.

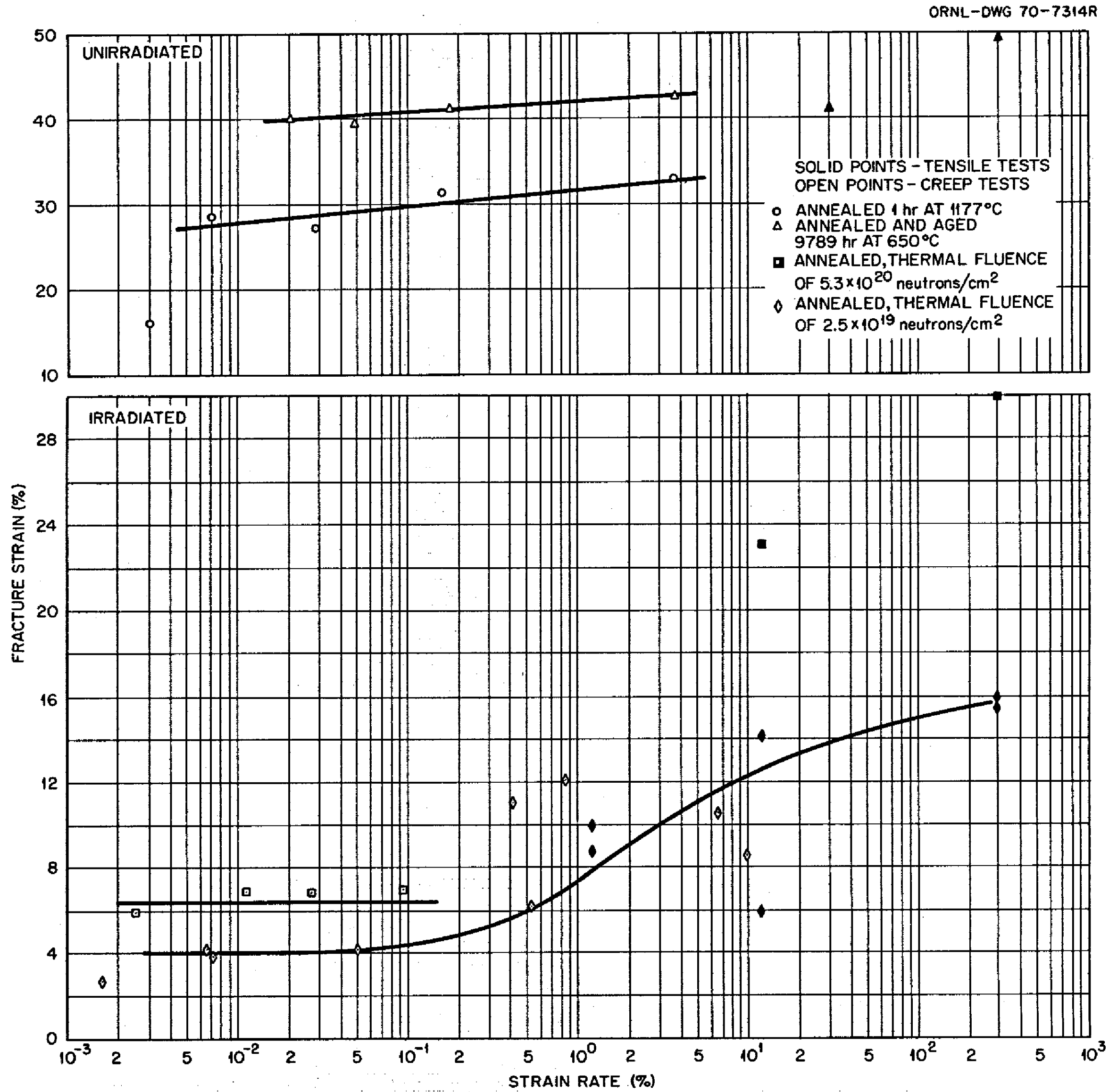

Fig. 43. Comparison of the Fracture Strains of Unirradiated and Irradiated Heat 67-504 at 650°C. [Data for samples aged for 9789 hr at 650°C and for those irradiated to 2.5 × 10^{19} neutrons/cm^2 from: H. E. McCoy, An Evaluation of the Molten-Salt Reactor Experiment Hastelloy N Surveillance Specimen — Third Group, ORNL-TM-2647 (1970).]

shown as a function of strain rate in Fig. 43. Aging increased the fracture strain of the unirradiated material. After irradiation the material irradiated to the lower fluence had the lowest fracture strain.

Several samples of heat 67-504 were subjected to tests that were interrupted. The results of these tests are summarized in Table 22. If strained continuously at 650°C at a strain rate of 0.05 min^{-1}, the

Table 22. Results of Interrupted Tensile Tests on Heat 67-504

Type of Test[a]	Test Temperature (°C)	Fracture Strain, %	
		Unirradiated	Irradiated
A	650	66.9	16.5
B	650	100.4	
C	650	109.0	
D	650	104.0	
E	650	95.4	25.8
A	760	35.5	8.7
F	760	96.0	23.7

[a]A — Run uninterrupted at a strain rate of 0.05 min^{-1}.

B — Strained 5%, held at temperature for 2 min, cycle repeated to failure.

C — Strained 5%, held at temperature for 10 min, cycle repeated to failure.

D — Strained 5%, held at temperature for 30 min, cycle repeated to failure.

E — Strained 5%, held at temperature for 60 min, cycle repeated to failure.

F — Strained 3%, held at temperature for 60 min, cycle repeated to failure.

material had a fracture strain of 66.9% if unirradiated and 16.5% if irradiated. If the material was strained 5% at 650°C then annealed 1 hr at 650°C and this pattern continued until failure, the unirradiated sample failed with 95.4% strain and the irradiated sample with 25.8% strain. A sequence of tests was performed on unirradiated samples at 650°C in which the annealing time was varied from 2 to 60 min; the results show that this variable had little effect on the fracture strain. At a test temperature of 760°C the fracture strain was 35.5% for an unirradiated sample and 8.7% for an irradiated material. Samples were also tested by straining 3%, annealing 1 hr at 760°C, straining 3%, and repeating this sequence until failure. The fracture strains were 96.0 and 23.7% for the unirradiated and irradiated samples, respectively. These tests have demonstrated that there is not, for each test temperature, a unique strain at which failure occurs; rather, the fracture strain depends upon the loading history.

Metallographic Examination of Test Samples

The tensile samples that were tested at 25°C at a strain rate of 0.05 min^{-1} and at 650°C at a strain rate of 0.002 min^{-1} were examined. An irradiated sample of heat 5085 from the core that was tested at 25°C is shown in Fig. 44. The fracture is primarily intergranular. There is a high frequency of edge cracking that extends to a depth of about 4 mils. The microstructure in the 4-mil region near the surface etches differently. At a 650°C test temperature (Fig. 45) the fracture is intergranular with no evidence of plastic deformation of the individual grains except adjacent to the fracture. This sample also had the modified structure and edge cracks that extend 10 mils into the sample. The control samples of heat 5085 that were annealed for 22,533 hr at 650°C in static barren fuel salt are shown in Figs. 46 and 47. The sample shown in Fig. 46 was tested at 25°C. The fracture is predominantly intergranular, but there are no edge cracks. There is a very thin layer near the surface where the structure is modified slightly. The microstructure is generally characterized by large M_6C-type carbides, many of which cracked during deformation, and a network of almost continuous carbides along the grain and twin boundaries. When tested at 650°C (Fig. 47) the fracture is intergranular. There is some edge cracking, but not as frequently as noted in Fig. 45 for the irradiated sample. Another factor that should be considered in comparing Figs. 45 and 47 is that the irradiated sample in Fig. 45 failed after straining only 5% (Table 4, p. 18), whereas the unirradiated sample in Fig. 47 strained 24% (Table 3, p. 17) before fracturing. The higher strain should have increased the number and depth of edge cracks. The observed opposite trend indicates some influence of the exposure to the reactor environment on the fracture characteristics near the surface.

Heat 5065 was also exposed to the core for 22,533 hr at 650°C. The microstructure of a sample tested at 25°C is shown in Fig. 48. The

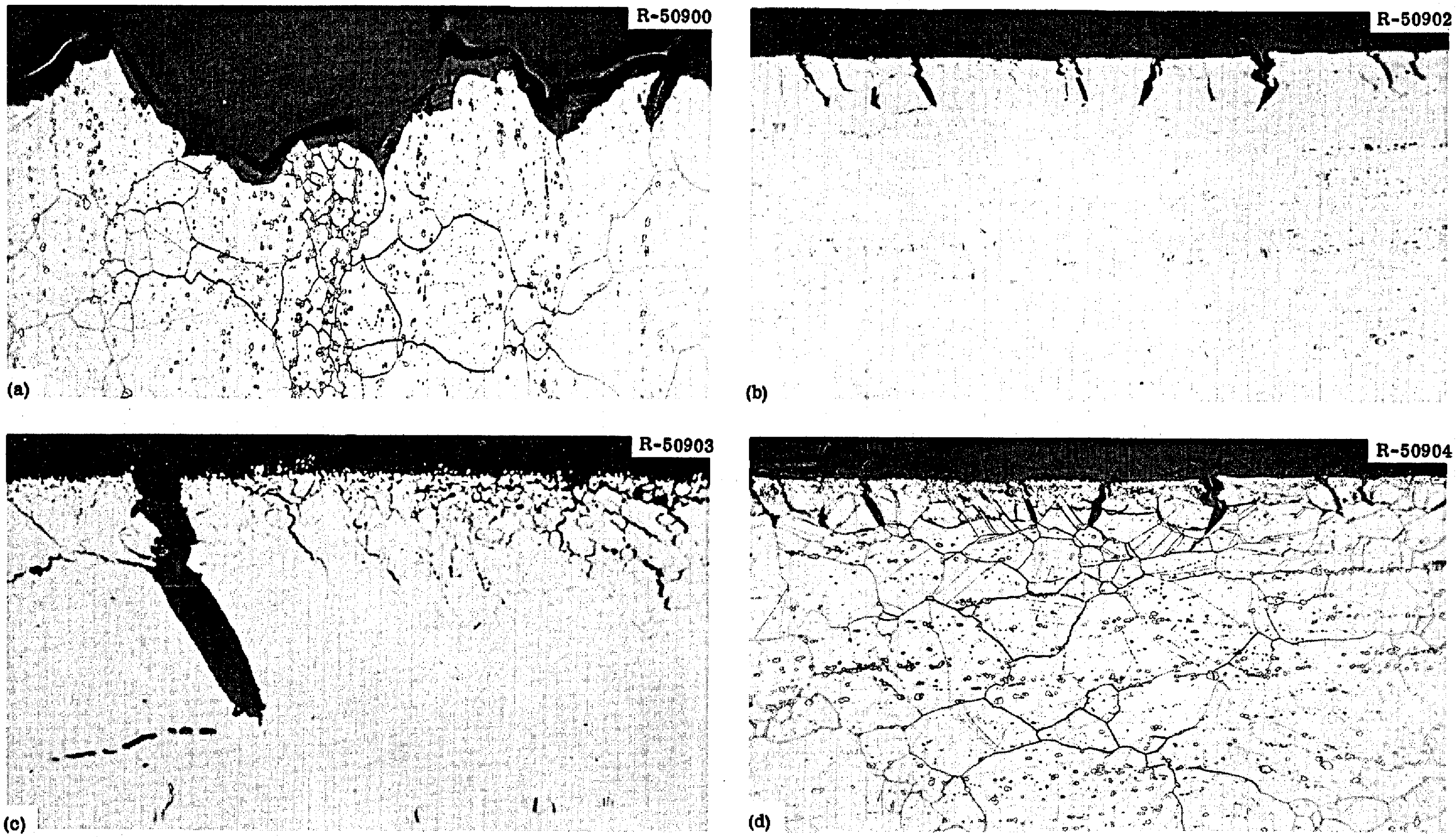

Fig. 44. Photomicrographs of a Hastelloy N (Heat 5085) Sample Tested at 25°C After Being Exposed to the MSRE Core for 22,533 hr at 650°C and Irradiated to a Thermal Fluence of 1.5×10^{21} neutrons/cm^2. (a) Fracture, etched. 100×. (b) Edge, as polished. 100×. (c) Edge, as polished. 500×. (d) Edge, etched. 100×. Etchant: glyceria regia. Reduced 27%.

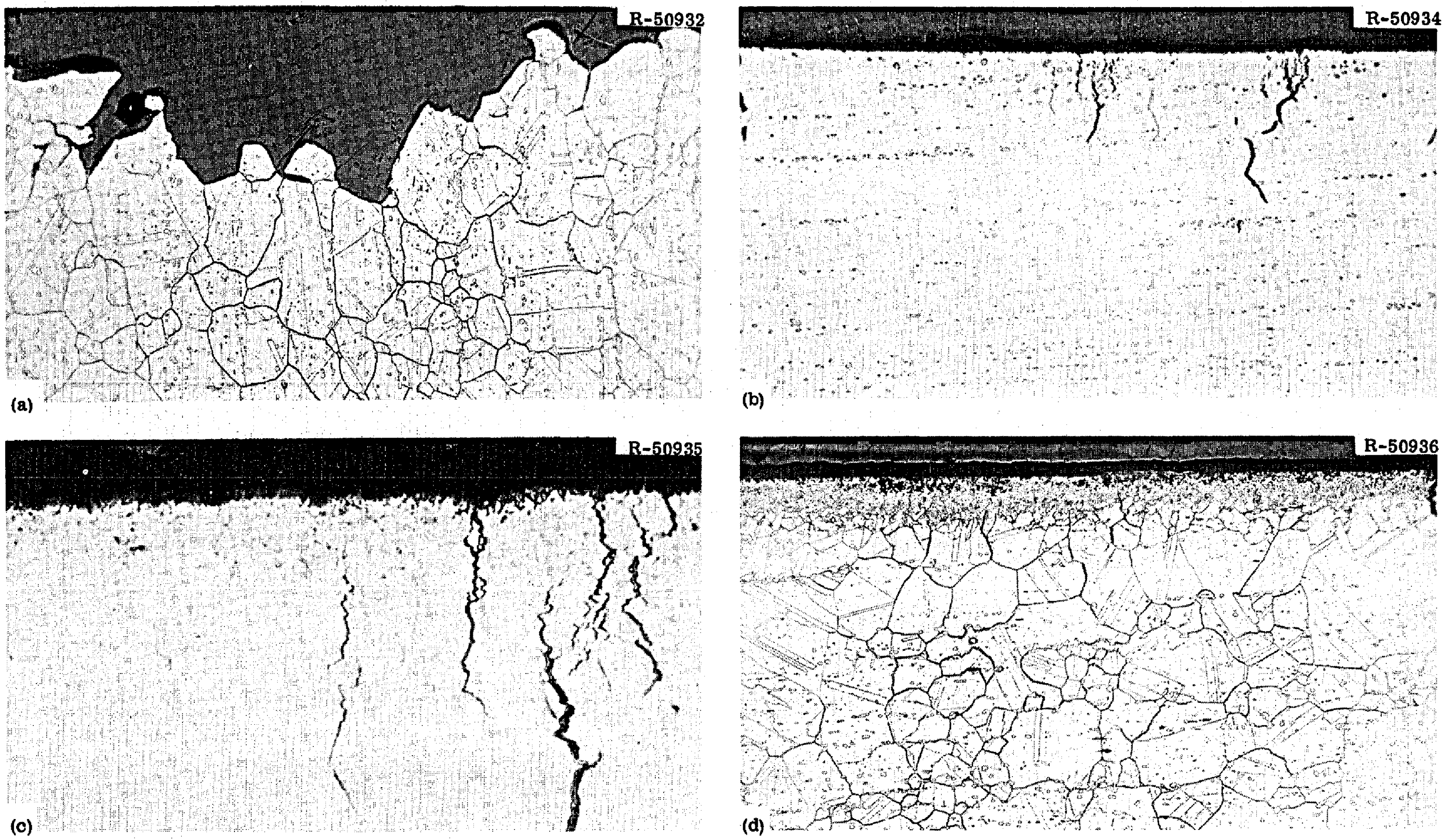

Fig. 45. Photomicrographs of a Hastelloy N (Heat 5085) Sample Tested at 650°C After Being Exposed to the Core of the MSRE for 22,533 hr at 650°C and Irradiated to a Thermal Fluence of 1.5×10^{21} neutrons/cm^2. (a) Fracture, etched. 100×. (b) Edge, as polished. 100×. (c) Edge, as polished. 500×. (d) Edge, etched. 100×. Etchant: glyceria regia. Reduced 27%.

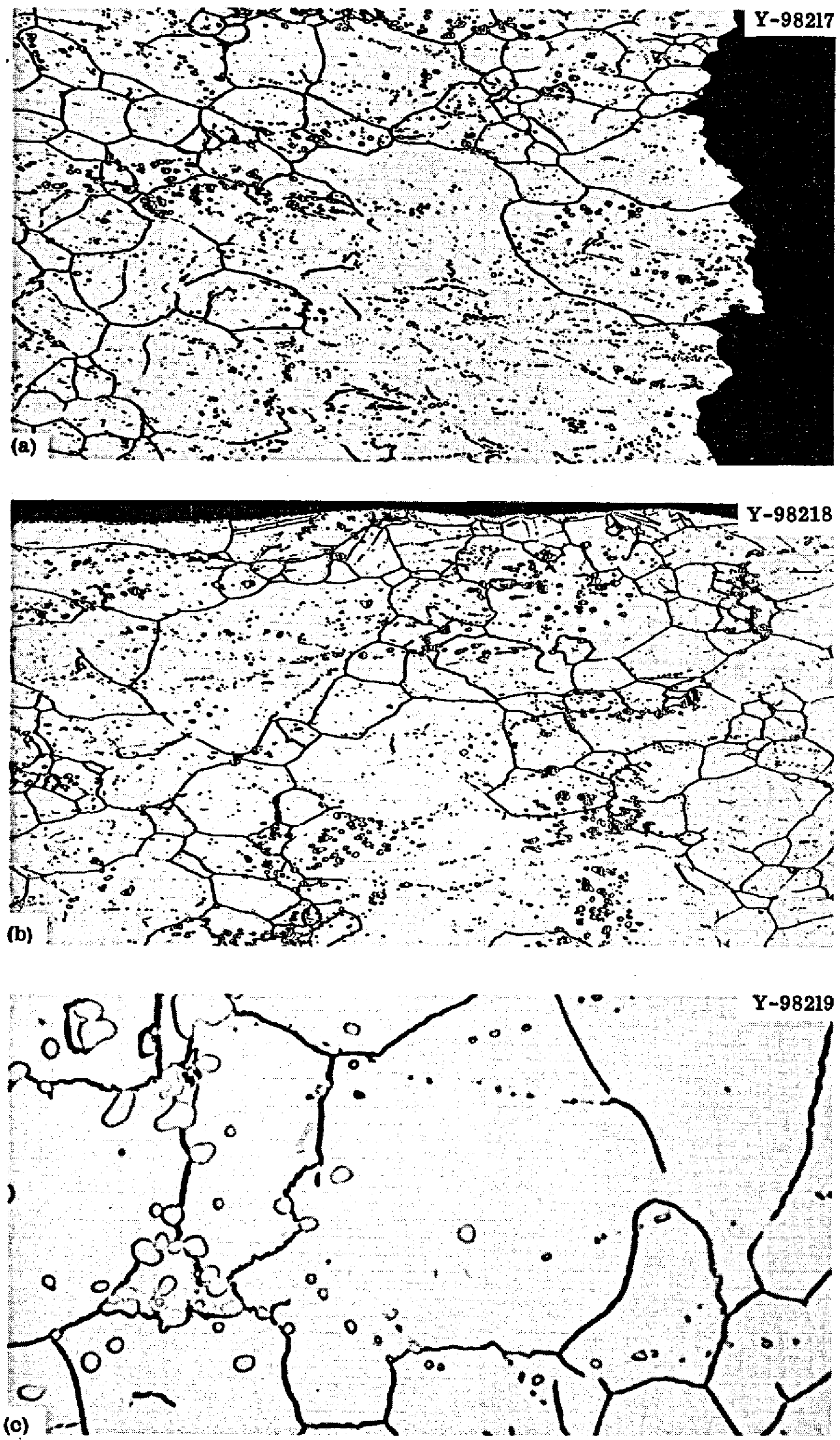

Fig. 46. Typical Photomicrographs of a Hastelloy N (Heat 5085) Sample Tested at 25°C After Being Exposed to Static Barren Fuel Salt for 22,533 hr at 650°C. (a) Fracture, etched. 100×. (b) Edge near fracture, etched. 100×. (c) Representative unstressed structure, etched. 500×. Etchant: glyceria regia. Reduced 24.5%.

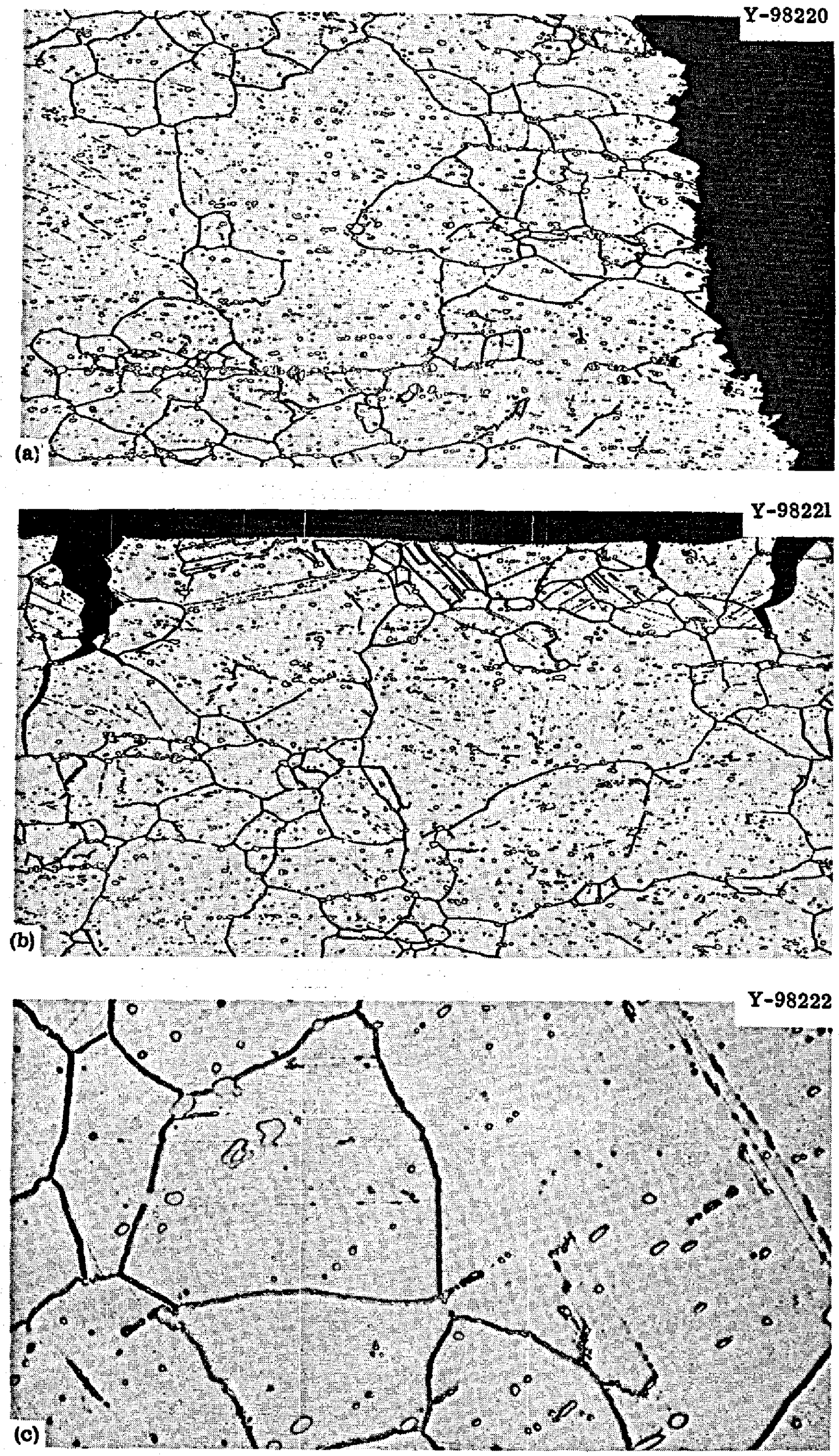

Fig. 47. Typical Photomicrographs of a Hastelloy N (Heat 5085) Sample Tested at 650°C (Strain Rate 0.002 min^{-1}) After Being Exposed to Static Barren Fuel Salt for 22,533 hr at 650°C. (a) Fracture. 100×. (b) Edge near fracture. 100×. (c) Representative unstressed structure. 500×. Etchant: glyceria regia. Reduced 25%.

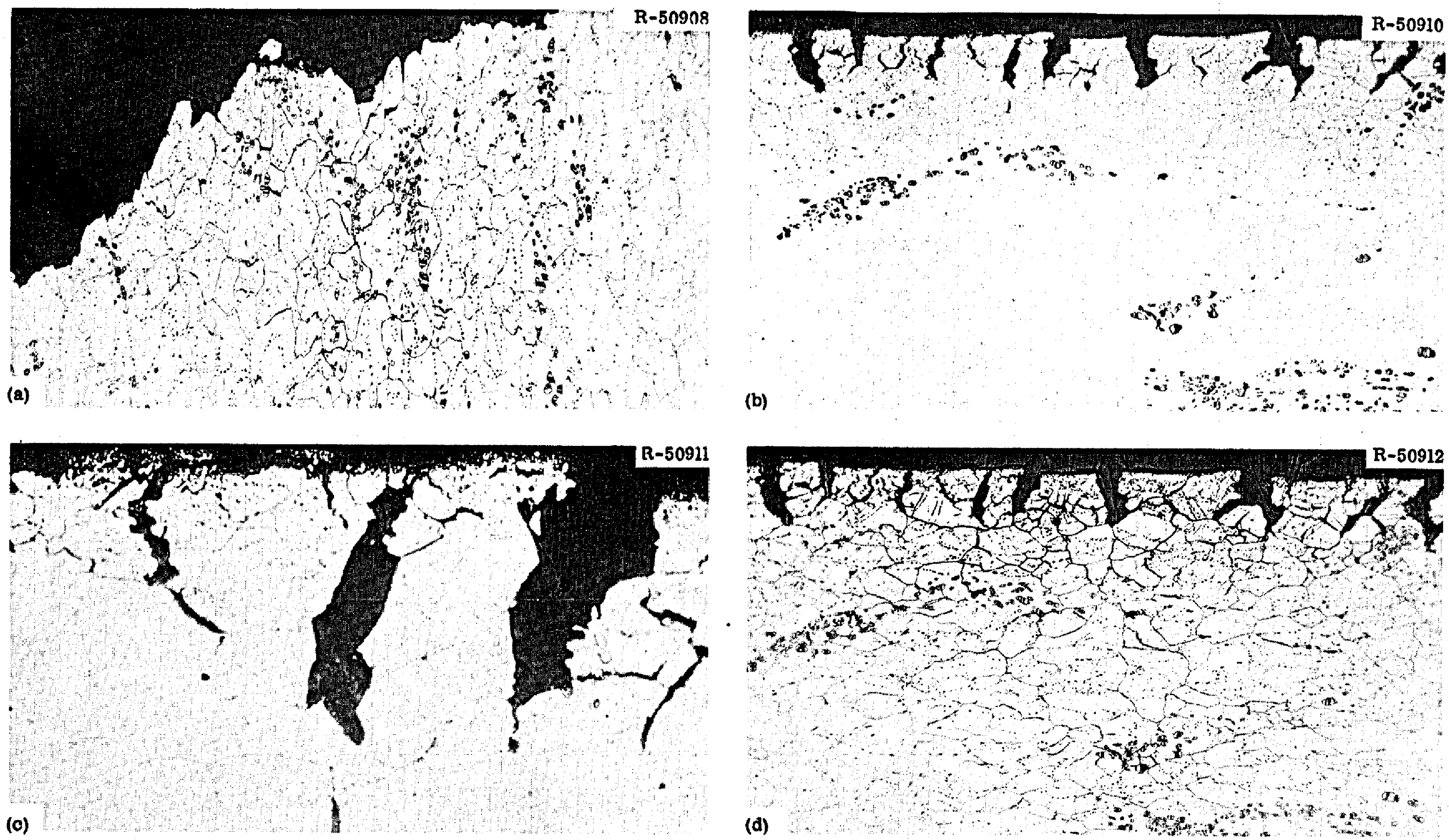

Fig. 48. Photomicrographs of a Hastelloy N (Heat 5065) Sample Tested at 25°C After Being Exposed to the MSRE Core for 22,533 hr at 650°C and Irradiated to a Thermal Fluence of 1.5×10^{21} neutrons/cm^2. (a) Fracture, etched. 100×. (b) Edge, as polished. 100×. (c) Edge, as polished. 500×. (d) Edge, etched. 100×. Etchant: glyceria regia. Reduced 26%.

fracture is mixed transgranular and intergranular. The same structural modification and edge cracking that were noted in heat 5085 (Fig. 44) are also present in heat 5065. A sample of heat 5065 tested at 650°C is shown in Fig. 49. The fracture is intergranular with little evidence of deformation of the adjacent grains. The microstructure at the edge is modified to a depth of about 4 mils, and cracks extend to a depth of about 10 mils. A control sample tested at 25°C is shown in Fig. 50. The fracture is mixed transgranular and intergranular, and the grains are elongated in the direction of stressing. There is no edge cracking. There are copious amounts of carbides, both of the large primary carbides and the finer carbides formed during the long annealing treatment at 650°C. The microstructure of a control sample of heat 5065 tested at 650°C (Fig. 51) shows an intergranular fracture and some edge cracking. Again the frequency of cracking is less than that noted for the irradiated material shown in Fig. 49.

Heat 7320 was exposed to the MSRE core for 7244 hr at 650°C. Typical micrographs of a sample tested at 25°C are shown in Fig. 52. The fracture is predominantly transgranular and the flow lines and the elongated grains attest to the deformation of the matrix. There are some edge cracks to a depth of about 3 mils, but the microstructure is not modified at the sample surface. Microstructures of an irradiated sample tested at 650°C are shown in Fig. 53. The fracture is intergranular. There are edge cracks that extend to a depth of about 10 mils, but the microstructure is not modified near the surface. A control sample that was tested at 25°C is shown in Fig. 54. The fracture is transgranular with the grains being elongated in the direction of stressing. There is no edge cracking. The unstressed microstructure gives a hint of the very fine matrix precipitation that is present in this alloy. Photomicrographs of a control sample tested at 650°C are shown in Fig. 55. The fracture is intergranular, and there are no edge cracks such as were noted in the irradiated sample (Fig. 53).

Heat 67-551 was exposed in the MSRE core for 7244 hr at 650°C. The fracture at 25°C (Fig. 56) is mixed transgranular and intergranular, and grains have deformed extensively. The microstructure near the surface is not altered, but there are edge cracks that extend to a depth of about

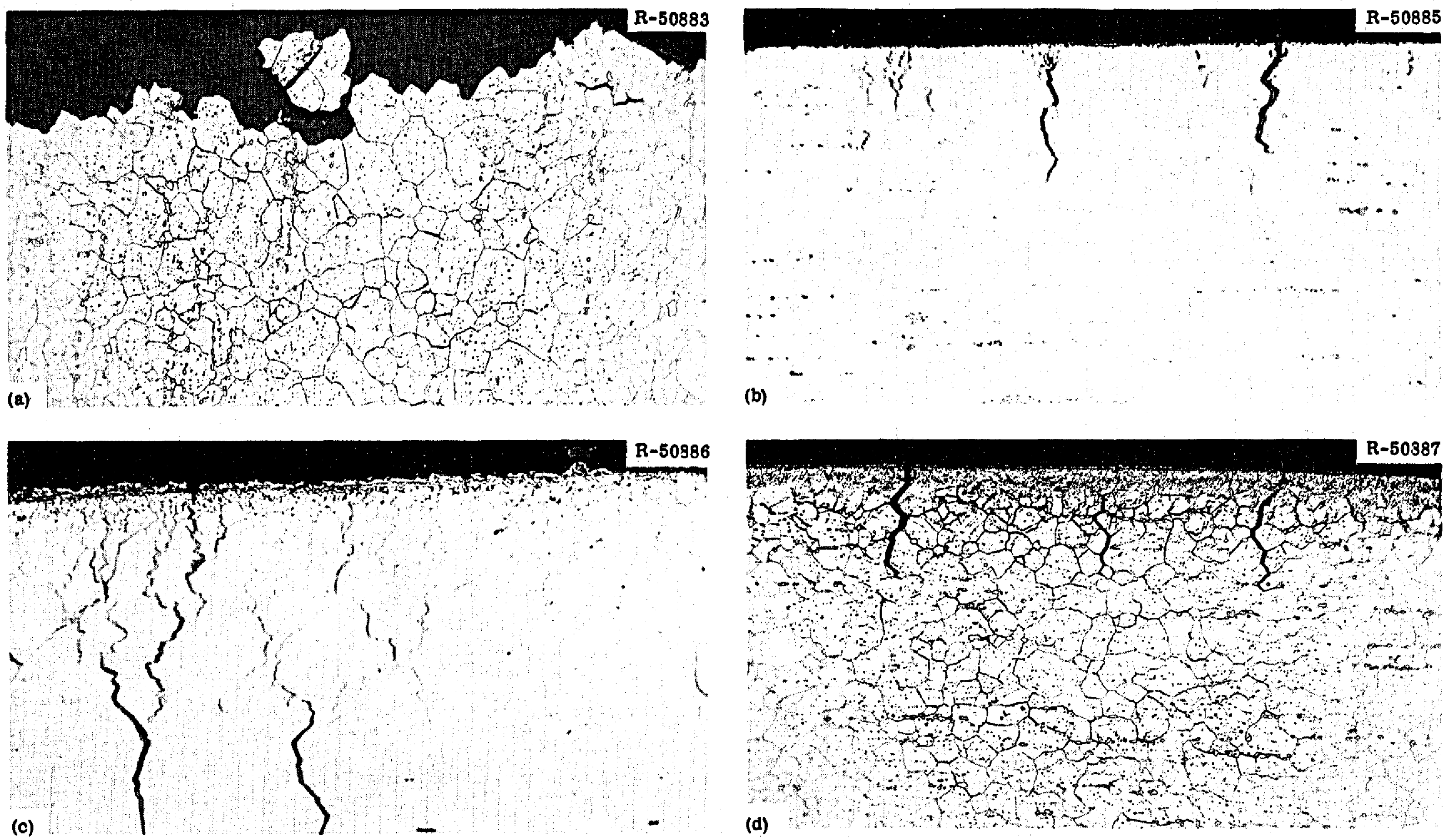

Fig. 49. Photomicrographs of a Hastelloy N (Heat 5065) Sample Tested at 650°C After Being Exposed to the Core of the MSRE for 22,533 hr at 650°C and Irradiated to a Thermal Fluence of 1.5×10^{21} neutrons/cm^2. (a) Fracture, etched. 100×. (b) Edge, as polished. 100×. (c) Edge, as polished. 500×. (d) Edge, etched. 100×. Etchant: glyceria regia. Reduced 26.5%.

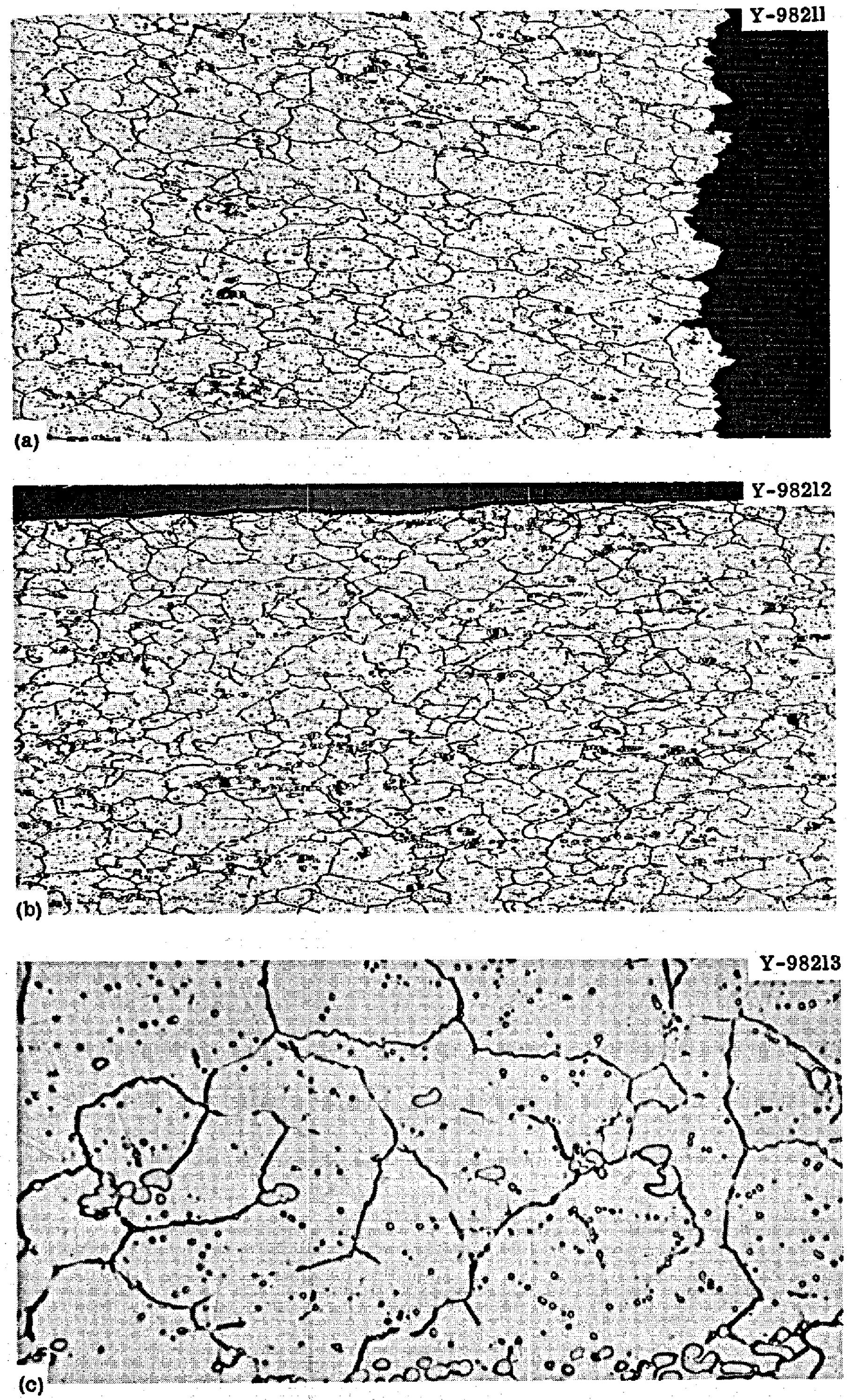

Fig. 50. Typical Photomicrographs of a Hastelloy N (Heat 5065) Sample Tested at 25°C After Being Exposed to Static Barren Fuel Salt for 22,533 hr at 650°C. (a) Fracture. 100X. (b) Edge near fracture. 100X. (c) Representative unstressed structure. 500X. Etchant: glyceria regia. Reduced 22%.

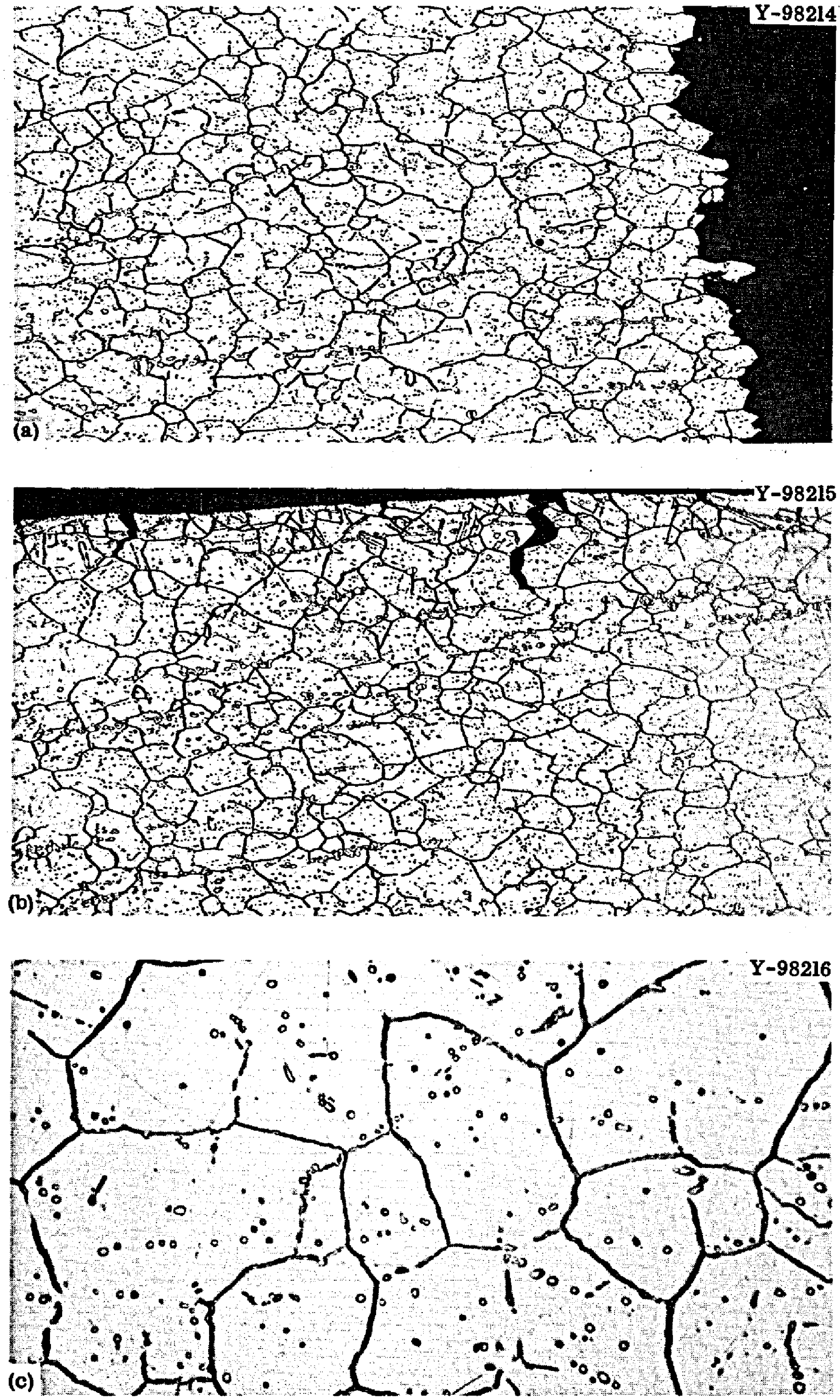

Fig. 51. Typical Photomicrographs of a Hastelloy N (Heat 5065) Sample Tested at 650°C (Strain Rate of 0.002 min^{-1}) After Being Exposed to Barren Fuel Salt for 22,533 hr at 650°C. (a) Fracture. 100×. (b) Edge near fracture. 100×. (c) Representative unstressed structure. 500×. Reduced 21.5%.

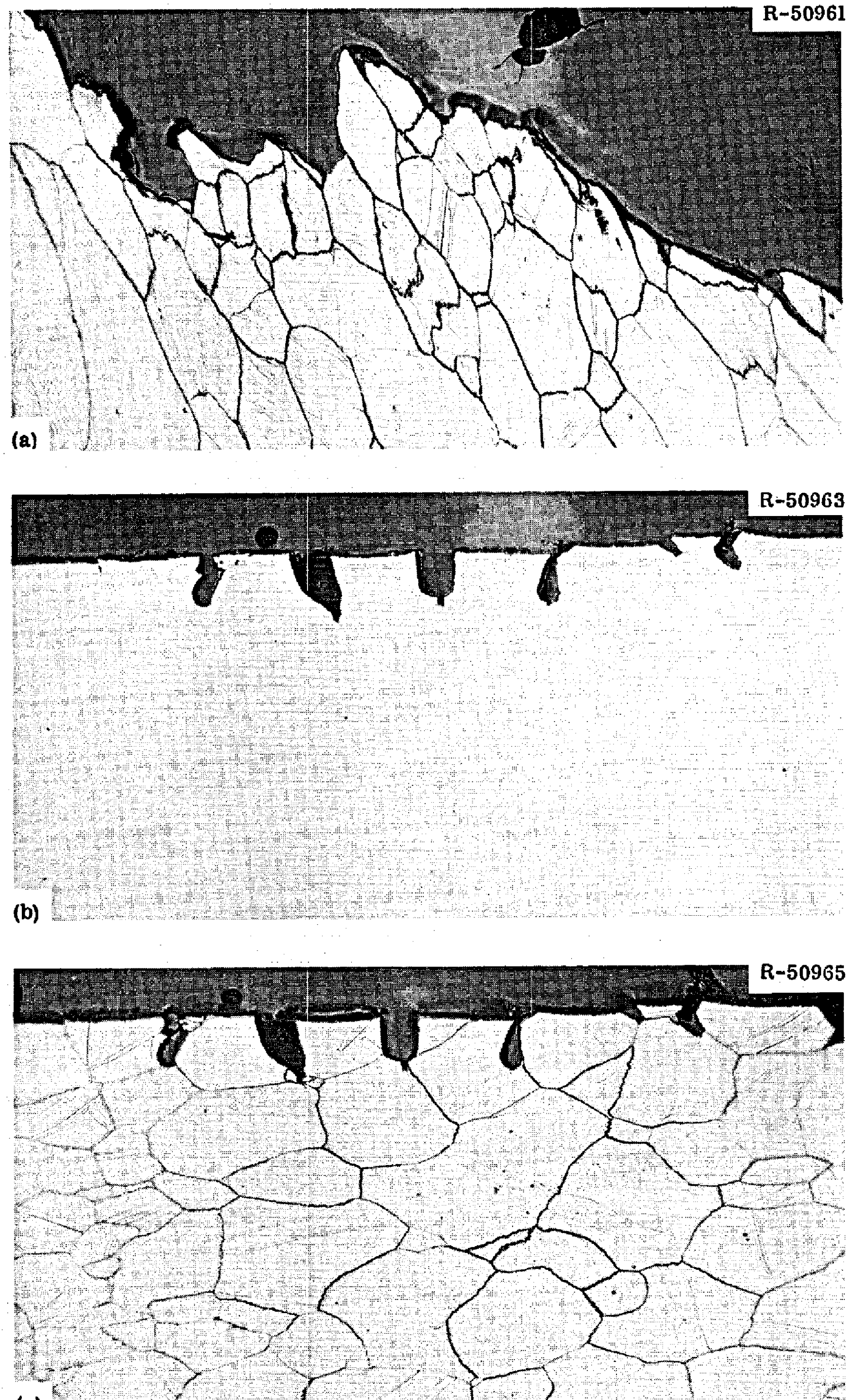

Fig. 52. Photomicrographs of a Modified Hastelloy N (Heat 7320) Sample Tested at 25°C After Being Exposed to the MSRE Core for 7244 hr at 650°C and Irradiated to a Fluence of 5.1×10^{20} neutrons/cm^2. (a) Fracture, etched. 100×. (b) Edge, as polished. 100×. (c) Edge, etched. 100×. Etchant: glyceria regia. Reduced 22%.

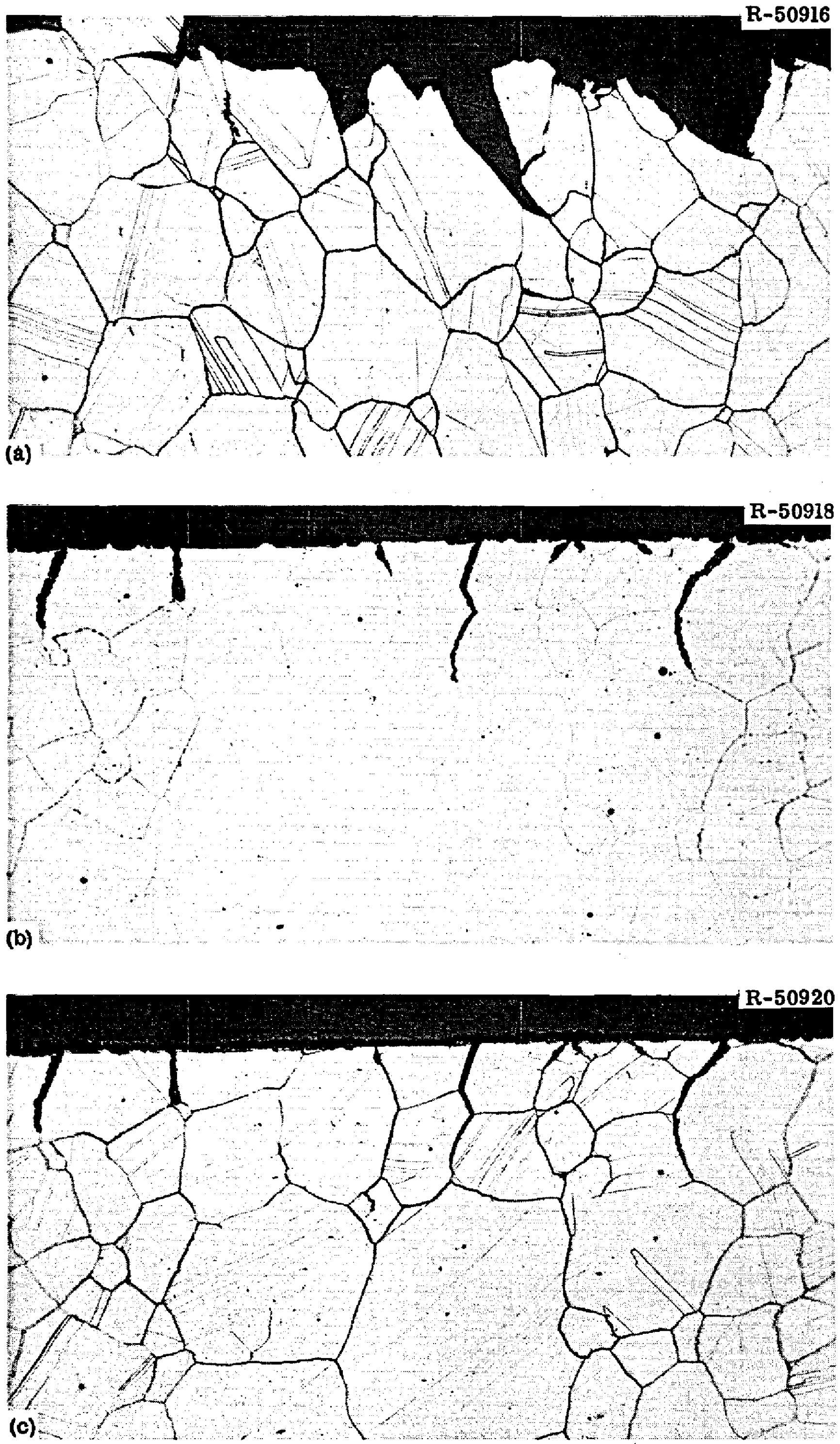

Fig. 53. Photomicrographs of a Modified Hastelloy N (Heat 7320) Sample Tested at 650°C (Strain Rate, 0.002 min^{-1}) After Being Exposed to the MSRE Core for 7244 hr at 650°C and Irradiated to a Fluence of 5.1×10^{20} neutrons/cm^2. (a) Fracture, etched. 100×. (b) Edge, as polished. 100×. (c) Edge, etched. 100×. Etchant: glyceria regia. Reduced 22%.

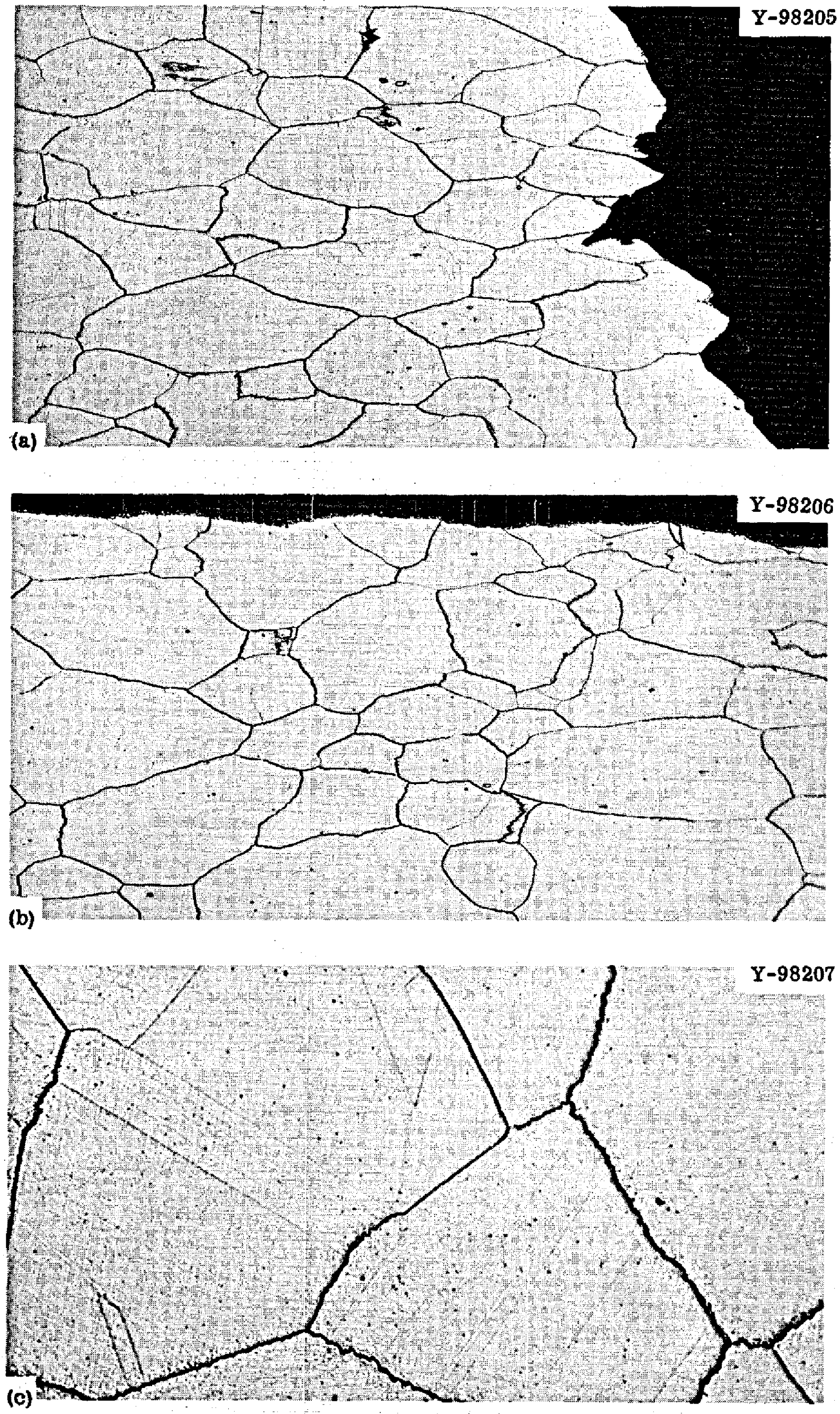

Fig. 54. Photomicrographs of a Modified Hastelloy N (Heat 7320) Sample Tested at 25°C After Being Exposed to Static Barren Fuel Salt for 7244 hr at 650°C. (a) Fracture. 100×. (b) Edge. 100×. (c) Typical unstressed microstructure. 500×. Etchant: glyceria regia. Reduced 22.5%.

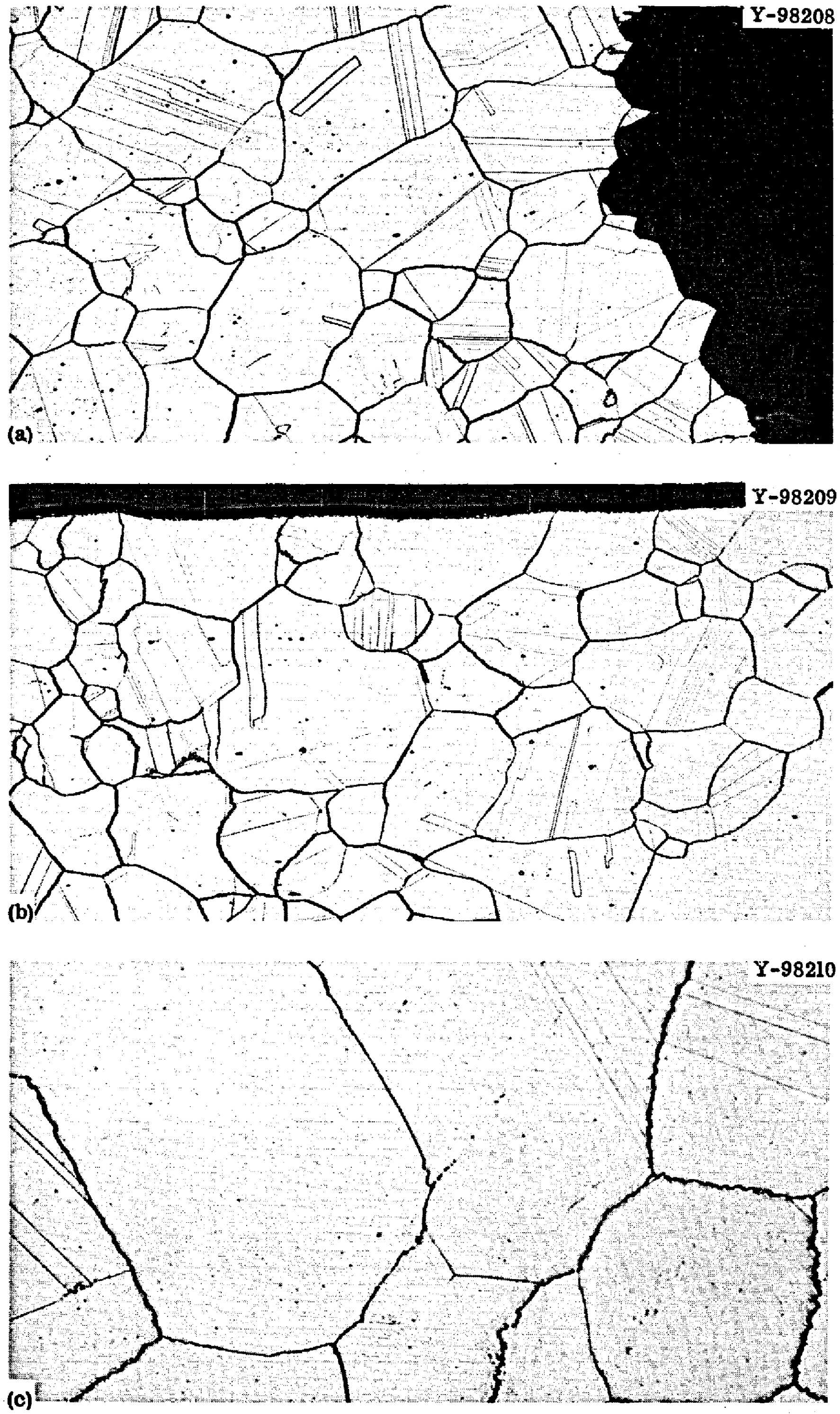

Fig. 55. Photomicrographs of a Modified Hastelloy N (Heat 7320) Sample Tested at 650°C (Strain Rate, 0.002 min^{-1}) After Being Exposed to Static Barren Fuel Salt for 7244 hr at 650°C. (a) Fracture. 100×. (b) Edge near fracture. 100×. (c) Typical unstressed microstructure. 500×. Etchant: gylceria regia. Reduced 23%.

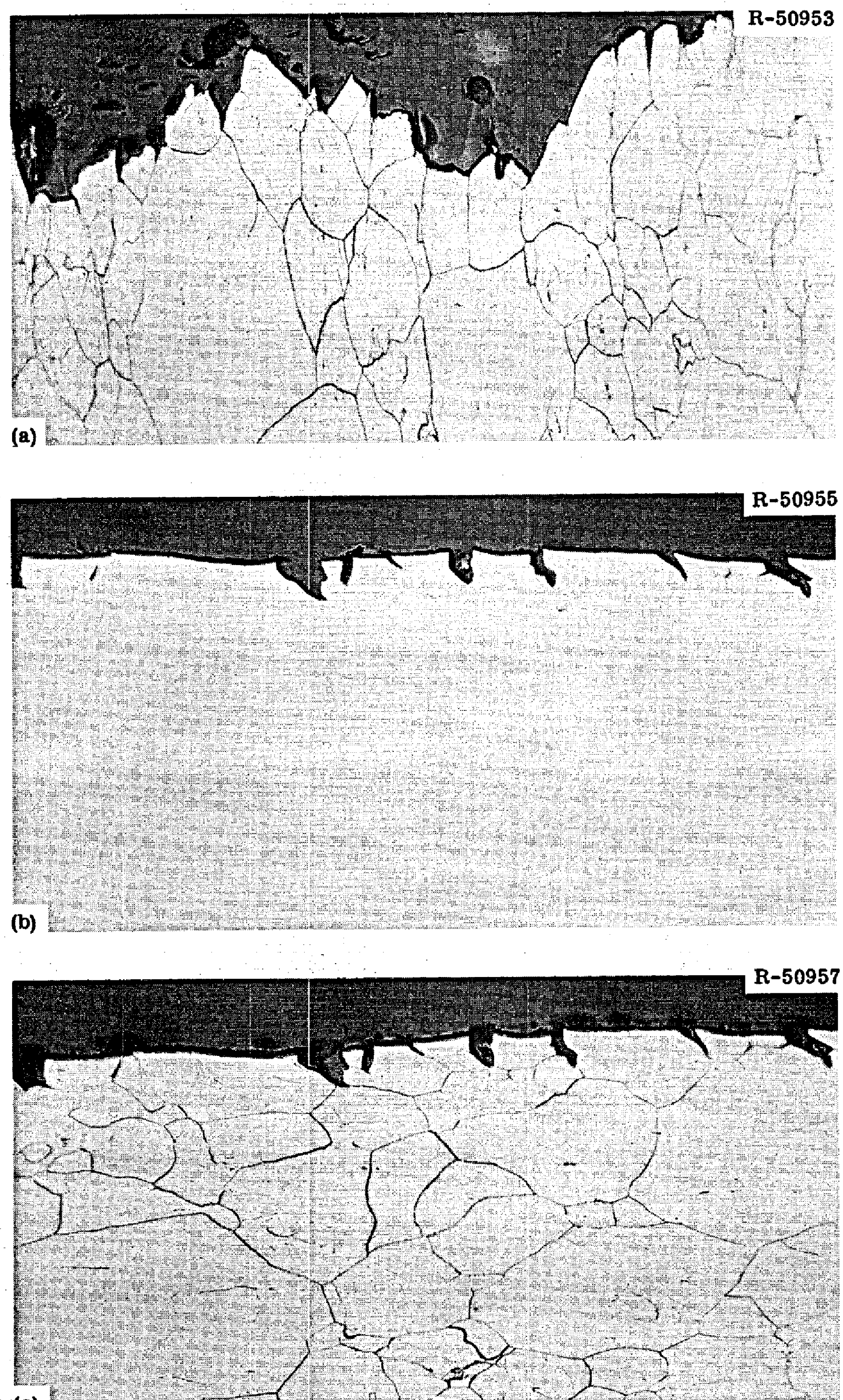

Fig. 56. Photomicrographs of a Modified Hastelloy N (Heat 67-551) Sample Tested at 25°C After Being Exposed to the MSRE Core for 7244 hr at 650°C and Irradiated to a Fluence of 5.1×10^{20} neutrons/cm^2. (a) Fracture, etched. 100×. (b) Edge, as polished. 100×. (c) Edge, etched. 100×. Etchant: glyceria regia. Reduced 21%.

2 mils. At a test temperature of 650°C the fracture is mixed intergranular and transgranular (Fig. 57). The microstructure near the edge is not modified, but edge cracks extend to a depth of about 8 mils. A control sample that was tested at 25°C is shown in Fig. 58. The fracture is largely transgranular, and there are no edge cracks nor structural modifications. The high magnification view shows the fine carbide precipitates that form during the long thermal anneal. At 650°C the fracture is intergranular with numerous intergranular cracks scattered throughout the sample (Fig. 59). A few cracks are near the surface, but these are to be expected in light of the 31.5% strain (Table 14, p. 40) that occurred in this sample before failure.

Heat 67-504 was exposed to the MSRE cell environment of N_2 + 2 to 5% O_2 for 17,033 hr at 650°C and had an oxide film of 1 to 2 mils: when tested at 25°C (Fig. 60) the fracture was mixed transgranular and intergranular, although most of the deformation occurred within the grains. There was no edge cracking. When tested at 650°C (Fig. 61) the fracture was primarily intergranular. There were edge cracks to a depth of 15 mils. Since there were no controls to compare with these samples, it is difficult to say whether the frequency and depth of cracking are greater than would be expected.

DISCUSSION OF RESULTS

The mechanical property changes of the standard Hastelloy N in both the irradiated and unirradiated conditions have followed very regular trends throughout its exposure in the MSRE and in the control facility. Heats 5065 and 5085 have been used throughout the surveillance program. Exposure to the static barren fuel salt up to 15,289 hr brought about a gradual reduction of the tensile fracture strains in both heats; further exposure up to 22,533 hr caused a slight improvement over the strains observed after 15,289 hr (Figs. 15 and 17, pp. 24 and 25). These changes were small compared with those observed after irradiation, and we attribute them to the precipitation of grain-boundary carbides. These changes in tensile properties occurred without detectable change in the creep strength at 650°C (Figs. 19 and 25, pp. 30 and 34).

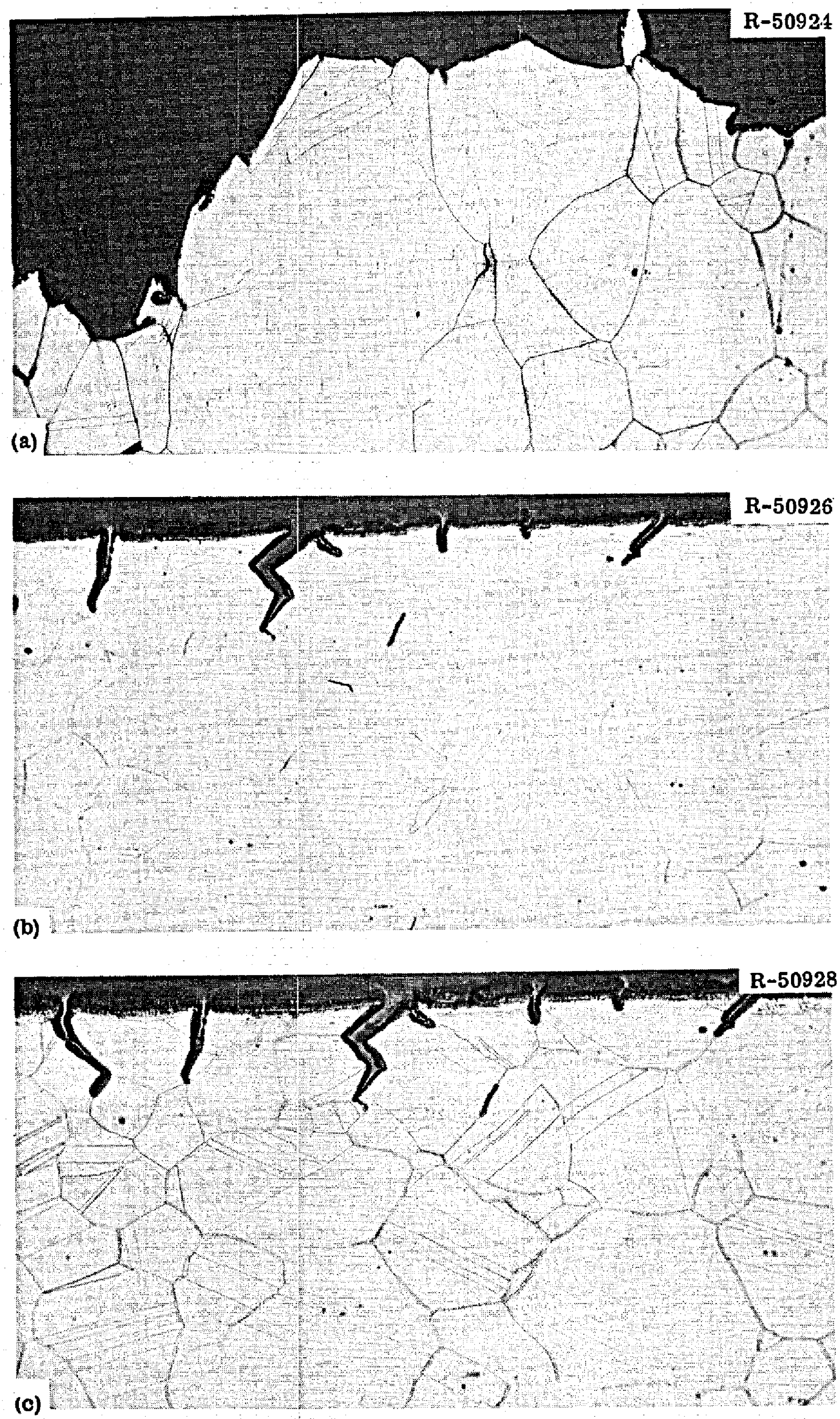

Fig. 57. Photomicrographs of a Modified Hastelloy N (Heat 67-551) Sample Tested at 650°C (Strain Rate, 0.002 min^{-1}) After Being Exposed to the MSRE Core for 7244 hr at 650°C and Irradiated to a Fluence of 5.1×10^{20} neutrons/cm^2. (a) Fracture, etched. 100×. (b) Edge, as polished. 100×. (c) Edge, etched. 100×. Etchant: glyceria regia. Reduced 20%.

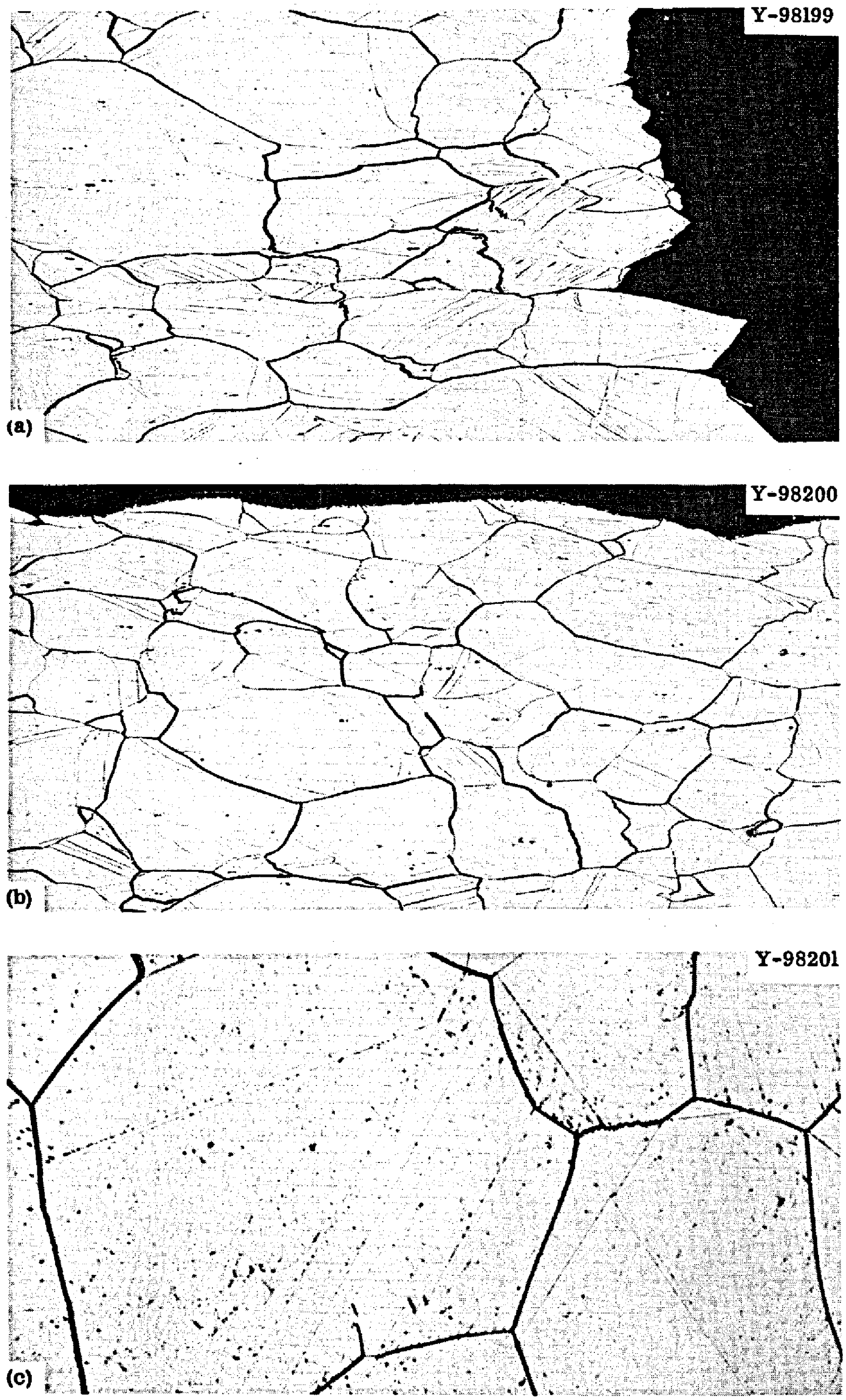

Fig. 58. Photomicrographs of a Modified Hastelloy N (Heat 67-551) Sample Tested at 25°C After Being Exposed to Static Barren Fuel Salt for 7244 hr at 650°C. (a) Fracture. 100X. (b) Edge. 100X. (c) Typical unstressed microstructure. 500X. Etchant: glyceria regia. Reduced 20.5%.

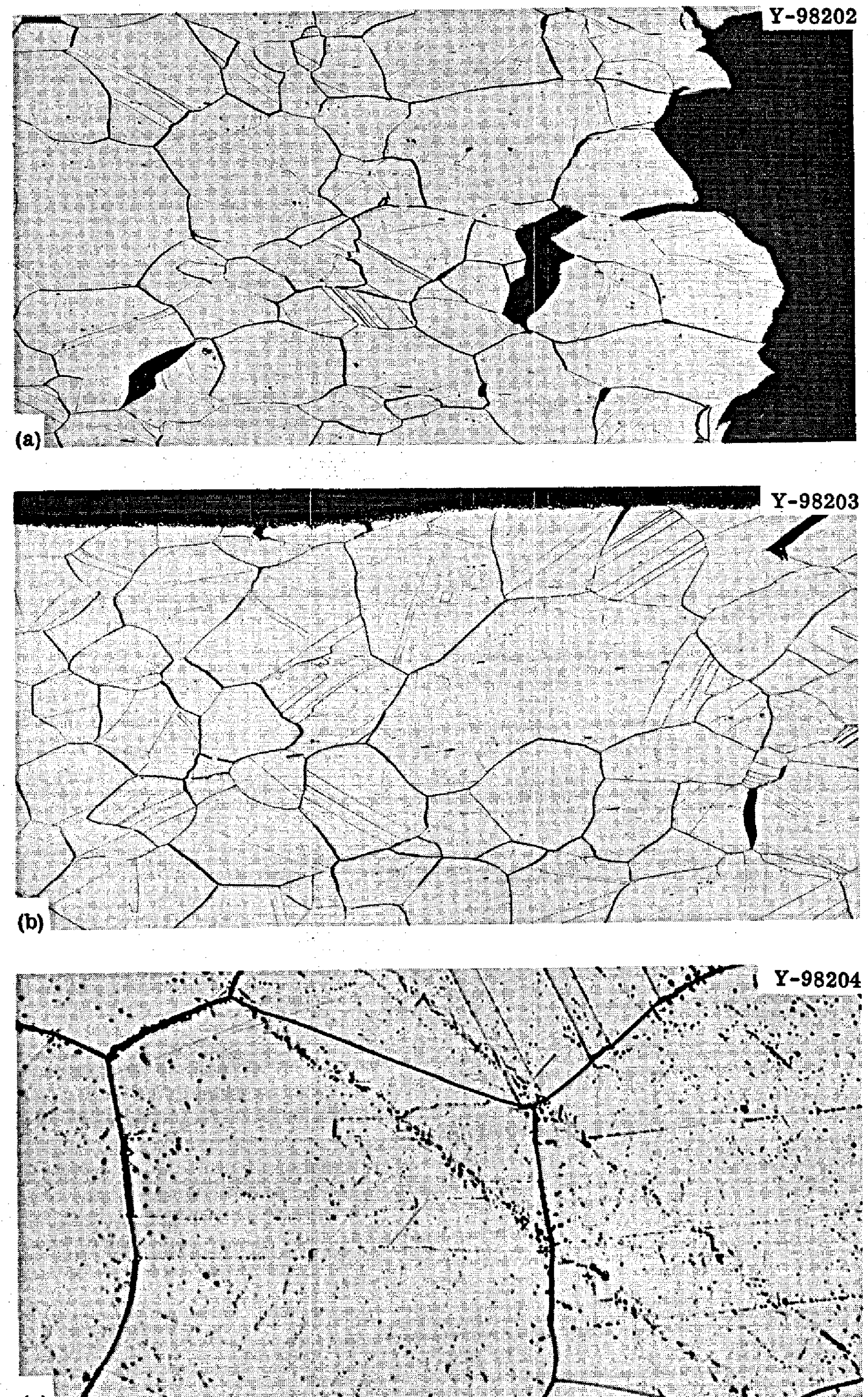

Fig. 59. Photomicrographs of a Modified Hastelloy N (Heat 67-551) Sample Tested at 650°C (Strain Rate, 0.002 min^{-1}) After Being Exposed to Static Barren Fuel Salt for 7244 hr at 650°C. (a) Fracture. 100×. (b) Edge near fracture. 100×. (c) Typical unstressed microstructure. 500×. Etchant: glyceria regia. Reduced 20.5%.

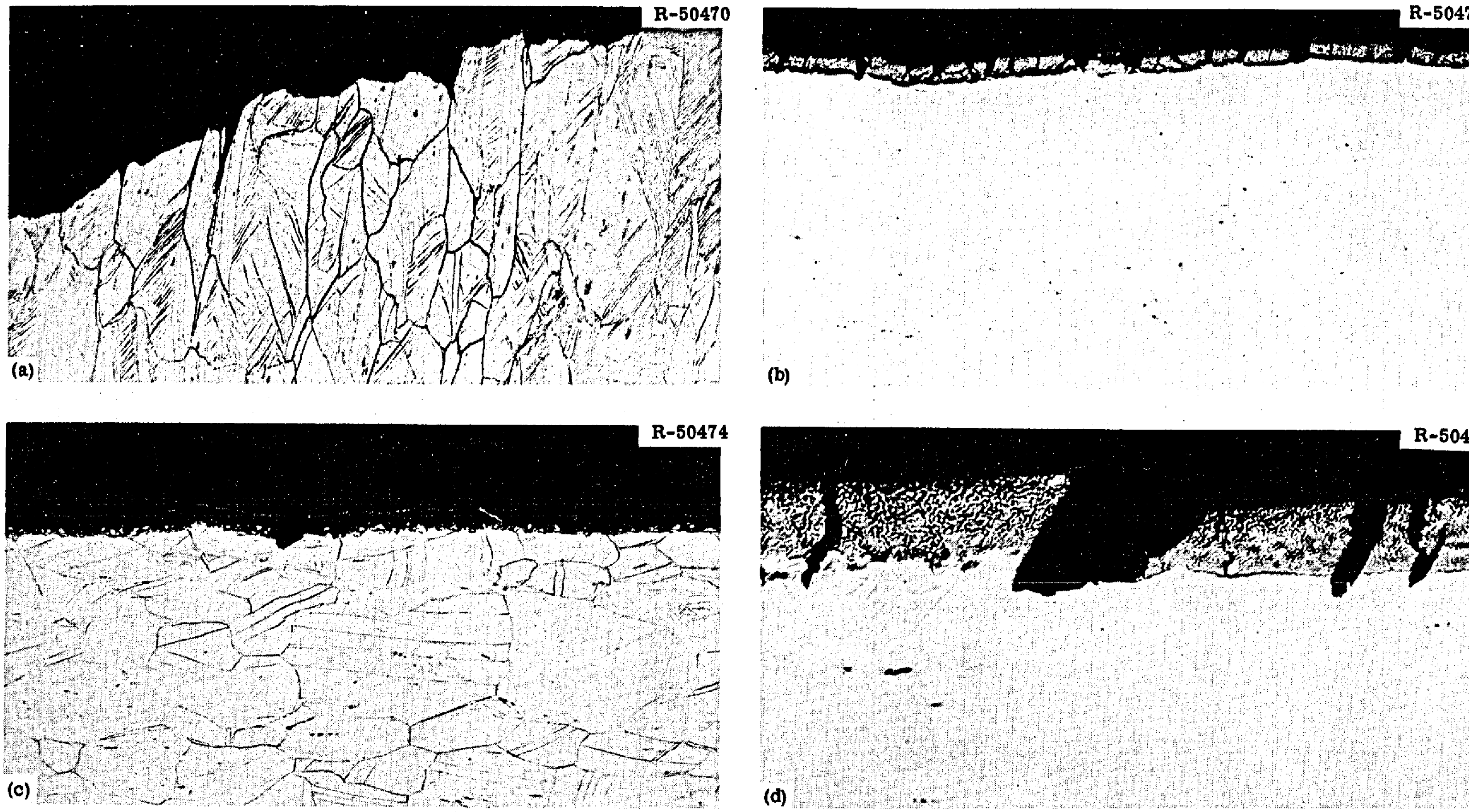

Fig. 60. Photomicrographs of a Modified Hastelloy N (Heat 67-504) Sample Tested at 25°C Following Exposure to the MSRE Cell Environment for 17,033 hr and Irradiation to a Fluence of 2.5×10^{19} neutrons/cm^2. (a) Fracture, etched. 100×. (b) Edge, as polished. 100×. (c) Edge, etched. 100×. (d) Edge, as polished. 500×. Etchant: glyceria regia. Reduced 27%.

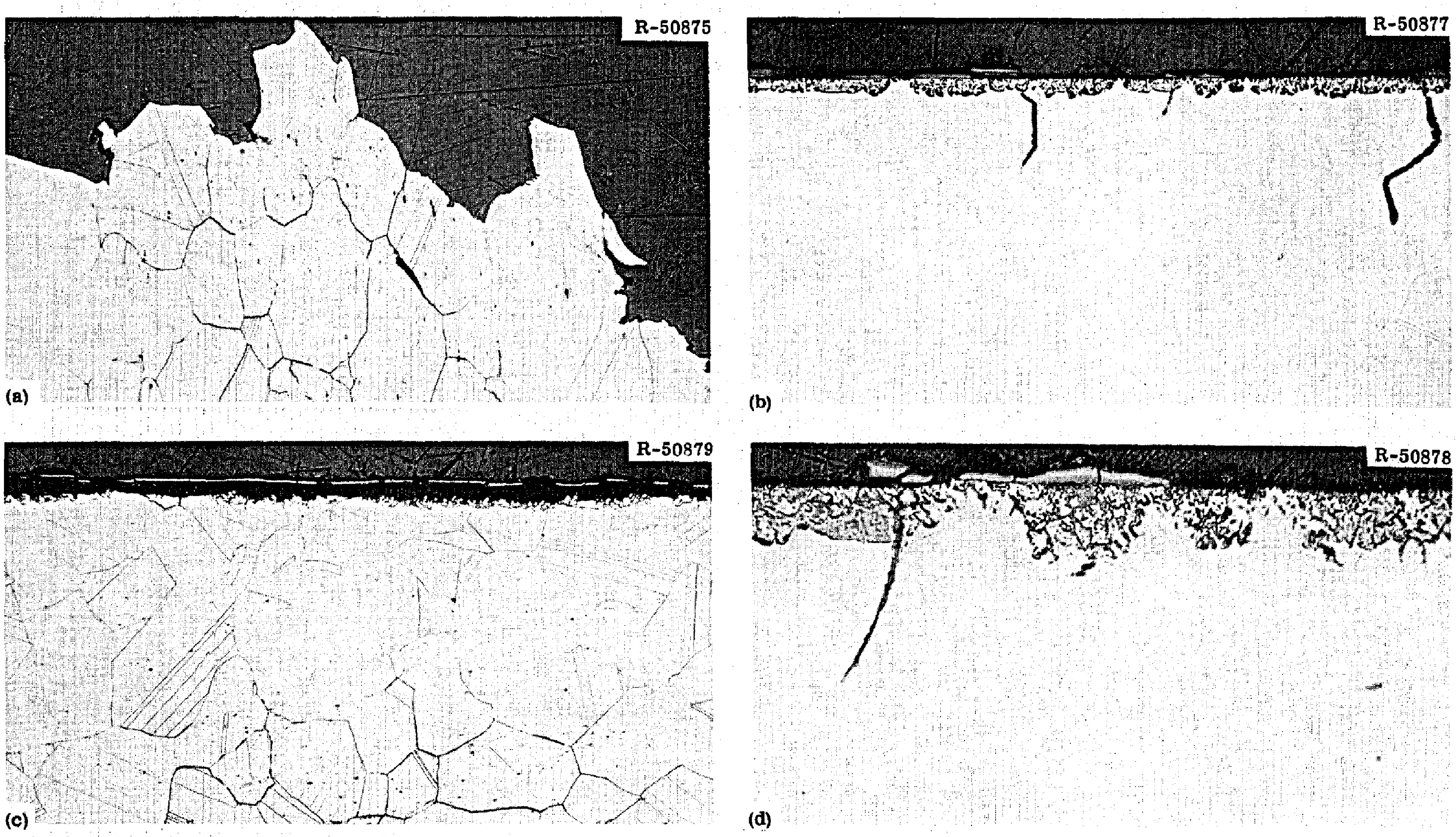

Fig. 61. Photomicrographs of a Modified Hastelloy N (Heat 67-504) Sample Tested at 650°C (Strain Rate, 0.002 min^{-1}) Following Exposure to the MSRE Cell Environment for 17,033 hr and Irradiated to a Fluence of 2.5×10^{19} neutrons/cm^2. (a) Fracture, etched. 100×. (b) Edge, as polished. 100×. (c) Edge, etched. 100×. (d) Edge, as polished. 500×. Etchant: glyceria regia. Reduced 25%.

Irradiation of both heats caused a general decrease of the fracture strain with increasing thermal fluence at test temperatures of 25 to 850°C. The fracture strains at low temperatures are lower for heat 5065. We attribute the reduction in fracture strain at low temperatures to precipitation of carbides and demonstrated previously that it can be recovered by annealing to coarsen the carbide.[12] We attribute the embrittlement at high temperatures to the helium formed by thermal transmutation of ^{10}B to form ^{4}He and ^{7}Li. This embrittlement cannot be recovered by annealing. The presence of helium in the material influences the creep properties at 650°C by reducing the rupture life and the strain at fracture; the creep rate is unaffected (Figs. 19 through 26, pp. 30 through 34). The effects on the rupture life are greater at higher stress levels and decrease to insignificant below about 10,000 psi. (The maximum operating stress[13] in the MSRE is 6000 psi.) The changes in the fracture strain are of utmost importance and are slightly dependent upon the thermal fluence (Figs. 21 and 26). Figure 23 shows more clearly the sensitivity of heat 5085 to the presence of helium and how this sensitivity at 650°C depends upon the strain rate. A thermal fluence of only 1.3×10^{19} neutrons/cm^2 produced about 1 ppm (atomic) He and reduced the fracture strain from 30 to 2% when the material was crept at a rate of 0.1%/hr. The strain rate results in the lowest fracture strains with slower rates resulting in slightly higher values. Figure 28, p. 36, shows that this same general behavior holds for heat 5065 although the amounts of helium produced are actually lower. The MSRE vessel has received a thermal fluence of about 4×10^{19} neutrons/cm^2, and Figs. 23 and 28 indicate that the fracture strains will not drop much more with continued operation. The control rod thimbles have received a thermal fluence of about 2×10^{21} neutrons/cm^2. They should be extremely brittle, but are normally subjected to only a slight compressive stress.

The greater strain rate sensitivity of the irradiated Hastelloy N at 650°C is illustrated in Figs. 22 and 27 for heats 5085 and 5065,

---

[12] H. E. McCoy, An Evaluation of the Molten-Salt Reactor Experiment Hastelloy N Surveillance Specimen — Third Group, ORNL-TM-2647 (1970).

[13] R. B. Briggs, ORNL, private communication.

respectively. For heat 5085 the fracture strain of the unirradiated material varies from 32 to 21%, a decrease of 34%, and the irradiated material varies from 9.3 to 0.5%, a decrease of 95%. For heat 5065 the corresponding reductions are 35% for the unirradiated material and 97% for the irradiated material.

The question of primary concern is whether the Hastelloy N has corroded more rapidly during the previous surveillance period than previously. We have at least three parameters or phenomena that can be observed or measured that likely are dependent upon the corrosion rate. The first measure is the chemical change of the salt during reactor operation. Since the chromium observed in the salt can hardly come from anywhere except the Hastelloy N, we cannot question this parameter as a measure of the corrosion rate. Second, we can observe changes in the microstructure. Figures 2, 3, and 4, pp. 9, 10, and 12, show typical changes, but these observations are difficult to interpret without additional information. Third, the mechanical properties themselves may be altered or the crack patterns that develop may be useful indications of the effects of corrosion on the mechanical properties. The property changes themselves are not very useful in this case because we have only matched sets of control samples and surveillance samples. The control samples are exposed to a static barren fuel salt that does not match the corrosiveness of the MSRE fuel circuit. The surveillance samples are exposed to a neutron fluence and to a more corrosive salt circuit. The irradiation effects predominate, so the effects of the added corrosion are not large enough to see by observing the mechanical property changes. Thus there are several measures of corrosion in the MSRE, but they are all subject to interpretation. Because of the importance of this subject, let us review the pertinent facts and observations.

1. Before the last period of operation, the salt was removed from the MSRE and processed to remove the uranium and replace it with ^{233}U. This processing left the salt fairly oxidizing, and it was necessary to adjust the oxidation potential by adding beryllium metal. The chromium content of the salt was only 40 ppm when placed in the reactor and rose over a few weeks to a level of about 100 ppm. This apparent corrosion could be accounted for by uniformly removing the chromium from the

Hastelloy N to a depth of 0.3 mil. The total increase of chromium in the salt during the entire MSRE operation would require uniform chromium extraction to a depth of 0.4 mil. However, the diffusion rate along the grain boundaries can be about 10^6 the rate through the bulk grains,[14] and it is more likely that chromium be removed to greater depths along the grain boundaries.

2. Electron microprobe examination of the sample in Fig. 5, p. 13, revealed a definite chromium gradient near the surface and a surface chromium concentration of nearly zero. A diffusion coefficient of 4×10^{-14} cm^2/sec for chromium was computed based on the shape of the profile which is in excellent agreement with the value of 2×10^{-14} cm^2/sec measured by Grimes et al.[15] (Fig. 62).

3. Complete loss of chromium from Hastelloy N does not result in the type of microstructural modification that was observed, not does it cause embrittlement.[16] We made laboratory melts containing from 0 to 9% Cr with the standard Hastelloy N base composition. The amount of carbide precipitate increases and the grain size decreases as the chromium content increases. The alloy is weaker in creep at 650°C without chromium, but the fracture strains are not dependent upon the chromium concentration.

4. Similar microprobe scans have been made on control samples where the modified structure is also present. The resolution is much better on these samples where the background radiation is not present. The gradients measured in a sample that had been in the control facility for 15,289 hr at 650°C are shown in Fig. 63. The chromium is depleted and the iron is enriched near the surface. These chemical modifications extend only a short distance into the material. These changes would not be expected to produce the microstructural changes.

---

[14] W. R. Upthegrove and M. J. Sinnot, "Grain-Boundary Self-Diffusion of Nickel," Trans. Am. Soc. Metals 50, 1031 (1958).

[15] W. R. Grimes, G. M. Watson, J. H. DeVan, and R. B. Evans, "Radio-Tracer Techniques in the Study of Corrosion by Molten Fluorides," pp. 559–574 in Conference on the Use of Radioisotopes in the Physical Sciences and Industry, September 6–17, 1960, Proceedings, Vol. III, International Atomic Energy Agency, Vienna, 1962.

[16] H. E. McCoy, Influence of Various Alloying Additions on the Strength of Nickel-Base Alloys (report in preparation).

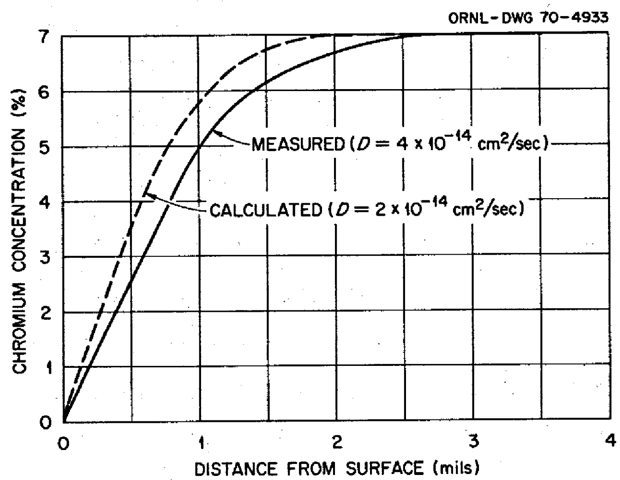

Fig. 62. Chromium Gradient in Hastelloy N Sample Exposed to the MSRE Core for 22,533 hr.

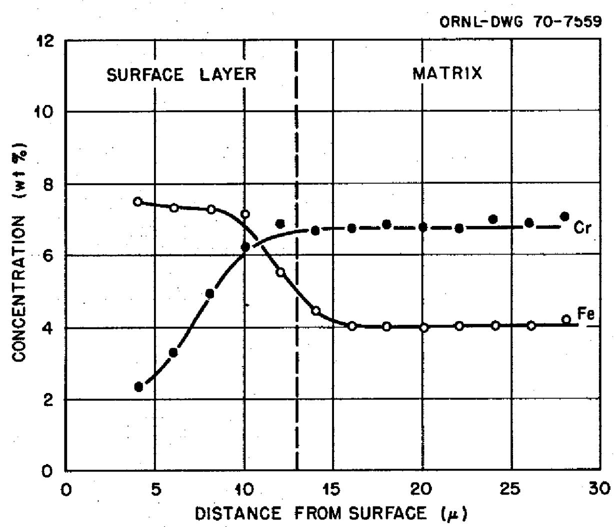

Fig. 63. Concentration Gradients in Hastelloy N (Heat 5085) Exposed to Static Barren Fuel Salt in the MSRE Control Vessel for 15,289 hr at 650°C.

5. The Hastelloy N straps that held the surveillance assembly together for 22,533 hr had intergranular surface cracks to a depth of about 3 mils (ref. 17) (see Fig. 2, p. 9). Straps that had been in the reactor for 7244 hr had cracks to a depth of 1.5 mils. The straps are 0.020 in. thick and should not be stressed during reactor operation, but

[17] W. H. Cook, MSR Program Semiann. Progr. Rept., Aug. 31, 1969, ORNL-4449, pp. 165–168.

they were handled considerably during disassembly. Thus one cannot conclude whether the cracks were formed during service or in handling afterwards. The microstructure was not modified near the surface of these straps.

6. A surface microstructural modification has been observed spasmodically during this entire program. The photomicrographs of the various lots of heat 5085 that were examined are presented in Fig. 64. The modified microstructure has been present to some degree in all samples including the irradiated and the control samples. It is difficult to say that the modification has grown any worse.

7. We have been able to produce a microstructural modification quite similar to that shown in Fig. 65 by sinterless grinding Hastelloy N and then annealing it for long periods of time in argon at 650°C (Fig. 65). Thus, the layer may well be associated with cold working and the manner in which this alters carbide deposition near the surface.

8. There is a definite tendency for the samples removed from the MSRE to show progressively more edge cracking during postirradiation testing as the time of exposure increases. As shown in Fig. 66 for samples stressed at 25°C, the frequency of edge cracks increases with exposure, but the maximum depth is constant at about 4 mils. The control samples do not show much edge cracking.

9. Microprobe scans on irradiated samples failed to reveal any fission products in the sample. However, the inability to analyze solely the material in a grain boundary makes it impossible to conclude that no fission products are entering the metal. We plan to dissolve progressive layers from the sample surfaces for chemical analysis to answer this question.

The observations on the alloys of modified Hastelloy N are quite important. Heats 7320 (0.5% Ti) and 67-551 (1.1% Ti) were exposed to the MSRE core for 7244 hr at 650°C. The properties of heat 7320 were not as good as we have observed for other 0.5% Ti-modified alloys irradiated at 650°C. However, the properties after irradiation in the MSRE are equivalent to those measured after irradiation in the ORR in a helium environment. The properties of heat 67-551 are outstanding. Both of

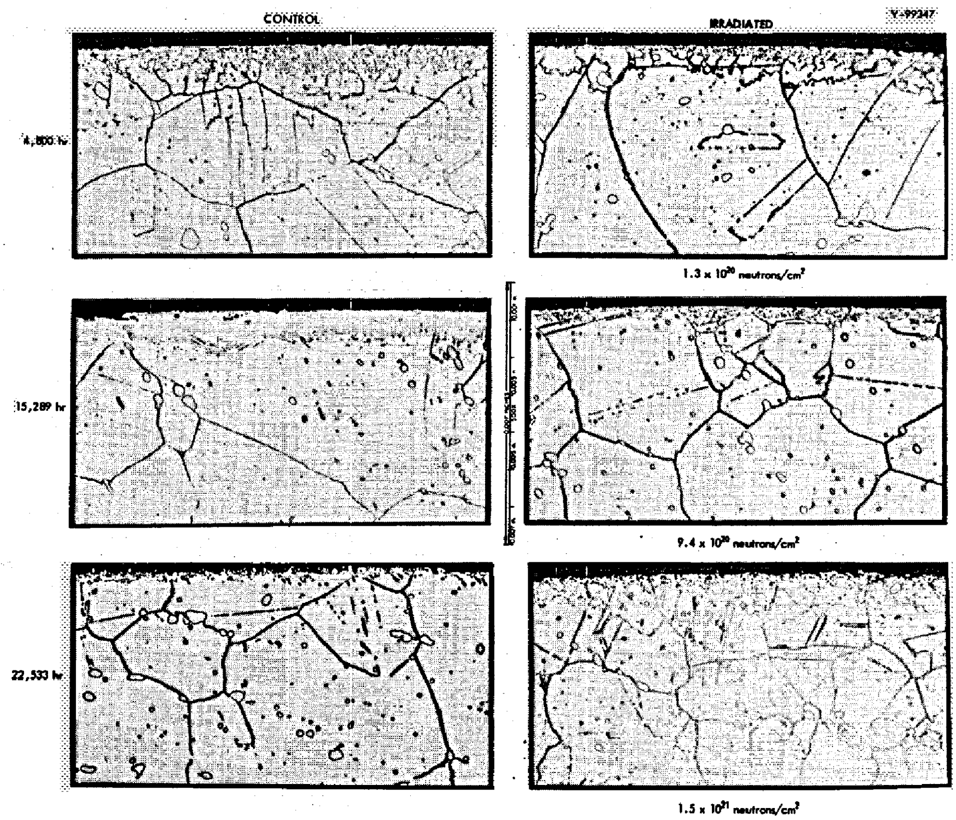

Fig. 64. Photomicrographs of Unstressed Hastelloy N (Heat 5085) Control and Irradiated Samples.

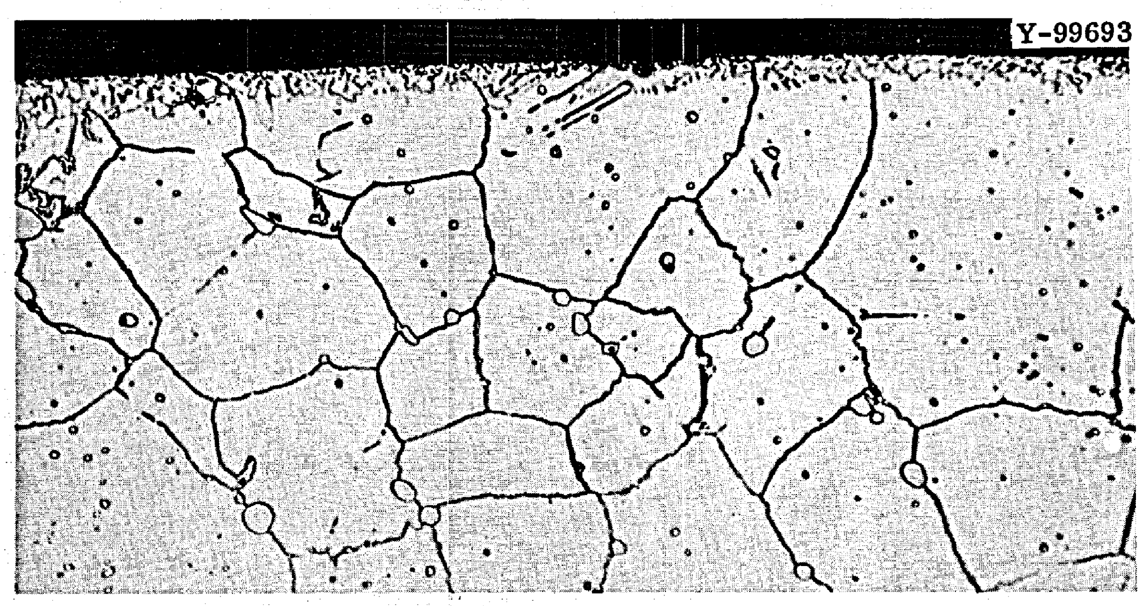

Fig. 65. Photomicrograph of Hastelloy N (Heat 5085) Rod That Was Annealed 1 hr at 1177°C, Sinterless Ground 5.2 mils, and Annealed for 4370 hr at 650°C in Argon. 500×. Etchant: glyceria regia.

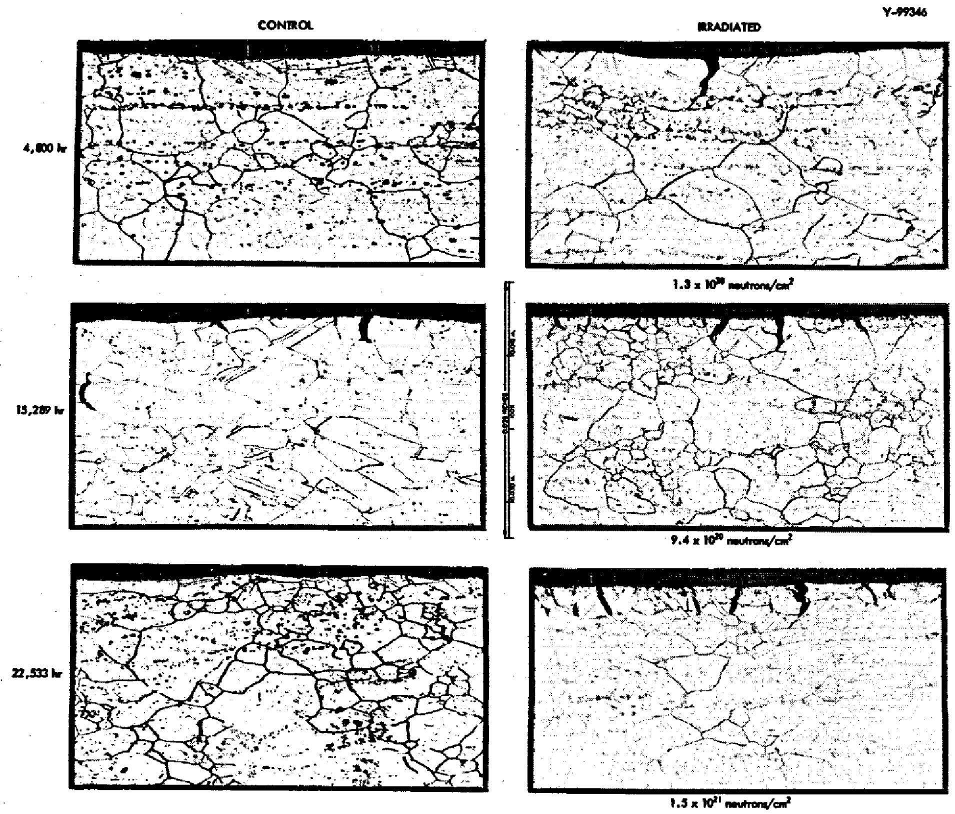

Fig. 66. Samples of Hastelloy N (Heat 5085) Stressed at 25°C. The control samples were exposed to static barren fuel salt for the indicated time and the irradiated samples were exposed to the core of the MSRE.

these heats seem to demonstrate some small property changes due to thermal aging. These changes are not large, but must be followed to longer times to make sure that they do not become large.

These two modified heats did not show a structural modification near the surface, but did exhibit edge cracking when tested. The frequency of edge cracks is much higher than noted for the controls.

One of the most confusing observations was the poor mechanical properties of heat 67-504 from outside the core. This heat was previously[18] exposed to the core for 9789 hr to a thermal fluence of 5.3×10^{20} neutrons/cm^2. The present group of samples outside the core

---

[18] H. E. McCoy, An Evaluation of the Molten-Salt Reactor Experiment Hastelloy N Surveillance Specimen — Third Group, ORNL-TM-2647 (1970).

was exposed to N_2 + 2 to 5% O_2 for 17,033 hr and received a thermal fluence of 2.5×10^{19} neutrons/cm^2. The latter group had poorer mechanical properties than the group exposed to the higher fluence. The rupture life at a given stress level was less (Fig. 41, p. 54), the minimum creep rate higher (Fig. 42, p. 54), and the fracture strain lower (Fig. 43, p. 55). The photomicrographs in Figs. 60 and 61, pp. 76 and 77, show some surface oxidation but no other unusual features. Two heats should have been used, heat 67-502 (2% W + 0.5% Ti) and heat 67-504 (0.5% Hf). Postirradiation chemical analyses showed the presence of 0.5% Hf, but no tungsten was present. Hence, we have concluded that only heat 67-504 was included in these tests.

Our surveillance program has given us the opportunity to look at several alloys of modified composition. The creep properties of these heats are compared with those of standard Hastelloy N in Fig. 67. The curves were drawn through only four or five data points in each case, so slight differences in slope are not significant. The rupture lives of the modified alloys are within a factor of 2. The rupture lives of the irradiated, modified heats are about equivalent to those of unirradiated standard Hastelloy N. The creep rates, shown in Fig. 67(b), are lower for the modified alloys by as much as a factor of 3. Heats 67-502 and 67-504 have the lowest creep rates. The postirradiation fracture strains are shown in Fig. 67(c). Quite a range of fracture strains resulted with a minimum of about 0.5% for standard Hastelloy N and a minimum of about 7% for heat 67-551. Heats 67-502 and 67-504 had fracture strains of 6.4%; heat 7320 was not much better than standard Hastelloy N with only 2.8%.

None of the modified alloys have shown any adverse corrosion behavior in the salt. Thus, it would appear that we have several alloys that are suitable for use in future reactors that operate at 650°C. However, as discussed previously, these new alloys are very sensitive to irradiation temperature and the proposed 700°C operating temperature of a breeder is too high for these alloys.[19] Present work offers encouragement that an alloy that is stable at 700°C can be developed by adding

---

[19]H. E. McCoy *et al.*, *MSR Program Semiann. Progr. Rept. Aug. 31, 1969*, ORNL-4449, p. 184.

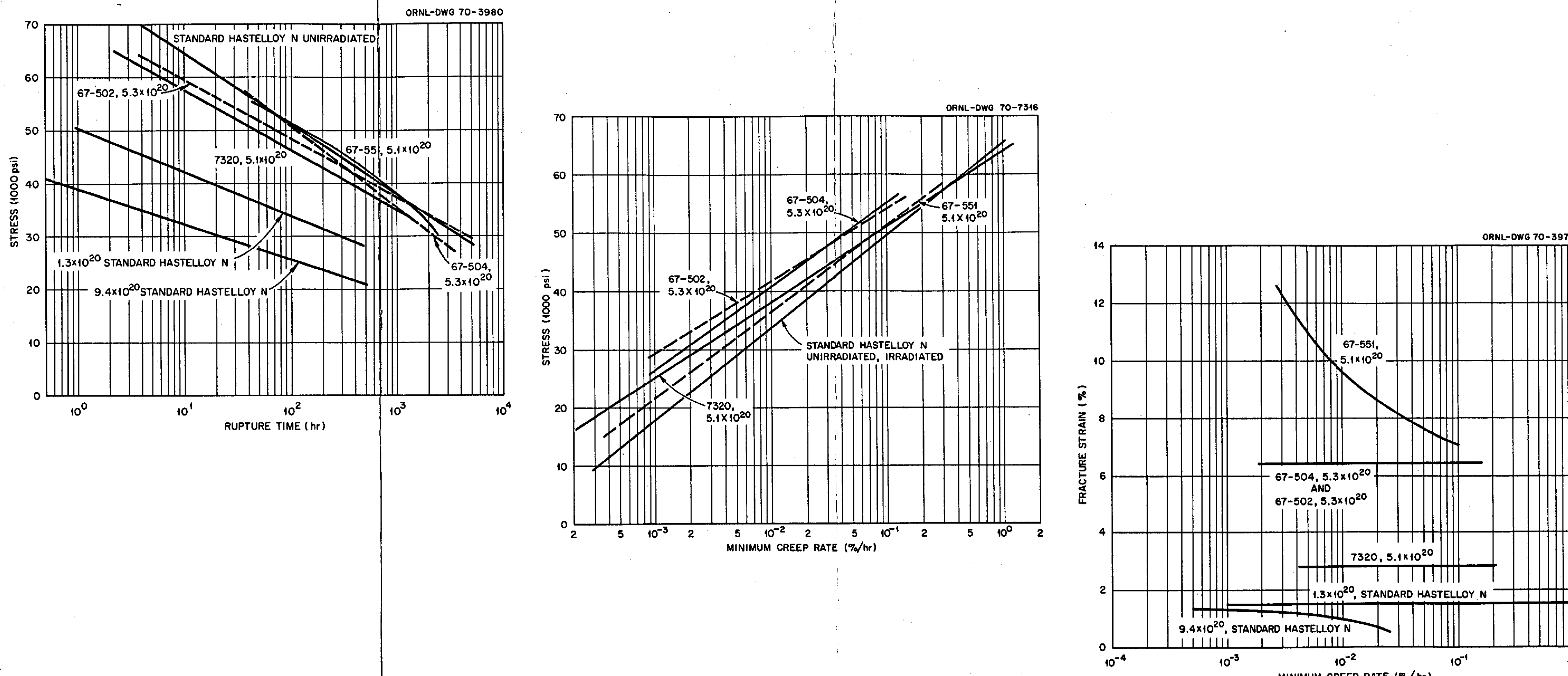

Fig. 67. Postirradiation Creep Properties at 650°C of Several Modified Alloys That Were Included in the Surveillance Program. The thermal fluence and heat numbers are shown by each line (see Table 1, p. 4, for the chemical composition).

larger amounts of titanium or combined amounts of these elements along with niobium and hafnium.

SUMMARY AND CONCLUSIONS

The heats of Hastelloy N used in fabricating the MSRE have shown a systematic deterioration of mechanical properties with increasing neutron fluence. The material exposed for the longest period of time in the core has reached a thermal fluence of 1.5×10^{21} neutrons/cm^2 and a fast fluence (> 50 kev) of 1.1×10^{21} neutrons/cm^2. These values are quite close to those anticipated for future reactors with a 30-year design life. The ductility of the material was too low, but the microstructure was free of irradiation-induced voids and defects other than helium bubbles. Several heats of the modified alloys have been exposed to the MSRE and these have better postirradiation properties. They also seem to have good corrosion resistance.

The standard Hastelloy N removed from the core shows some evidence of corrosion. The corrosion seems generally to be due to the selective removal of chromium, as predicted by prenuclear tests. Some observations that have not been explained adequately are (1) the presence of grain-boundary cracks in the straps that held parts of the surveillance assembly together, (2) the modified microstructure near the surface, and (3) the formation of intergranular cracks originating from the surface when irradiated materials are strained.

One of the modified alloys, heat 67-504, was exposed to the cell environment. This heat had been previously exposed to the MSRE. The fluence was higher in the core, but the postirradiation properties were superior to those of the material exposed to the cell environment. We presently have no explanation for the observed behavior.

ACKNOWLEDGMENTS

The author is indebted to many people for assisting in this study: W. H. Cook and A. Taboada for design of the surveillance assembly and insertion of the specimens; W. H. Cook and R. C. Steffy for measurements of flux; J. R. Weir, Jr., R. E. Gehlbach, and C. E. Sessions for review of the manuscript; E. J. Lawrence and J. L. Griffith for assembling the surveillance and control specimens in the fixture; P. Haubenreich and the MSRE Operation Staff for the extreme care with which they inserted and removed the surveillance specimens; E. M. King and the Hot Cell Operation Staff for developing techniques for cutting long rods into individual specimens, determining specimen straightness, and assistance in running creep and tensile tests; B. C. Williams, B. McNabb, and H. W. Kline for running tensile and creep tests on surveillance and control specimens; J. Feltner for processing the test data; H. R. Tinch and N. M. Atchley for metallography of the control and surveillance specimens; Frances Scarboro of The Metals and Ceramics Division Reports Office for preparing the manuscript; and the Graphic Arts Department for preparing the drawings.

INTERNAL DISTRIBUTION

1–3. Central Research Library
4. ORNL Y-12 Technical Library
 Document Reference Section
5–24. Laboratory Records
25. Laboratory Records, ORNL RC
26. ORNL Patent Office
27. G. M. Adamson, Jr.
28. J. L. Anderson
29. R. F. Apple
30. W. E. Atkinson
31. C. F. Baes
32. S. J. Ball
33. C. E. Bamberger
34. C. J. Barton
35. H. F. Bauman
36. S. E. Beall
37. M. J. Bell
38. C. E. Bettis
39. D. S. Billington
40. R. E. Blanco
41. F. F. Blankenship
42. E. E. Bloom
43. R. Blumberg
44. E. G. Bohlmann
45. J. Braunstein
46. M. A. Bredig
47. R. B. Briggs
48. H. R. Bronstein
49. G. D. Brunton
50. S. Cantor
51. D. W. Cardwell
52. W. L. Carter
53. G. I. Cathers
54. O. B. Cavin
55. Nancy Cole
56. C. W. Collins
57. E. L. Compere
58. W. H. Cook
59. J. W. Cooke
60. L. T. Corbin
61. J. L. Crowley
62. F. L. Culler
63. D. R. Cuneo
64. J. E. Cunningham
65. J. M. Dale
66. J. H. DeVan
67. J. R. DiStefano
68. S. J. Ditto
69. W. P. Eatherly
70. J. R. Engel
71. J. I. Federer
72. D. E. Ferguson
73. J. H Frye, Jr.
74. W. K. Furlong
75. C. H. Gabbard
76. R. B. Gallaher
77. R. E. Gehlbach
78. L. O. Gilpatrick
79. G. Goldberg
80. W. R. Grimes
81. A. G. Grindell
82. R. H. Guymon
83. W. O. Harms
84. P. N. Haubenreich
85. R. E. Helms
86. J. R. Hightower
87–89. M. R. Hill
90. E. C. Hise
91. H. W. Hoffman
92. D. K. Holmes
93. P. P. Holz
94. A. Houtzeel
95. W. R. Huntley
96. H. Inouye
97. W. H. Jordan
98. P. R. Kasten
99. R. J. Kedl
100. C. R. Kennedy
101. R. T. King
102. S. S. Kirslis
103. J. W. Koger
104. H. W. Kohn
105. R. B. Korsmeyer
106. A. I. Krakoviak
107. T. S. Kress
108. J. A. Lane
109. R. B. Lindauer
110. E. L. Long, Jr.
111. A. L. Lotts
112. M. I. Lundin
113. R. N. Lyon
114. R. E. MacPherson

115. D. L. Manning
116. W. R. Martin
117. R. W. McClung
118–123. H. E. McCoy
124. D. L. McElroy
125. C. K. McGlothlan
126. C. J. McHargue
127. H. A. McLain
128. B. McNabb
129. L. E. McNeese
130. J. R. McWherter
131. A. S. Meyer
132. R. L. Moore
133. D. M. Moulton
134. T. R. Mueller
135. H. H. Nichol
136. J. P. Nichols
137. E. L. Nicholson
138. T. S. Noggle
139. L. C. Oakes
140. S. M. Ohr
141. P. Patriarca
142. A. M. Perry
143. T. W. Pickel
144. H. B. Piper
145. C. B. Pollock
146. B. E. Prince
147. G. L. Ragan
148. D. M. Richardson
149. R. C. Robertson
150. K. A. Romberger
151. M. W. Rosenthal
152. H. C. Savage
153. W. F. Schaffer
154. Dunlap Scott
155. J. L. Scott
156. C. E. Sessions
157. J. H. Shaffer
158. W. H. Sides
159. G. M. Slaughter
160. A. N. Smith
161. F. J. Smith
162. G. P. Smith
163. O. L. Smith
164. P. G. Smith
165. I. Spiewak
166. R. C. Steffy
167. R. A. Strehlow
168. R. W. Swindeman
169. J. R. Tallackson
170. R. E. Thoma
171. D. B. Trauger
172. W. E. Unger
173. G. M. Watson
174. J. S. Watson
175. H. L. Watts
176. C. F. Weaver
177. B. H. Webster
178. A. M. Weinberg
179. J. R. Weir
180. K. W. West
181. M. E. Whatley
182. J. C. White
183. R. P. Wichner
184. L. V. Wilson
185. Gale Young
186. H. C. Young
187. J. P. Young
188. E. L. Youngblood
189. F. C. Zapp

EXTERNAL DISTRIBUTION

190. G. G. Allaria, Atomics International
191. J. G. Asquith, Atomics International
192. D. F. Cope, RDT, SSR, AEC, Oak Ridge National Laboratory
193. C. B. Deering, Black and Veatch, Kansas City, Missouri
194. A. R. DeGrazia, AEC, Washington
195. H. M. Dieckamp, Atomics International
196. David Elias, AEC, Washington
197. A. Giambusso, AEC, Washington
198. J. E. Fox, AEC, Washington
199. F. D. Haines, AEC, Washington
200. C. E. Johnson, AEC, Washington

201. W. L. Kitterman, AEC, Washington
202. Kermit Laughon, AEC, OSR, Oak Ridge National Laboratory
203. C. L. Matthews, AEC, OSR, Oak Ridge National Laboratory
204–205. T. W. McIntosh, AEC, Washington
206. A. B. Martin, Atomics International
207. J. M. Martin, The International Nickel Company, Huntington, W. Va.
208. D. G. Mason, Atomics International
209. G. W. Meyers, Atomics International
210. D. E. Reardon, AEC, Canoga Park Area Office
211. T. C. Reuther, AEC, Washington
212. D. R. Riley, AEC, Washington
213. T. K. Roche, Stellite Division, Cabot Corporation, 1020 W. Park Ave., Kokomo, Ind. 46901
214. H. M. Roth, AEC, Oak Ridge Operations
215. M. Shaw, AEC, Washington
216. J. M. Simmons, AEC, Washington
217. T. G. Schleiter, AEC, Washington
218. W. L. Smalley, AEC, Washington
219. Earl O. Smith, Black and Veatch, Post Office Box 8405, Kansas City, Missouri 64114
220. S. R. Stamp, AEC, Canoga Park Area Office
221. E. E. Stansbury, The University of Tennessee
222. D. K. Stevens, AEC, Washington
223. R. F. Sweek, AEC, Washington
224. A. Taboada, AEC, Washington
225. M. J. Whitman, AEC, Washington
226. R. F. Wilson, Atomics International
227. Laboratory and University Division, AEC, Oak Ridge Operations
228–242. Division of Technical Information Extension